# DIAGONAL ERECTION BRIDGING FOR OPEN WEB STEEL JOISTS WITH FLUSH FRAME CONNECTIONS

A Thesis Presented for the
Master of Science
Degree
The University of Tennessee, Knoxville

James A Moore
August 2024

## ACKNOWLEDGEMENTS

This work was funded by the Steel Joist Institute (SJI). The joists were manufactured and delivered to the University of Tennessee, Knoxville campus by Vulcraft-Alabama. The support of both SJI and Vulcraft is gratefully acknowledged. The author thanks Dr. Mark Denavit, Pratik Poudel, Larry Roberts, Andy Baker, and Caroline Dykes for their support performing the physical experiments.

## ABSTRACT

Open web steel joists are highly slender structural members that are susceptible to lateral-torsional buckling before bracing is installed. The stability of joists needs to be properly assessed to ensure safety and efficiency during erection. Current practice for joists is based on a strength equation derived by Minkoff in the 1970s. This equation was derived for the common case of joists with bearing seat connections. Flush frame connections for joists have been recently developed. These connections are similar in form to single-plate shear connections and can provide more restraint than bearing seat connections. With more restraint, less bracing may be required, however, the magnitude of the benefit is unknown. The objective of this research is to quantify the strength of unbraced open web steel joists with flush frame connections and to modify the Minkoff equation to improve its accuracy for joists with flush frame connections. Physical testing of four joists sizes and a variety of connection details, making up 60 different configurations, was conducted. The joists with flush frame connections supported more load than the joists of the same designation with bearing seat connections in almost all cases. Based on the experimental results, a modification to the Minkoff equation, specifically a new effective length factor for joists with flush frame connections, is proposed. The proposed modification will enable engineers to preserve the efficiency of open web steel joists while also ensuring safety during erection.

## TABLE OF CONTENTS

## LIST OF TABLES

## LIST OF FIGURES

# CHAPTER ONE

# INTRODUCTION

Open web steel joists are efficient and economical structural members. Their efficiency is achieved, in part, through judicious use of bracing, which allows these relatively slender members to be designed near their plastic capacity. The design of bracing, also referred to as bridging, for open web steel joists is generally divided into three stages in the life of the structure (Green and Holtermann 2008). Erection bridging is required when a joist is not stable under its own self-weight and the weight of one erector. Construction bridging is required prior to the application of construction loads (i.e., any load other than the erector, joists, and bridging bundles). Once attached, metal decking (except for standing seam roofs) provides sufficient lateral support to the top chord, but permanent bridging is required to provide lateral support to the bottom chord and web members, especially when the joist is subject to uplift forces. Requirements for these different stages vary, but the bridging for the different stages are not different physical members. Erection bridging can serve as construction bridging and permanent bridging as the structure evolves through the different stages.

Bridging is generally either horizontal or diagonal (Figure 1). Horizontal bridging consists of continuous members that span through the joists, are welded to each joist, and are anchored at each end. Diagonal bridging connects the top chord of one joist to the bottom chord of an adjacent joist, is generally bolted, and is also anchored. Diagonal bridging must be connected at its intersection by bolt or weld to function properly and prevent rigid body movement (Green et al. 2008).

A typical process of erection for steel building starts with the columns then framing members along column lines (e.g., steel girders, joist girders, or column joists) to "box out" the frame. Wire rope bracing can be used to stabilize the frame which induces axial forces in the framing members along column lines. The SJI *Specifications* (2020) requires joist girders to be proportioned such that they can be erected without bridging. An OSHA rule requires that column joists with spans of 60 ft or less be designed with sufficient strength to allow one employee to release the hoisting cable without the need for erection bridging (OSHA 2001). Given the challenges in achieving this level of stability for column joists, OSHA issued a policy that erectors would be in compliance with the requirement by (1) installing bridging or otherwise stabilizing the joist prior to releasing the hoisting cable, or (2) releasing the cable without having a worker on the joist. Joist manufacturers attach a "danger tag" to column joists that have not been designed to support an erector without bridging (Green and Holtermann 2008).

Joists not on a column line are typically not subject to significant axial forces during erection. However, bridging may still be required for these members since they are susceptible to lateral-torsional buckling. Requirements for diagonal erection bridging are included in SJI *Specifications* (2020) Section 5.5.2.1.

For joist spans 60 ft or less in length, bolted diagonal erection bridging is required if the entry for the joist is shaded red in the SJI Load Tables. For these joists, the row of bridging nearest the

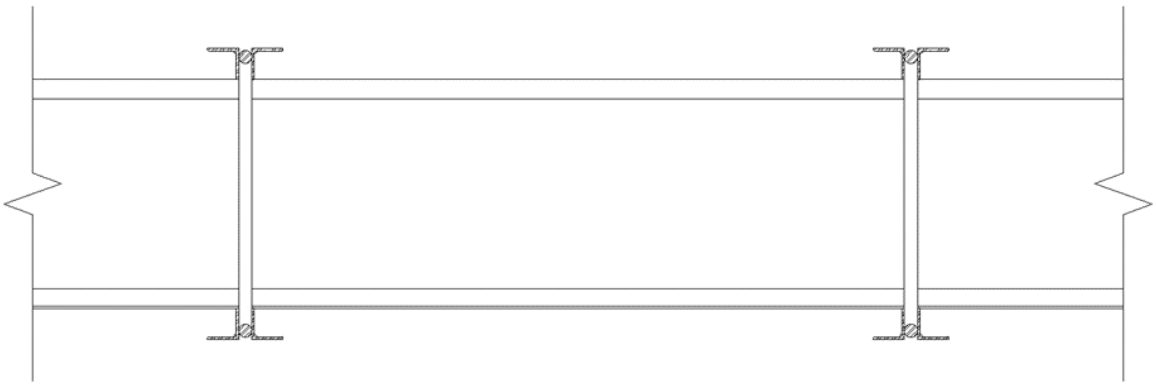

(a) Horizontal bridging

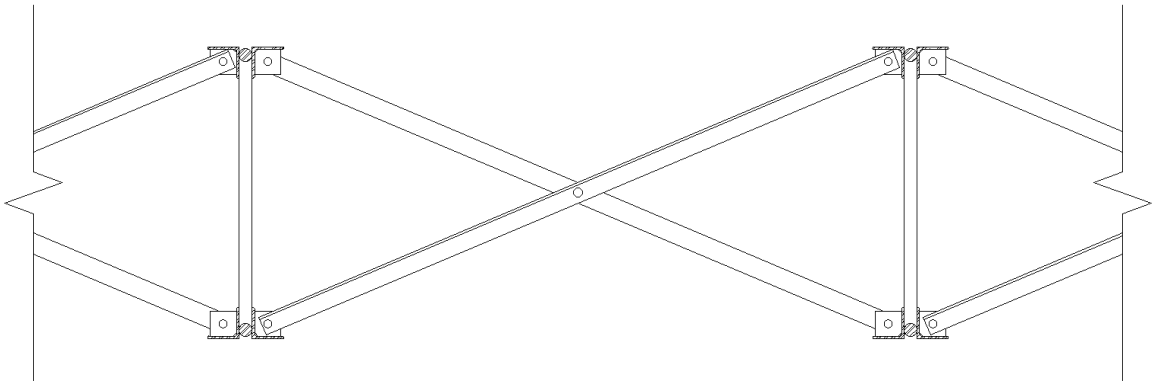

(b) Diagonal bridging

Figure 1. Example Illustrations of Bridging Details

midspan must be diagonal bridging with bolted connections at chords and intersections (i.e., bolted diagonal erection bridging) and hoisting cables must not be released until this row of bridging is completely installed. If the joist is not in the red shaded area in the SJI Load Tables, then welded horizontal bridging is permitted and this bridging can be installed after the hoisting cables are released. The red shaded area in the SJI Load Table was determined based on the Minkoff equation.

For joist spans greater than 60 ft in length, requirements for erection bridging are indicated by blue or gray shading in the SJI Load Tables. All joists with spans between 60 and 100 ft are shaded blue. For these joists, hoisting cables must not be released until the two rows of bridging nearest the third points are completely installed and anchored. All joists with spans of 100 ft to 240 ft are shaded gray. For these joists, hoisting cables must not be released until all rows of bridging are completely installed and anchored. In both cases, all rows of bridging must be diagonal bridging with bolted connections at chords and intersections. Additionally, when the joist spacing is less than 70% of the joist depth, bolted horizontal bridging is required in addition to bolted diagonal erection bridging.

In the absence of a standard SJI section number designation, erection bridging requirements (for joist spans 60 ft or less in length) can be determined by matching the joist design to an equivalent standard joist or by using the Minkoff equation (SJI *Specifications* (2020) Equation 5.5-1) which is described in detail in Chapter 2.

Minkoff presented only limited validation of his eponymous equation but recommended experimental testing to verify the accuracy of the equation. Ziemian et al. (2004) described a series of experimental studies to investigate the validity of the Minkoff equation. The tests included a variety of joists ranging from 10 in. to 32 in. deep and a variety of conditions for the bearing connection (e.g., bolts vs. welds and with or without vertical stabilizer plates at the bottom chord). Loads were applied at the top chord at midspan until an out-of-plane displacement of the span divided by 120 was observed. Ziemian et al. (2004) observed strengths lower than that estimated by the Minkoff equation. The differences were attributed to initial out-of-straightness and connection stiffness. The average limit load for the weakest connection configuration was half that of the strongest connection configuration. Vertical stabilizer plates at the bottom chord increased the strength by approximately 10%.

Requirements for erection bridging are also included in OSHA standard 1926.757(d) (OSHA 2001). Similar to SJI, OSHA has erection bridging requirement tables where the maximum length for a joist designation is listed and if the length of a certain joist exceeds the table value, then erection bridging is required. For joists less than 60 ft., OSHA requires 1) a midspan row of bolted diagonal bridging 2) hoisting cables not to be released until the diagonal bridging is bolted and anchored and 3) allowing only one erector on the joist until all bridging is installed and anchored. For joists between 60 ft. and 100 ft., OSHA requires 1) all rows of bridging be bolted diagonal bridging 2) two rows of bolted diagonal bridging be installed nearest to third points along the span of the joist 3) hoisting cables not to be released until the diagonal bridging is bolted and anchored and 4) allowing no more than two erectors on the joist until all bridging is

installed and anchored. For joists between 100 ft. and 144 ft., OSHA requires 1) all rows of bridging be bolted diagonal bridging 2) hoisting cables not to be released until the diagonal bridging is bolted and anchored and 3) allowing no more than two erectors on the joist until all bridging is installed and anchored. When joists are greater than 144 ft., they are to be installed and braced using the OSHA Regulations §1926.756 for Beams and columns and not §1926.757 for Open web steel joist.

## Flush Frame Connections

Typical open web steel joists have bearing seats that sit atop the supporting member as shown in Figure 2. Open web steel joists with flush frame connections have plates at the joist ends that are bolted to plates attached to the supporting members such that the top of the joist is flush with the top of the supporting member. Figure 3 shows two potential details for flush frame connections of joists to wide flange girders. Flush frame connections can also be made to joist girders.

The in-plane rotational stiffness of a flush frame connection is significantly greater than that for a traditional bearing seat connection. Due to the increased connection stiffness and the composite action of the girder made available by the flush framing, floor systems using flush frame connections are more capable of mitigating vibration than traditional joist floor systems (Murray and Davis 2020; Davis and Murray 2022).

The out-of-plane rotational stiffness and torsional stiffness of flush frame connections can also be greater than that of traditional bearing seat connections. These characteristics can help increase resistance to lateral-torsional buckling during erection, potentially leading to less need for erection bridging. The Minkoff equation was derived assuming no lateral deflection or twist at the member ends, thus greater torsional stiffness cannot be included in the derivation. However, the benefit of additional out-of-plane rotational stiffness can be expressed through the effective length factor, $k$, which was not part of the original derivation, but is included in the version of the Minkoff equation included in the SJI *Specifications* (2020).

Joists with flush frame connections are also supported lower relative to the joist's center of gravity than joists with typical bearing seat connections. The location of support can affect stability, but it is not a factor in the Minkoff equation since twist and lateral deflection were assumed to be zero at the supports in the derivation of the equation.

## Objective and Scope

The objective of this research is to develop design guidance for the erection stability of open web steel joists with flush frame connections. Physical testing of open web steel joists without bridging was performed. Experiments consisted of in-plane loading to determine critical loads and out-of-plane loading to determine torsional and rotational stiffnesses. Many configurations of flush frame joists were evaluated with variations in connection plate type, connection plate thicknesses, connection eccentricity, and the number of bolts installed. The experimental results were compared to results from the Minkoff equation to quantify the accuracy of the Minkoff equation and identify an appropriate effective length factor for use in the equation for open web

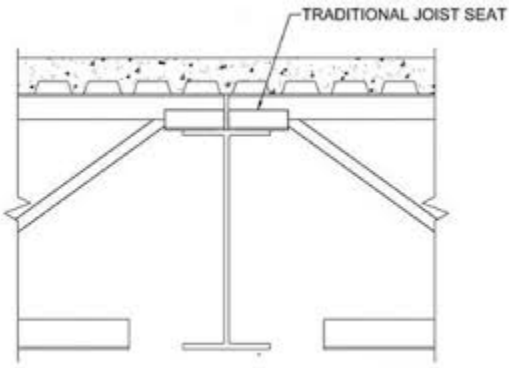


Figure 2. Typical Bearing Seat Joist Connection (Murray and Davis 2020)

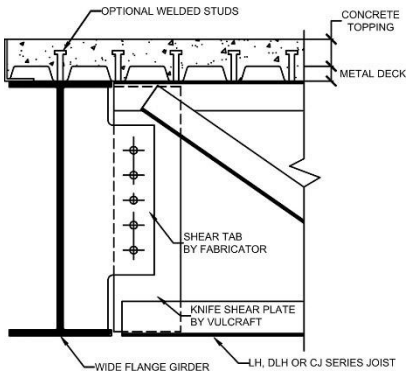


(a) Full-depth connection

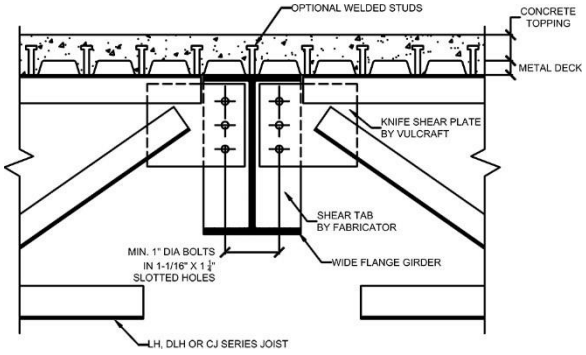


(b) Top-chord connection

Figure 3. Flush Frame Connection Details (Vulcraft 2023)

steel joists with flush frame connections. Numerical analyses, using models calibrated to the results of the experiments, were also performed to expand the range of investigation.

# CHAPTER TWO

# THE MINKOFF EQUATION

Minkoff derived Equation 1 from the governing differential equation for lateral-torsional buckling using the Rayleigh-Ritz method (Minkoff 1975). The derivation assumed that the joist was a simply supported beam with ends prevented from twist and lateral deflection and that the joist remained elastic. Uniform load acting through the centroid of the cross section (i.e., self-weight) and a point load acting at some height at mid-span (i.e., an erector) were considered. The lateral deflection and twist were assumed to be in the shape of a half-sine wave. Equation 1 does not include an effective length factor, *k*. The assumed boundary conditions and deformed shape correspond to an effective length factor of *k* = 1.0 and thus the factor was not included in the original derivation.

$$(wL)^2\left(\frac{\pi^2+3}{24}\right)^2+(wL)\left[\left(\frac{\pi^2+3}{12}\right)\left(\frac{P}{16}\right)(\pi^2+4)-\frac{\pi^4 EI_y}{2L^3}\left(\frac{\beta_x(\pi^2-3)}{24}-\frac{y_o}{2}\right)\right]+\left[\frac{P(\pi^2+4)}{16}\right]^2-\frac{\pi^4 EI_y}{2L^3}\left[\frac{\pi^4 EC_w}{2L^3}+\frac{\pi^2 GJ}{2L}+\frac{P\beta_x(\pi^2-4)}{16}-Pa_e\right]=0 \quad (1)$$

where

$C_w$ = warping constant (in.$^6$)
E = modulus of elasticity (= 29,000,000 psi for steel)
G = shear modulus (= 0.385E = 11,165,000 psi for steel)
$I_y$ = joist moment of inertia about y-axis (in.$^4$)
J = St. Venant torsion constant (in.$^4$)
L = joist span (in.)
P = point load (lb.)
w = uniform load (lb./in.)
$a_e$ = vertical location of load P with respect to shear center (in.)
(the value of $a_e$ is positive when the point of load application is above the shear center)
$y_o$ = distance from centroid of cross section to shear center (in.)
$\beta_x$ = cross-sectional parameter (in.)

A variety of cross-sectional geometric properties are used in the Minkoff equation. They are computed as follows. Key dimensions are also shown in Figure 4.

The joist effective depth, $d_e$, is computed as

$$d_e = d - y_t - y_b \quad (2)$$

where

d = joist total depth (in.)
$y_b$ = distance from the bottom of the bottom chord to the centroid of the bottom chord (in.)

$y_t$ = distance from the top of the top chord to the centroid of the top chord (in.)

The distance from the centroid of the top chord to the centroid of the cross section, *y*, is computed as

$$y = \frac{A_b d_e}{A_t + A_b} \quad (3)$$

where
$A_b$ = cross-sectional area of the bottom chord (in.$^2$)
$A_t$ = cross-sectional area of the top chord (in.$^2$)

The joist moment of inertia about the *y*-axis, $I_y$, is the sum of the contributions from the top chord and bottom chord.

$$I_y = I_{yt} + I_{yb} \quad (4)$$

where
$I_{yb}$ = bottom chord moment of inertia about the *y*-axis (in.$^4$)
$I_{yt}$ = top chord moment of inertia about the *y*-axis (in.$^4$)

The joist moment of inertia about the *x*-axis, $I_x$, is based on the parallel axis theorem, neglecting the small contribution of the chords about their own axes.

$$I_x = A_t y^2 + A_b (d_e - y)^2 \quad (5)$$

The distance from the centroid of the cross section to the shear center, $y_o$, is computed as

$$y_o = -y + \frac{I_{yb} d_e}{I_y} \quad (6)$$

The value of $y_o$ will be negative if the shear center is above the centroid.

The St. Venant torsion constant, *J*, is computed as

$$J = \frac{1}{3}(A_t t_t^2 + A_b t_b^2) \quad (7)$$

where
$t_b$ = thickness of the bottom chord angles (in.)
$t_t$ = thickness of the top chord angles (in.)

The warping constant, $C_w$, is computed as

$$C_w = \frac{d_e^2 I_{yb} I_{yt}}{I_y} \quad (8)$$

The cross-sectional parameter, $\beta_x$, is related to the asymmetry of the joist and is computed as

$$\beta_x = \frac{1}{I_x}[A_b(d_e - y)^3 - A_t y^3] - 2y_o \quad (9)$$

## The Minkoff Equation in the SJI Specifications

For use in practice, Equation 1 can be rewritten as a quadratic equation of $W = wL$ and solved using the quadratic equation as shown in Equation 10. Equation 10 is included in SJI *Specifications* (2020) Section 5.5.2.1. This equation was modified from the original Minkoff equation by inclusion of an effective length factor, *k*.

$$W = \frac{-b + \sqrt{b^2 - 4ac}}{2a} \quad (10a)$$

$$a = \left(\frac{\pi^2 + 3}{24}\right)^2 \quad (10b)$$

$$b = P\left(\frac{\pi^2 + 3}{12}\right)\left(\frac{\pi^2 + 4}{16}\right) - \frac{\pi^4 E I_y}{2(kL)^3}\left[\beta_x\left(\frac{\pi^2 - 3}{24}\right) - \frac{y_o}{2}\right] \quad (10c)$$

$$c = P^2\left(\frac{\pi^2 + 4}{16}\right)^2 - \frac{\pi^4 E I_y}{2(kL)^3}\left[P\left(\beta_x \frac{\pi^2 - 4}{16} - a_e\right) + \frac{\pi^4 E C_w}{2(kL)^3} + \frac{\pi^2 GJ}{2kL}\right] \quad (10d)$$

The vertical location of load *P* with respect to shear center, $a_e$, is positive when the point of load application is above the shear center. In the SJI *Specifications* (2020), the load from the erector is assumed to act at the joist center of gravity, thus $a_e = y_o$. The load is more destabilizing the higher it acts (i.e., greater values of $a_e$). Galambos (1993) described the weight of the erector as acting at the centroid of the top flange.

The SJI *Specifications* (2020) define the effective length factor, *k*, equal to 0.85. The effective length factor does not appear in the original derivation by Minkoff (1975), which essentially corresponds to $k = 1$. Galambos (1993) defined the effective length factor as $k = 1.00$ if the ends of the joist are not welded down and $k = 0.85$ if one end of the joist is welded down.

Once the total uniform load that causes lateral buckling, *W*, is computed using Equation 10a, the magnitude of the uniform load that causes lateral buckling, $w_u$, is computed by dividing by the joist span, $w_u = W/L$. Erection bridging is not required if the joist self-weight, $w_{actual}$, is less than the buckling load (i.e., $w_{acutal} < w_u$). Erection bridging is required if the joist self-weight is greater than or equal to the buckling load (i.e., $w_{acutal} \geq w_u$).

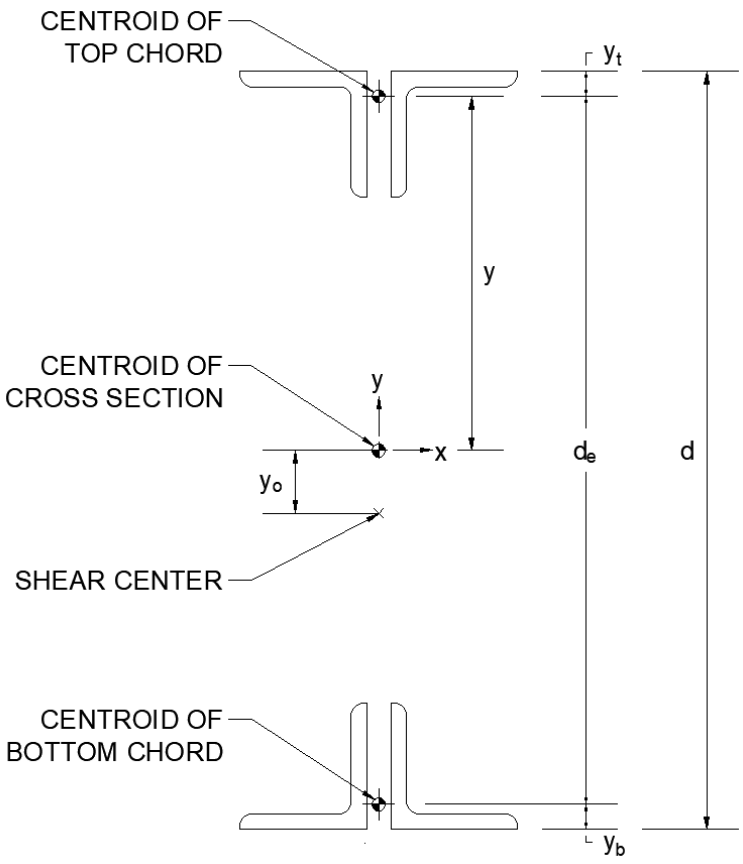


Figure 4. Joist Cross Section

## Calculation of the Critical Point Load

Equation 10 is for calculating the uniform load that causes buckling with a given point load. In this research, for comparisons to the experimental results, the opposite was needed: an equation for calculating the point load that causes buckling with a given uniform load. Equation 10 was derived noting that Equation 1 is a quadratic function of *wL*. Equation 1 is also a quadratic function of *P*, and thus a similar derivation can be applied to determine the critical value of *P*. Equation 11 shows the result of such a derivation and is used in this work to determine the point load that causes buckling with a given uniform load.

$$P = \frac{-b + \sqrt{b^2 - 4ac}}{2a} \tag{11a}$$

$$a = \left(\frac{\pi^2 + 4}{16}\right)^2 \tag{11b}$$

$$b = wL\left(\frac{\pi^2 + 3}{12}\right)\left(\frac{\pi^2 + 4}{16}\right) - \frac{\pi^4 E I_y}{2(kL)^3}\left[\beta_x\left(\frac{\pi^2 - 4}{16}\right) - a_e\right] \tag{11c}$$

$$c = wL^2\left(\frac{\pi^2 + 3}{24}\right)^2 - wL\left(\frac{\pi^4 E I_y}{2(kL)^3}\right)\left[\beta_x\left(\frac{\pi^2 - 3}{24}\right) - \frac{y_o}{2}\right] - \frac{\pi^4 E I_y}{2(kL)^3}\left(\frac{\pi^4 E C_w}{2(kL)^3} + \frac{\pi^2 G J}{2kL}\right) \tag{11d}$$

# CHAPTER THREE

# EXPERIMENTAL INVESTIGATION

An experimental investigation was performed in this work in which open web steel joists without bridging were subjected to in-plane and out-of-plane bending. These tests provided data against which the Minkoff equation was evaluated, and numerical models were validated. The tests were similar to those performed by Ziemian et al. (2004).

## Materials and Methods

Twelve joists were fabricated by a joist manufacturer for this project as listed in Table 1. The twelve consisted of four joist designations, each with one of three end connection types: a bearing seat connection, a full depth flush frame connection, and a top chord flush frame connection. Figure 5 shows the two types of flush frame joist end connections. The geometry and member sizes for each joist are presented in the Appendix.

Table 2 lists various lengths for each joist. The design length was selected to be the same for each of the three joists of the same designation. For the flush frame joists, the design length was defined as centerline of the bolt holes to centerline of the bolt holes. For the bearing seat joists, the design length was defined as the span minus 4 in. (SJI 2020). The span for the flush frame joists is the design length plus the distance from the centerline of the bolt holes to the centerline of the supporting member on each end. Since this distance varied from 3 in. to 12 in. among the configurations tested, the joist spans also varied. The span at which erection bridging is required per the SJI Load Tables is also listed in Table 2. The joist spans were selected to be similar to these limiting values.

Table 3 lists weight data for the joists. The weight of each joist was measured with a crane scale. The approximate joist weight from the SJI Load Tables and measured joist weight divided by the design length are provided for reference. The chord and web members of the flush frame joists were the same as the corresponding bearing seat joist. The larger weight of the flush frame joists is due to the end plates. For the bearing seat joists, the measured joist weight divided by the design length is close to the approximate joist weight from the SJI Load Tables.

Dimensions of the chord angles for each joist are listed in Table 4 with full details of the joists presented in the Appendix. The joists were made primarily from rolled angles. All interior web members were single angles that were crimped when the leg length exceeded the chord angle separation. The end diagonals were round or square bar for bearing seat joists J11, J21, and J31 and double angles for bearing seat joist J41 and all the flush frame joists.

Each bearing seat joist was tested in only one configuration while the flush frame joists were tested in several configurations each. A test matrix outlining the connection configurations is shown in Table 5. There was a total of 15 connection configurations: 1 for the bearing seat joists, 6 for the full depth flush frame joists, and 8 for the top chord flush frame joists. The configurations for the flush frame joists vary in connection eccentricity (i.e., the distance from the centerline of the support to the centerline of the bolt holes), girder connection plate type, and

Table 1. Joists Selected for Testing

| Index | Name | Joist Designation | End Connection |
|---|---|---|---|
| 1 | J11 | 18K3 | Bearing Seat |
| 2 | J12 | 18K3 | Full Depth Flush Frame |
| 3 | J13 | 18K3 | Top Chord Flush Frame |
| 4 | J21 | 30K7 | Bearing Seat |
| 5 | J22 | 30K7 | Full Depth Flush Frame |
| 6 | J23 | 30K7 | Top Chord Flush Frame |
| 7 | J31 | 30K12 | Bearing Seat |
| 8 | J32 | 30K12 | Full Depth Flush Frame |
| 9 | J33 | 30K12 | Top Chord Flush Frame |
| 10 | J41 | 32LH08 | Bearing Seat |
| 11 | J42 | 32LH08 | Full Depth Flush Frame |
| 12 | J43 | 32LH08 | Top Chord Flush Frame |

Table 2. Joists Selected for Testing – Length Data

| Index | Name | Design Length | Centerline of holes to centerline of holes | Joist Span | Span at which erection bridging is required |
|---|---|---|---|---|---|
| 1 | J11 | 31'-8" | n/a | 32'-0" | 31' |
| 2 | J12 | 31'-8" | 31'-8" | 32'-8" to 33'-8" | 31' |
| 3 | J13 | 31'-8" | 31'-8" | 32'-2" to 33'-8" | 31' |
| 4 | J21 | 43'-8" | n/a | 44'-0" | 44' |
| 5 | J22 | 43'-8" | 43'-8" | 44'-8" to 45'-8" | 44' |
| 6 | J23 | 43'-8" | 43'-8" | 44'-2" to 45'-8" | 44' |
| 7 | J31 | 53'-8" | n/a | 54'-0" | 54' |
| 8 | J32 | 53'-8" | 53'-8" | 54'-8" to 55'-8" | 54' |
| 9 | J33 | 53'-8" | 53'-8" | 54'-2" to 55'-8" | 54' |
| 10 | J41 | 59'-8" | n/a | 60'-0" | 55' |
| 11 | J42 | 59'-8" | 59'-8" | 60'-8" to 61'-8" | 55' |
| 12 | J43 | 59'-8" | 59'-8" | 60'-2" to 61'-8" | 55' |

Table 3. Joists Selected for Testing – Weight Data

| Index | Name | Joist Weight (lbs) | Joist Weight Divided by Design Length (lbs/ft) | Approximate Joist Weight (lbs/ft) |
|---|---|---|---|---|
| 1 | J11 | 217 | 6.85 | 6.4 |
| 2 | J12 | 287 | 9.06 | 6.4 |
| 3 | J13 | 269 | 8.49 | 6.4 |
| 4 | J21 | 373 | 8.54 | 9.6 |
| 5 | J22 | 569 | 13.03 | 9.6 |
| 6 | J23 | 431 | 9.87 | 9.6 |
| 7 | J31 | 735 | 13.70 | 15 |
| 8 | J32 | 953 | 17.76 | 15 |
| 9 | J33 | 796 | 14.83 | 15 |
| 10 | J41 | 963 | 16.14 | 17 |
| 11 | J42 | 1177 | 19.73 | 17 |
| 12 | J43 | 1013 | 16.98 | 17 |

Table 4. Dimensions of Chord Angles

| | | Joist Series | | | |
|---|---|---|---|---|---|
| **Parameter** | **Units** | **J1** | **J2** | **J3** | **J4** |
| Top Chord Leg Length | in. | 1.5 | 2 | 2 | 2.5 |
| Top Chord Leg Thickness | in. | 0.155 | 0.137 | 0.250 | 0.212 |
| Bottom Chord Leg Length | in. | 1.25 | 1.5 | 2 | 2.5 |
| Bottom Chord Leg Thickness | in. | 0.133 | 0.155 | 0.216 | 0.212 |
| Angle Separation | in. | 1 | 1 | 1 | 1 |

Table 5. Test Matrix (Connection Configurations)

| Index | Name | Connection Eccentricity, *a* (in.) | Joist Connection | Joist Connection Plate | Girder Connection Plate Type | Girder Connection Plate Thickness (in.) |
|---|---|---|---|---|---|---|
| 1 | JX1 | n/a | Bearing Seat | n/a | n/a | n/a |
| 2 | JX2a | 6 | Flush Frame | Full Depth | Tab | 1/4 |
| 3 | JX2b | 9 | Flush Frame | Full Depth | Tab | 1/2 |
| 4 | JX2c | 12 | Flush Frame | Full Depth | Tab | 1/2 |
| 5 | JX2d | 6 | Flush Frame | Full Depth | Full Depth | 1/4 |
| 6 | JX2e | 9 | Flush Frame | Full Depth | Full Depth | 1/2 |
| 7 | JX2f | 12 | Flush Frame | Full Depth | Full Depth | 1/2 |
| 8 | JX3a | 3 | Flush Frame | Top Chord | Tab | 1/4 |
| 9 | JX3b | 6 | Flush Frame | Top Chord | Tab | 1/4 |
| 10 | JX3c | 9 | Flush Frame | Top Chord | Tab | 1/2 |
| 11 | JX3d | 12 | Flush Frame | Top Chord | Tab | 1/2 |
| 12 | JX3e | 3 | Flush Frame | Top Chord | Full Depth | 1/4 |
| 13 | JX3f | 6 | Flush Frame | Top Chord | Full Depth | 1/4 |
| 14 | JX3g | 9 | Flush Frame | Top Chord | Full Depth | 1/2 |
| 15 | JX3h | 12 | Flush Frame | Top Chord | Full Depth | 1/2 |

girder connection plate thickness. The girder connection plate was either a tab plate that was only welded to the girder web or a full depth plate that was welded to the girder web and flanges. The two types are shown in Figure 5. The girder connection plate thickness was 1/4 in. for connection eccentricities of 3 and 6 in. and 1/2 in. for connection eccentricities of 9 and 12 in. Joists with the full depth flush frame configuration could not be tested with 3 in. connection eccentricity because the joist depth exceeded the flange clearance of the girder.

Guidance from SJI on the design of flush frame connections suggests using 1) 1 in. diameter bolts, 2) a minimum of three bolts, 3) a single vertical row of bolts, 4) 1 in. thick joist end plates, and 5) short slots in either the shear tab or joist end plate. The flush frame joists fabricated for this project had 1 in. thick connection plates to match the spacing between the chord members. The connections were made with (3) 1 in. diameter bolts at each end according to SJI recommended practice. These bolts are larger than necessary for strength, even if the joists were loaded to their allowable strength. The size of the bolts is recommended to allow the holes in the joist connection plate to be punched. For the experiments, standard holes were used in the joist connection plates and girder connection plates. Slotted holes were not needed since the column assembly had sufficient adjustability to construct the specimens and the applied loads were relatively low resulting in small end rotations that could be accommodated by standard holes. The bolts were tightened with a wrench to a snug-tight condition.

The fifteen connection configurations listed in Table 5 were tested with each of the four joist designations resulting in 60 total configurations. The names of the configurations are denoted in the designation column of Table 5 but with the "X" replaced by a number corresponding to the joist designation. For example, configuration J11 was an 18K3 bearing seat joist, designation J12a was an 18K3 full depth flush frame joist, and designation J13a was an 18K3 top chord flush frame joist. Joist designations ending in "2a" through "2c" are connected to a girder tab plate, joist designation ending in "2d" through "2f" are connected to a full depth girder plate. Joist designations ending in "3a" through "3d" are connected to a girder tab plate, joist designations ending in "3e" through "3h" are connected to a full depth girder plate.

Several configurations were tested with only one or two of the three bolts installed at each end of the joist. Specifically, configurations J32b, J32e, J33d, J33h, J42a, J42d, J43a, and J43e had one additional set of tests with only two bolts at either end of the joist and configuration J13a had two additional sets of tests with either one or two bolts at either end of the joist.

The components of the experiment consist of a column assembly, a girder assembly, and safety catches as shown in Figure 6. The column assembly was secured to the lab's strong floor at either end of the joist and supported the girder assembly. The girder assemblies supported the joist. Each girder assembly was designed to have two configurations, a shear tab connection plate on one side and a full depth shear connection plate on the other side as shown in Figure 7. Four girder assembly pairs, varying in connection plate thickness and eccentricity, were fabricated for the project. Two safety catches were secured to the strong floor near midspan to keep the joist from deflecting too far or causing permanent deformation in the joist.

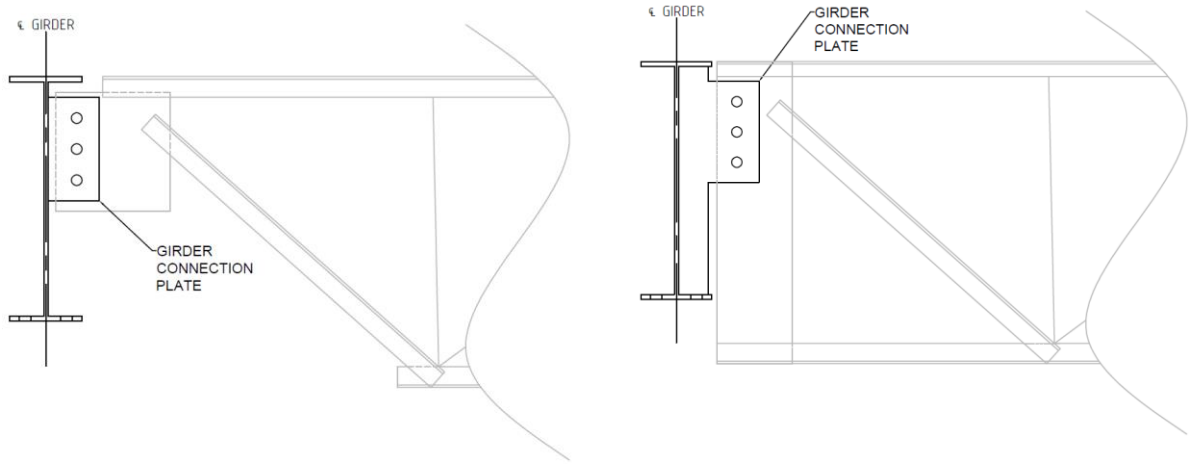


(a) Top Chord Flush Frame Connection with Tab Girder Plate

(b) Full Depth Flush Frame Connection with Full Depth Girder Plate

Figure 5. End Connection Plates

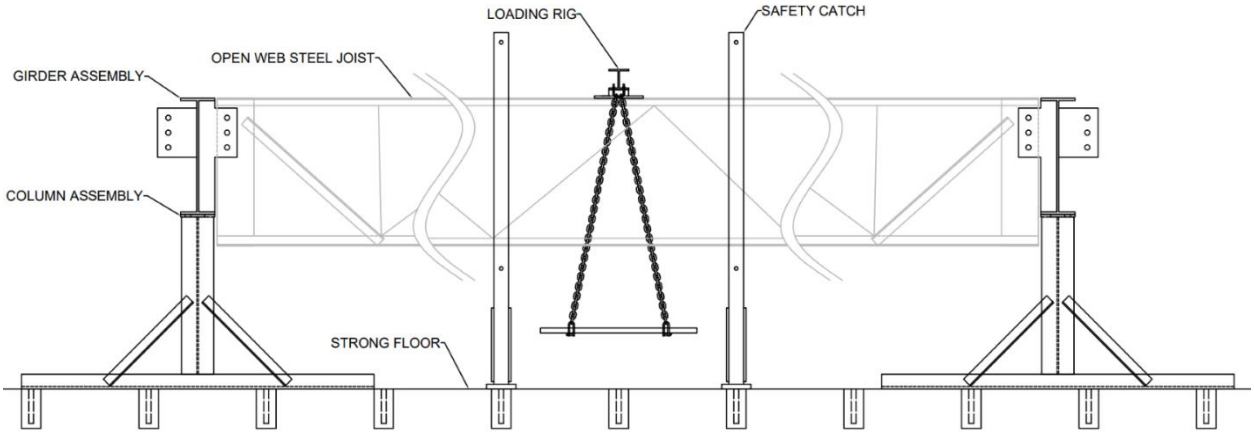


Figure 6. In-Plane Bending Experiment Set-up

Out-of-plane deflection of the top chord and the bottom chord of the joists was measured using string potentiometers. The string potentiometers were oriented horizontally perpendicular to the joist. A small hole was drilled to the outstanding leg edge of each chord and the strings of the potentiometers were secured to the outstanding legs with metal S-hooks. The string potentiometer on the bottom chord was located at midspan. The string potentiometer on the top chord was located 4 in. from midspan to avoid the knife edge plate and load rig set up at midspan.

For consistency, the flush-frame joists were installed such that the direction of the out-of-straightness was towards the girder-side connection plates as shown in Figure 8. Joist out-of-straightness was measured once the joist was installed but before any tests were conducted. A string was pulled above the middle of the top chord at each end. The out-of-straightness was measured at midspan with a measuring tape to the nearest $1/16^{th}$ of an inch.

## Out-of-Plane Bending Tests

Out-of-plane bending tests were performed on each joist configuration to measure lateral stiffness. Two tests were performed, one subjecting the joist to a transverse lateral load at the top chord and another subjecting the joist to a transverse lateral load at the bottom chord. Figure 9 shows how load was applied. A scissor jack created tension in a rope with a hook that connected to the joist at midspan. A load cell was installed in-line with the rope to record the tension load on the joist chord. Data was collected at a frequency of 10 Hz throughout the duration of each test. The test was stopped after approximately 4 in. of deflection was achieved.

A line was fit to the data recorded between 20 percent of the maximum load and 80 percent of the maximum load. The slope of the best fit line was taken as the stiffness. Example measurements for joist J21 are shown in Figure 10 along with a dashed line indicating the line of best fit.

## In-Plane Bending Tests

In-plane bending tests were performed to subject the joists to downward vertical load to measure the lateral-torsional buckling strength of the joists. Roughly 50 steel angles were weighed on a scale and their weights were written on their surfaces. The steel angle loads were applied by hand to the loading rig. After the placement of each steel angle the string potentiometer measurements and the weight written on the angle were recorded on paper.

The test was stopped after approximately $L/100$ deflection out-of-plane was achieved at midspan, where $L$ is the design length.

The loading rig was placed at midspan and included a grate to support the steel angle loads under the joist, chains to transfer the load to a spreader beam, and a knife edge support to ensure that the load was vertical. The knife edge angle was welded to the bottom of the spreader beam and the knife edge seat plate was bolted to the top chord of the joist. Figure 11 shows how the load was applied 1/2 in. above the top of the top chord. The loading rig and other experiment features are shown in Figure 12.

(a) Shear Tab Connection Plate (b) Full Depth Shear Connection Plate

Figure 7. Girder Assemblies (1/2 in. Plate with 12 in. Eccentricity Shown)


(a) Joist placement used for experiments (b) Joist placement avoided for experiments

Figure 8. Plan View of Joist Installation with Respect to Out-of-Straightness


Figure 9. Out-of-Plane Bending Experiment Set-up

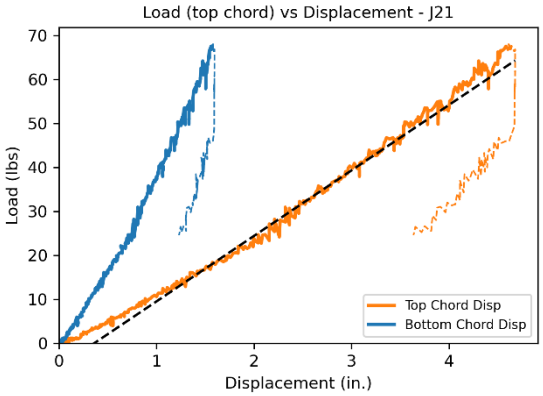


(a) Loading at Top Chord

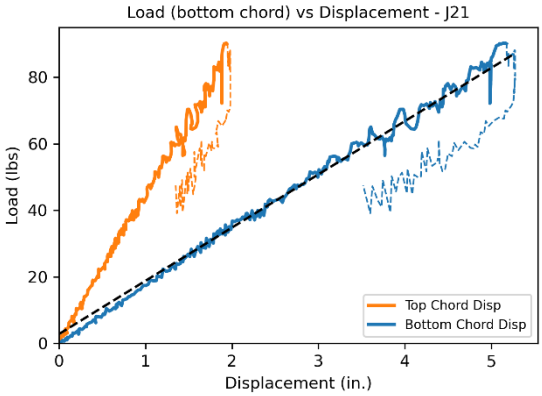


(b) Loading at Bottom Chord

Figure 10. Example Stiffness Results for Joist J21

The load and displacement data were used to compute two separate critical loads: one based on a deflection limit and another using the Southwell plot method.

The deflection limit load was defined as the load at which the out-of-plane deflection at midspan, $L/120$ occurs, where $L$ is the design length. The $L/120$ limit was used in previous studies and is related to the comfort of a person traversing an unbraced joist to the midspan (Ziemian et al. 2004). The critical load based on deflection is the point at which the top chord displacement intersects the deflection limit of $L/120$ as shown in Figure 13.

The Southwell plot method was used to quantify the critical buckling load. The plot has deflection on the $y$ axis and deflection divided by applied load on the $x$ axis as shown in Figure 14. A straight line was fit to the data with deflection greater than 25% of the maximum recorded deflection. The 25% limit was chosen to exclude the nonlinear toe region that occurred early in the dataset of the joist experiments. The slope of the line is the Southwell critical buckling load. The Southwell plot method was originally developed for buckling of columns but is also satisfactory for beams that undergo lateral-torsional buckling (Mandal and Calladine 2002). The Southwell plot method has also been used to obtain an experimental estimate of the theoretical elastic buckling strength for structural steel beams undergoing elastic lateral-torsional buckling (Slein et al. 2020).

## Results

The joists exhibited typical lateral-torsional buckling behavior in the in-plane bending experiments as shown in Figure 15. At low loads the change in deflection was small as each angle weight was placed on the loading rig. The change in deflection with each angle weight increased with increasing load. Much of the observed deflection occurred with the addition of the last few angle weights. The lateral movement of the top chord was greater than that of the bottom chord resulting in twist of the joist. Deflection was not measured at the ends of the joists, however, based on visual observations, twist at the ends of the joists appeared to be fully restrained and out-of-plane rotation at the ends appeared to be partially restrained.

Results for each of the joist and connection configurations are listed in Table 6. Data for each configuration includes the Southwell buckling load and load at deflection limit from the in-plane bending test; top and bottom chord stiffnesses from the out-of-plane bending tests; and the measured out-of-straightness.

## Strength

In all cases, the Southwell buckling load is greater than the load at the deflection limit. The magnitude of the deflection for a given applied load depends on the out-of-straightness. A more out-of-straight joist will reach the deflection limit at a lower load. The Southwell buckling load, in effect, corrects for differences in out-of-straightness by extrapolating to the point of infinite deflection. Accordingly, the difference between the Southwell buckling load and the deflection limit load depends on the out-of-straightness as shown in Figure 16.

Figure 11. Knife Edge for In-Plane Bending Experiments

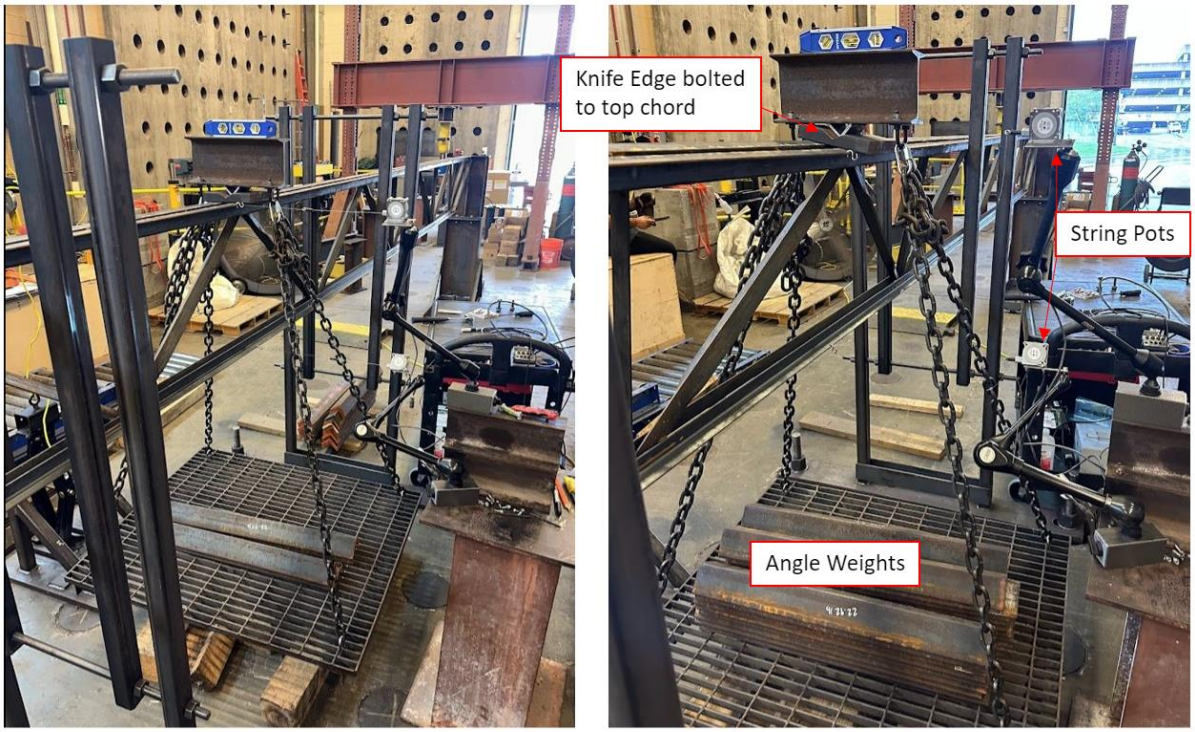


Figure 12. In-Plane Bending Experiment Set-up

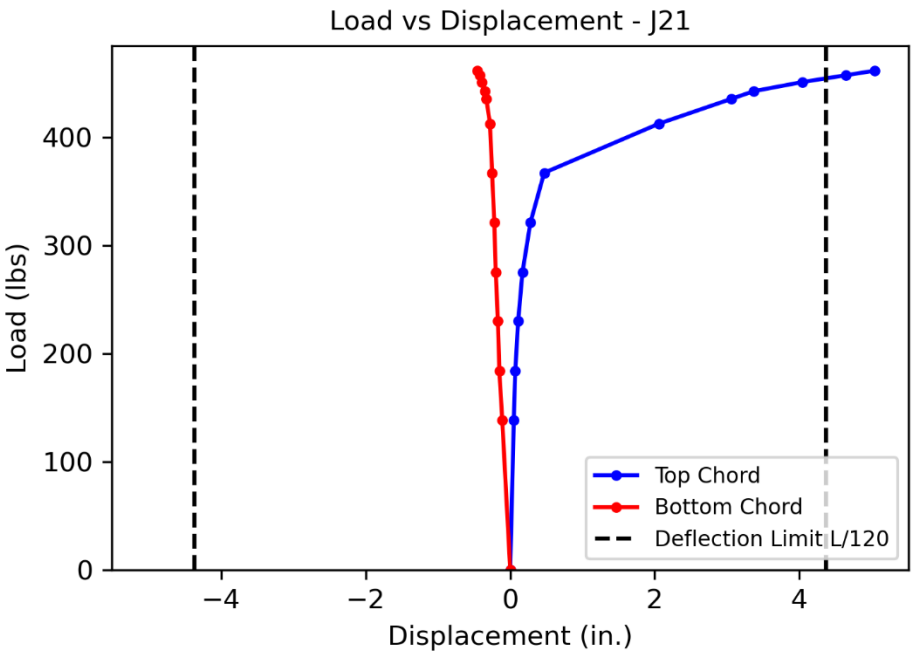


Figure 13. Deflection Limit Critical Load Example

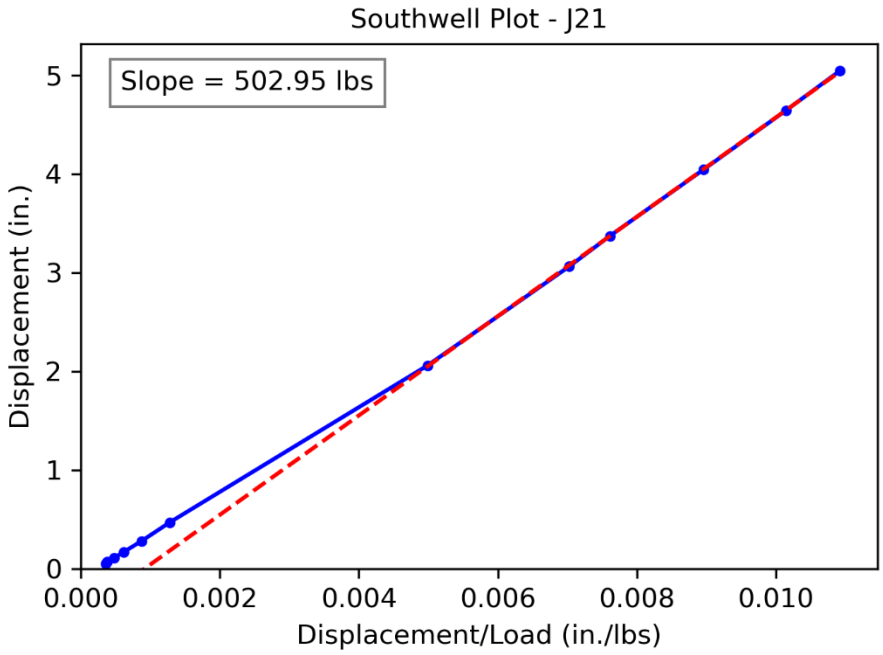


Figure 14. Southwell Critical Buckling Load Example

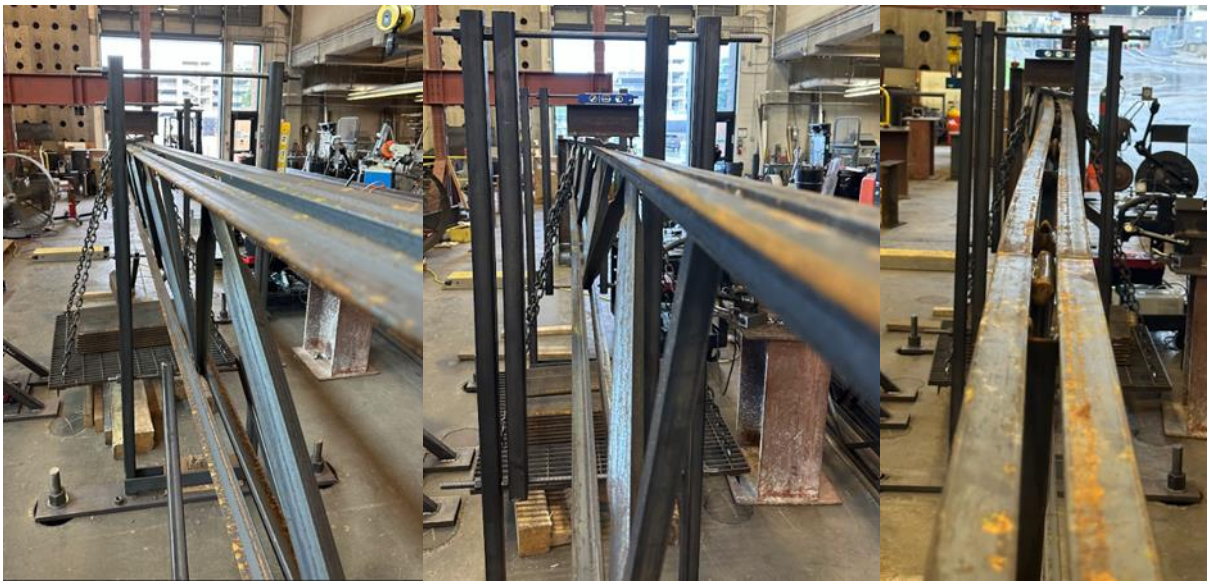

Figure 15. Photos of Deflected Joists

Table 6. Experimental Results

| Specimen | Southwell Buckling Load (lbs) | Load at Deflection Limit (lbs) | Top Chord Stiffness (lbs/in.) | Bottom Chord Stiffness (lbs/in.) | Out-of-straightness (in.) |
|---|---|---|---|---|---|
| J11 | 709 | 632 | 24.7 | 30.5 | 1/8 |
| J12a | 861 | 754 | 27.0 | 30.9 | 1/2 |
| J12b | 801 | 695 | 56.1 | 59.0 | 1/2 |
| J12c | 928 | 833 | 46.1 | 68.1 | 1/2 |
| J12d | 801 | 719 | 27.5 | 28.4 | 3/8 |
| J12e | 874 | 722 | 31.7 | 30.7 | 1/2 |
| J12f | 878 | 770 | 33.2 | 26.2 | 9/16 |
| J13a | 882 | 785 | 22.9 | 26.3 | 5/8 |
| J13b | 721 | 642 | 25.3 | 26.8 | 1/4 |
| J13c | 836 | 666 | 22.5 | 22.9 | 5/8 |
| J13d | 866 | 798 | 55.8 | 61.2 | 1/4 |
| J13e | 994 | 734 | 58.6 | 43.2 | 1 |
| J13f | 849 | 775 | 36.9 | 28.8 | 1/2 |
| J13g | 865 | 789 | 32.5 | 26.9 | 1/4 |
| J13h | 882 | 762 | 36.2 | 35.2 | 1/2 |
| J21 | 506 | 455 | 14.9 | 16.0 | 1/4 |
| J22a | 917 | 720 | 17.9 | 20.9 | 9/16 |
| J22b | 924 | 692 | 15.7 | 24.7 | 7/16 |
| J22c | 908 | 748 | 21.1 | 25.0 | 5/8 |
| J22d | 996 | 766 | 16.9 | 20.6 | 11/16 |
| J22e | 948 | 740 | 21.1 | 28.0 | 3/8 |
| J22f | 947 | 738 | 18.7 | 27.2 | 1/2 |
| J23a | 913 | 830 | 19.8 | 16.3 | 1/8 |
| J23b | 877 | 790 | 15.4 | 19.5 | 3/16 |
| J23c | 886 | 780 | 18.4 | 14.2 | 1/4 |
| J23d | 922 | 750 | 23.8 | 22.3 | 1/8 |
| J23e | 998 | 793 | 21.1 | 18.8 | 9/16 |
| J23f | 890 | 776 | 36.9 | 19.8 | 1/4 |
| J23g | 930 | 846 | 32.5 | 18.5 | 1/8 |
| J23h | 933 | 819 | 36.2 | 23.1 | 1/8 |

Table 6. Experimental Results (continued)

| Specimen | Southwell Buckling Load (lbs) | Load at Deflection Limit (lbs) | Top Chord Stiffness (lbs/in.) | Bottom Chord Stiffness (lbs/in.) | Out-of-straightness (in.) |
|---|---|---|---|---|---|
| J31 | 469 | 354 | 12.6 | 5.6 | 7/16 |
| J32a | 720 | 544 | 12.9 | 25.7 | 3/4 |
| J32b | 964 | 623 | 27.6 | 51.2 | 1 3/4 |
| J32c | 761 | 626 | 12.8 | 46.8 | 1/2 |
| J32d | 785 | 596 | 12.9 | 27.3 | 7/8 |
| J32e | 832 | 627 | 17.4 | 34.9 | 7/8 |
| J32f | 823 | 589 | 29.3 | 46.7 | 1 |
| J33a | 804 | 658 | 16.4 | 29.2 | 1/4 |
| J33b | 846 | 661 | 14.7 | 26.1 | 1/4 |
| J33c | 845 | 680 | 14.7 | 16.5 | 1 |
| J33d | 774 | 654 | 18.8 | 27.1 | 1/4 |
| J33e | 875 | 723 | 15.4 | 24.7 | 1 |
| J33f | 763 | 636 | 14.5 | 23.0 | 7/16 |
| J33g | 847 | 700 | 16.1 | 23.1 | 1 |
| J33h | 794 | 711 | 17.5 | 27.6 | 1/2 |
| J41 | 735 | 493 | 15.5 | 26.3 | 2 1/4 |
| J42a | 918 | 507 | 17.5 | 30.0 | 2 3/8 |
| J42b | 950 | 535 | 12.0 | 30.5 | 2 1/4 |
| J42c | 881 | 477 | 17.4 | 27.6 | 2 3/4 |
| J42d | 895 | 531 | 14.1 | 18.1 | 2 |
| J42e | 934 | 571 | 14.9 | 27.9 | 2 3/8 |
| J42f | 831 | 480 | 13.8 | 27.0 | 2 1/4 |
| J43a | 840 | 588 | 11.7 | 19.1 | 1 1/2 |
| J43b | 670 | 488 | 15.3 | 24.7 | 1 1/2 |
| J43c | 752 | 571 | 14.8 | 36.5 | 1 1/2 |
| J43d | 720 | 545 | 24.5 | 51.7 | 1 1/4 |
| J43e | 852 | 680 | 12.9 | 28.5 | 7/8 |
| J43f | 717 | 573 | 11.5 | 24.9 | 1 3/8 |
| J43g | 757 | 617 | 17.2 | 39.9 | 1 1/4 |
| J43h | 700 | 589 | 18.1 | 47.7 | 1 1/8 |

Figure 17 and Figure 18 show the buckling loads for flush frame joists with a tab girder-side connection plate normalized by the buckling loads for the same joist designation but with a bearing seat connection. The average normalized loads for the J1, J2, J3, and J4 series joist configurations are 1.19, 1.80, 1.74, and 1.11, respectively, for the Southwell buckling load; and 1.17, 1.67, 1.80, and 1.08, respectively, for the deflection limit load. In a few cases (i.e., J42c, J43b, and J43d), the normalized strength is less than 1.0, indicating that the joist with a flush frame connection buckled at a lower load than the joist with a bearing seat connection. However, on average, the joists with flush frame connections buckled at higher loads than those with bearing seat connections, with the most significant difference observed for the J2 and J3 series joists.

Figure 19 and Figure 20 show the buckling loads for flush frame joists with a full-depth girder-side connection plate, again normalized by the buckling loads for the same joist designation but with a bearing seat connection. The average normalized loads for the J1, J2, J3, and J4 series joist configurations are 1.24, 1.89, 1.74, and 1.10, respectively, for the Southwell buckling load; and 1.19, 1.72, 1.85, and 1.17, respectively, for the deflection limit load. Like before, in a few cases (i.e., J42f, J43f, and J43h), the normalized strength is less than 1.0, indicating that the joist with a flush frame connection buckled at a lower load than the joist with a bearing seat connection. However, on average, the joists with flush frame connections again exhibited higher buckling loads than those with bearing seat connections, with the most significant difference observed for the J2 and J3 series joists.

Buckling loads for the joists with a full-depth girder-side connection plate were somewhat greater than those with a tab girder-side connection plate. Comparing average normalized loads, an increase of +0.05, +0.09, +0.00, and +0.01 was observed for J1, J2, J3, and J4 series joists, respectively, for the Southwell buckling loads and an increase of +0.02, +0.05, +0.05, and +0.09 was observed for J1, J2, J3, and J4 series joists, respectively, for the deflections limit loads.

Figure 21 and Figure 22 show the buckling loads for top chord flush frame joists normalized by the buckling loads for the same joist designation but with a bearing seat connection. The average normalized loads for the J1, J2, J3, and J4 series joist configurations are 1.22, 1.83, 1.74, and 1.02, respectively for the Southwell buckling load; and 1.18, 1.76, 1.92, and 1.18, respectively for the deflection limit load. In a few cases (i.e., J43b, J43d, J43f, and J43g), the normalized strength is less than 1.0, indicating that the joist with a flush frame connection buckled at a lower load than the joist with a bearing seat connection. However, on average, the joists with flush frame connections buckled at higher loads than those with bearing seat connections, with the most significant difference observed for the J2 and J3 series joists.

Figure 23 and Figure 24 show the buckling loads for full depth flush frame joists, again normalized by the buckling loads for the same joist designation but with a bearing seat connection. The average normalized loads for the J1, J2, J3, and J4 series joist configurations are 1.21, 1.87, 1.73, and 1.23, respectively for the Southwell buckling load; and 1.18, 1.61, 1.70, and 1.05, respectively for the deflection limit load. Like before, in a few cases (i.e., J42c and J42f), the normalized strength is less than 1.0, indicating that the joist with a flush frame connection

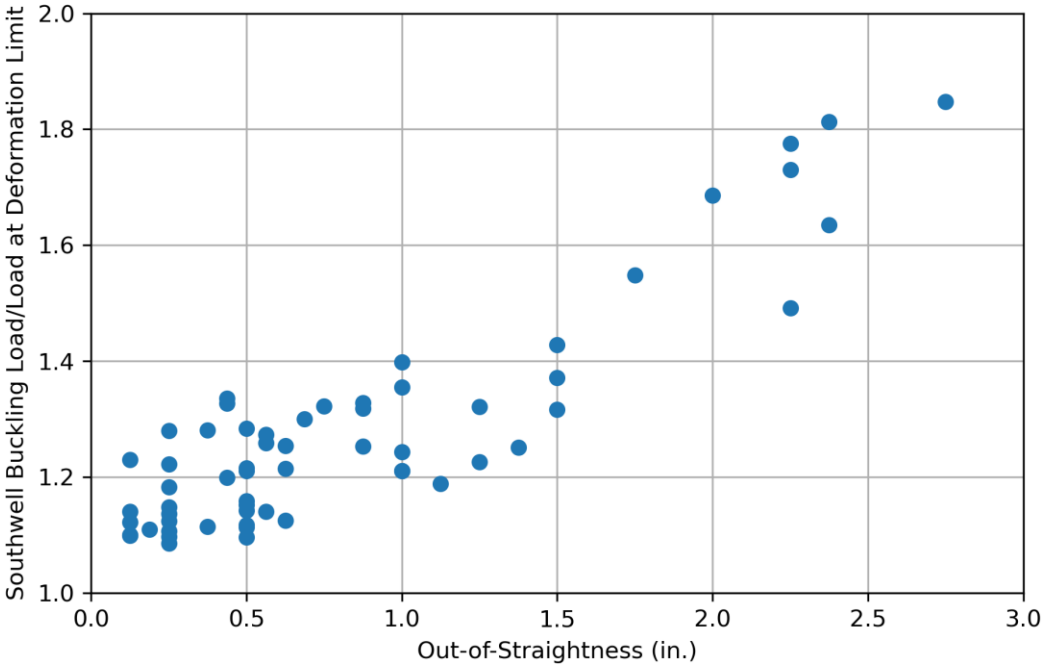


Figure 16. Impact of Out-of-Straightness on Southwell Buckling Loads

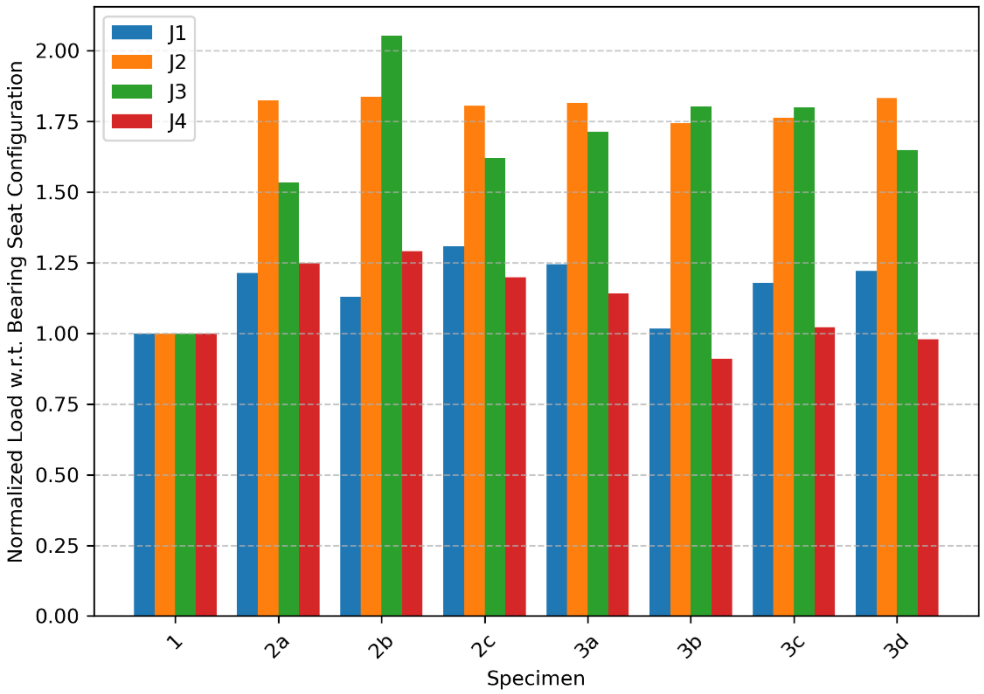


Figure 17. Joists with Tab Girder-Side Connection Plate – Southwell Buckling Load

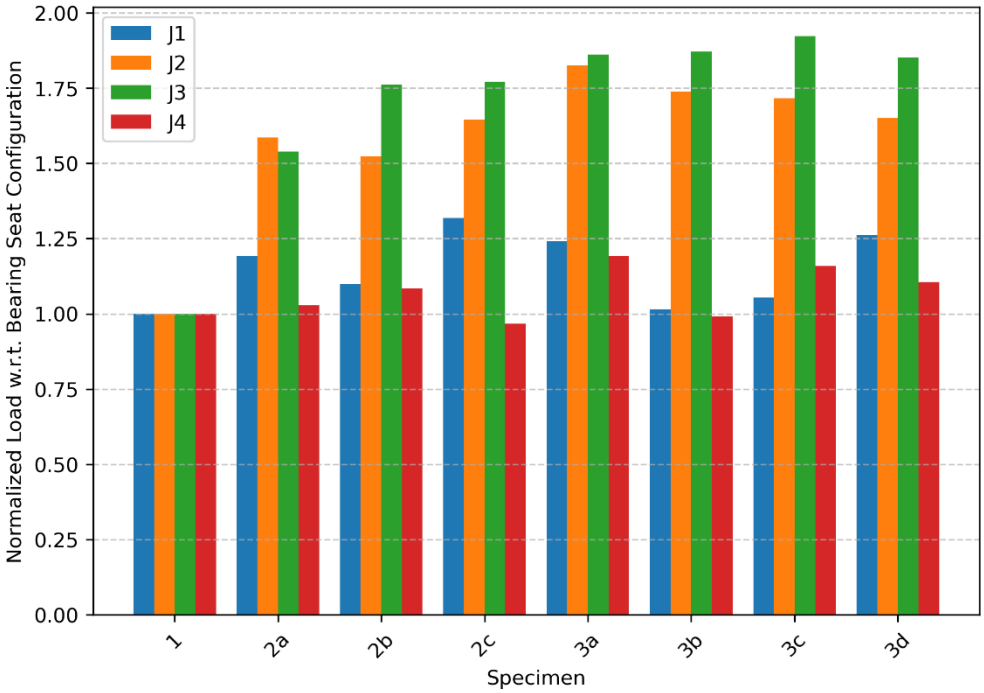


Figure 18. Joists with Tab Girder-Side Connection Plate – Deflection Limit Load

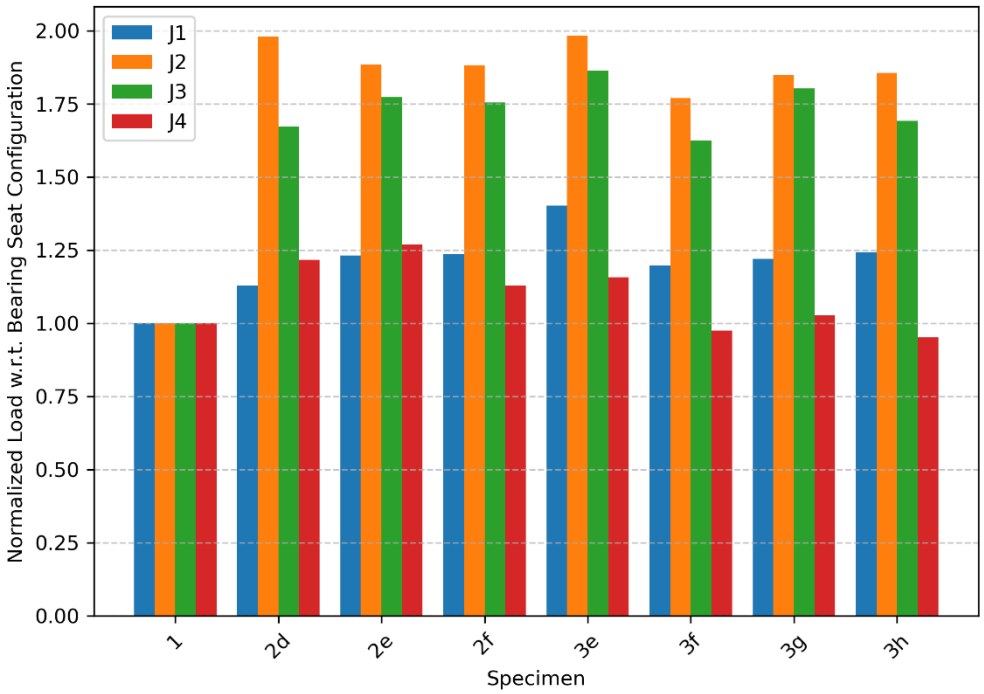


Figure 19. Joists with Full Depth Girder-Side Connection Plate – Southwell Buckling

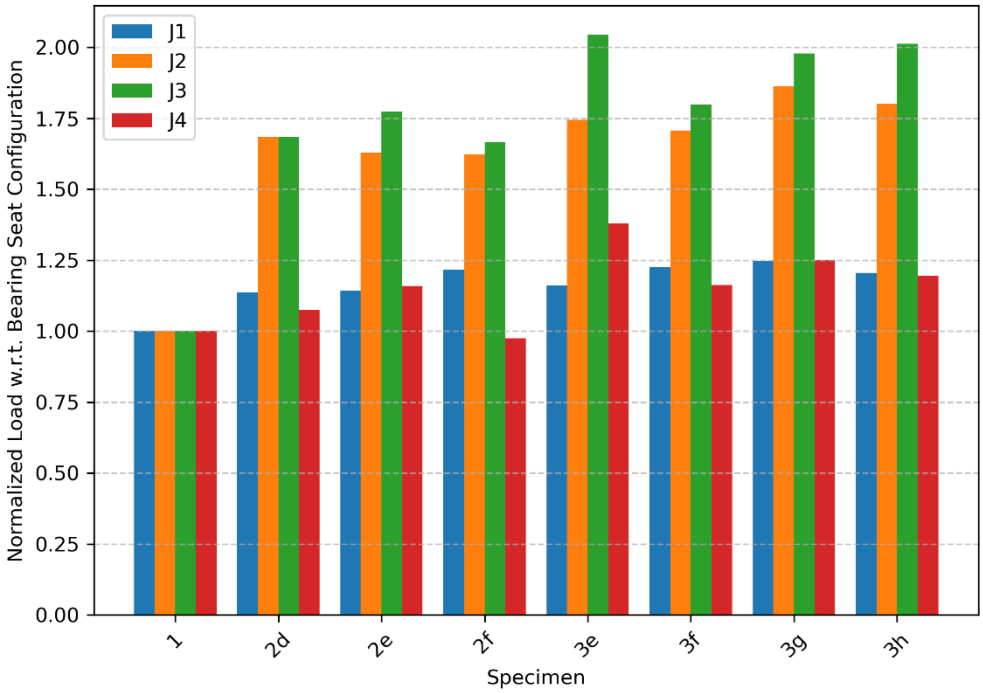


Figure 20. Joists with Full Depth Girder-Side Connection Plate – Deflection Limit

buckled at a lower load than the joist with a bearing seat connection. However, on average, the joists with flush frame connections again exhibited higher buckling loads than those with bearing seat connections, with the most significant difference observed for the J2 and J3 series joists.

No clear trend was observed in the differences between buckling loads for the top chord flush frame joists and the full-depth flush frame joists. Comparing average normalized Southwell buckling loads, the full-depth flush frame joists were as strong or stronger than the top chord flush frame joists with a difference of -0.01, +0.04, -0.01, and +0.21 for J1, J2, J3, and J4 series joists, respectively. Comparing average normalized deflection limit loads, the tab flush frame joists were as strong or stronger than the full-depth flush frame joists with a difference of 0.00, -0.15, -0.18, and -0.13 for J1, J2, J3, and J4 series joists, respectively.

Figure 25 and Figure 26 show how the critical loads vary with connection eccentricity. Note, however, that the girder-side connection plate thickness also varied with connection eccentricity. The plate was 1/4 in. thick for eccentricities of 3 and 6 in. and 1/2 in. thick for eccentricities of 9 and 12 in. (Table 5). In general, the critical load decreases from 3 in. to 6 in., increases from 6 in. to 9 in., and decreases from 9 in. to 12 in. The critical load at 6 in. eccentricity was lower than that for 3 in. eccentricity for most joists. This difference could have been caused by a reduced connection stiffness with the higher eccentricity. The critical load at 9 in. eccentricity was greater than that for 6 in. eccentricity for most joists. The girder-side connection plate was thicker for the connections with 9 in. eccentricity, leading to an apparent increase in stiffness despite the greater eccentricity. The critical load at 12 in. eccentricity was lower than that for 9 in. eccentricity for most joists, continuing the observed trend of decreasing stiffness with increasing eccentricity for a given plate thickness.

## Comparison to Minkoff Equation

Equation 11a was used to compute the critical load given a distributed load equal to the self-weight, taken as the joist weight divided by the design length from Table 3 for the bearing seat joist of each designation. The joist weight divided by the design length was higher for the joists with flush frame connections due to the connection plates at the ends. Extra weight at the ends has minimal impact on buckling behavior. The vertical location of the point load with respect to the shear center, $a_e$, was computed as

$$a_e = y_t + y + y_o + 0.5 \text{ in.} \quad (12)$$

where

$y_t$ = distance from the top of the top chord to the centroid of the top chord
$y$ = distance from the centroid of the top chord to the centroid of the cross section
$y_o$ = distance from the centroid of the cross section to the shear center
0.5 in. = depth of knife edge plate

The cross-sectional properties and other parameters used in the Minkoff equation are listed in

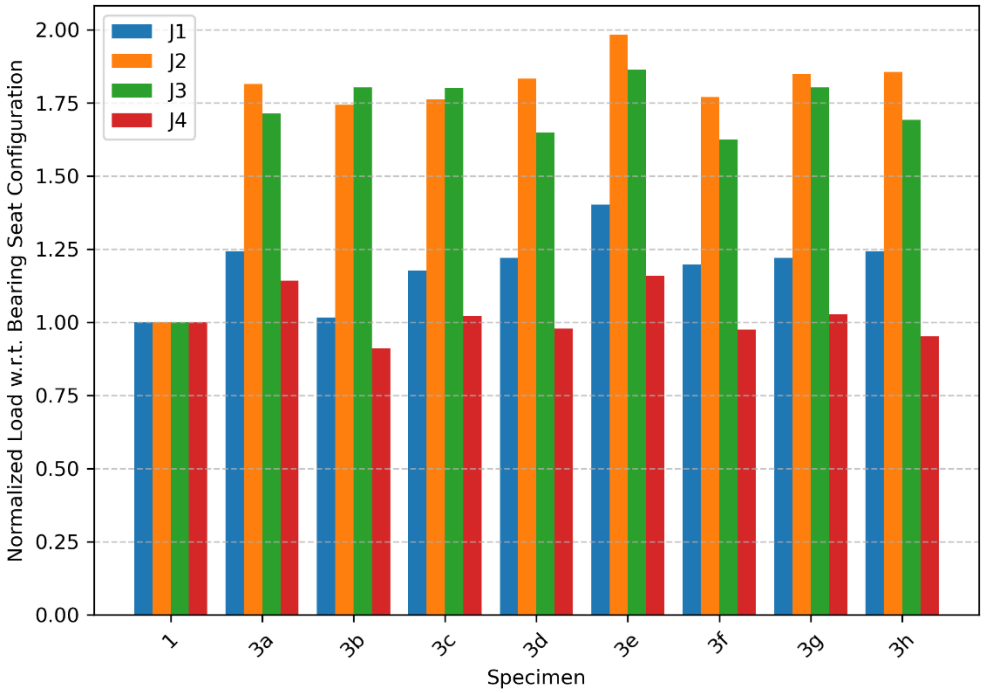


Figure 21. Top Chord Flush Frame Joists – Southwell Buckling

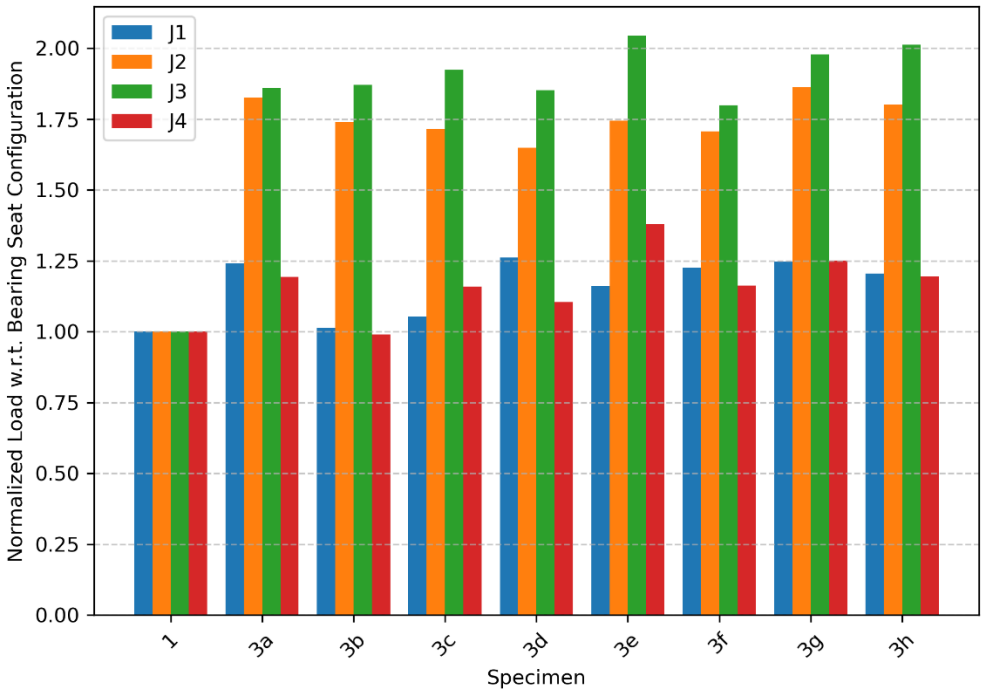


Figure 22. Top Chord Flush Frame Joists – Deflection Limit

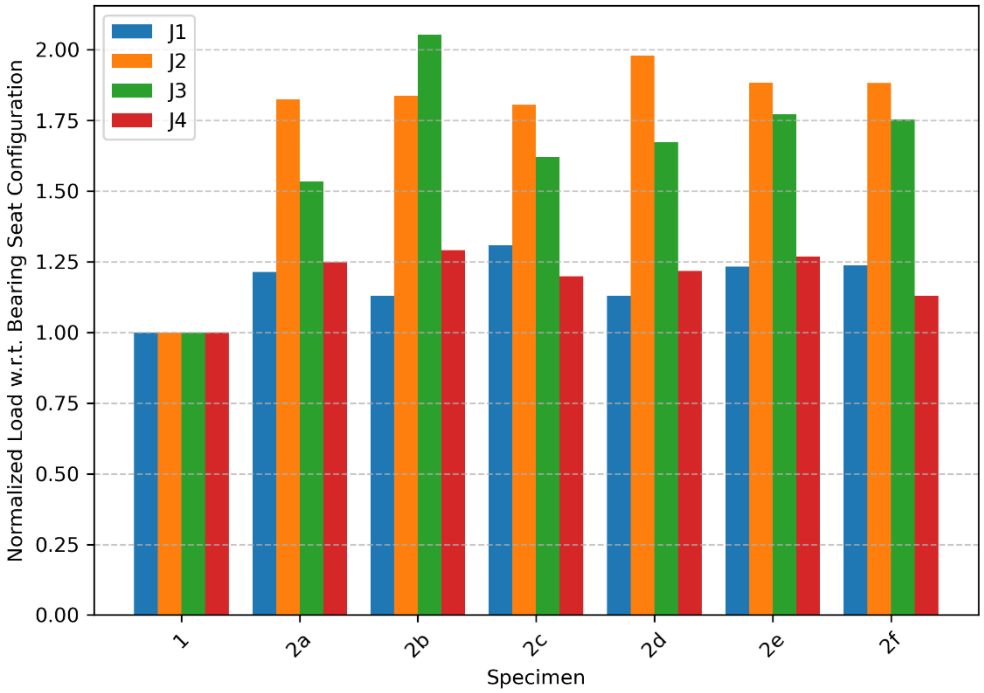


Figure 23. Full Depth Flush Frame Joists – Southwell Buckling

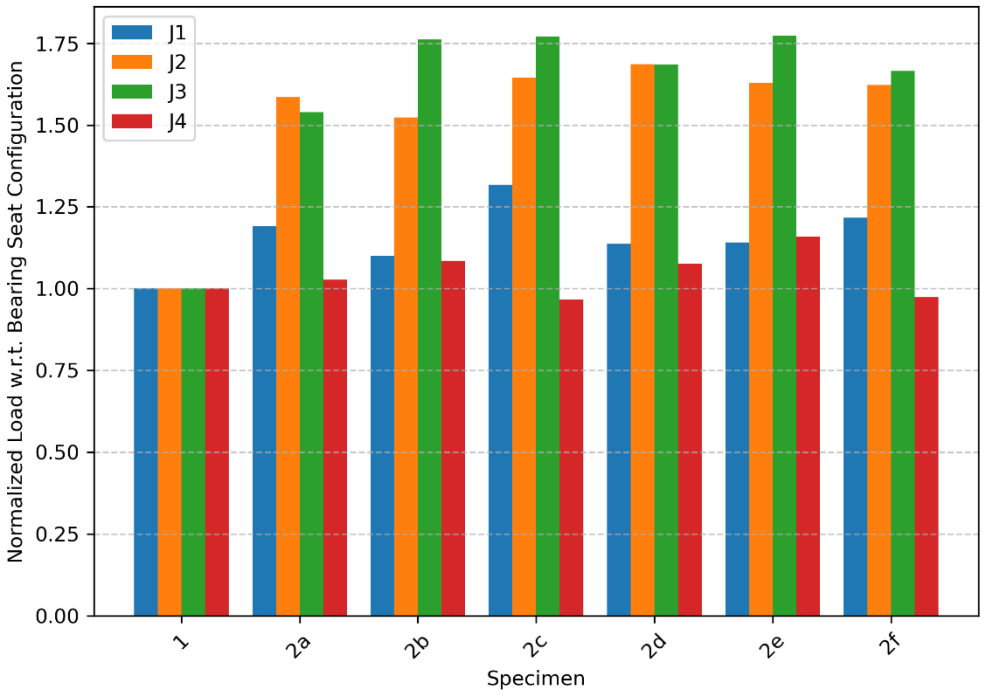


Figure 24. Full Depth Flush Frame Joists – Deflection Limit

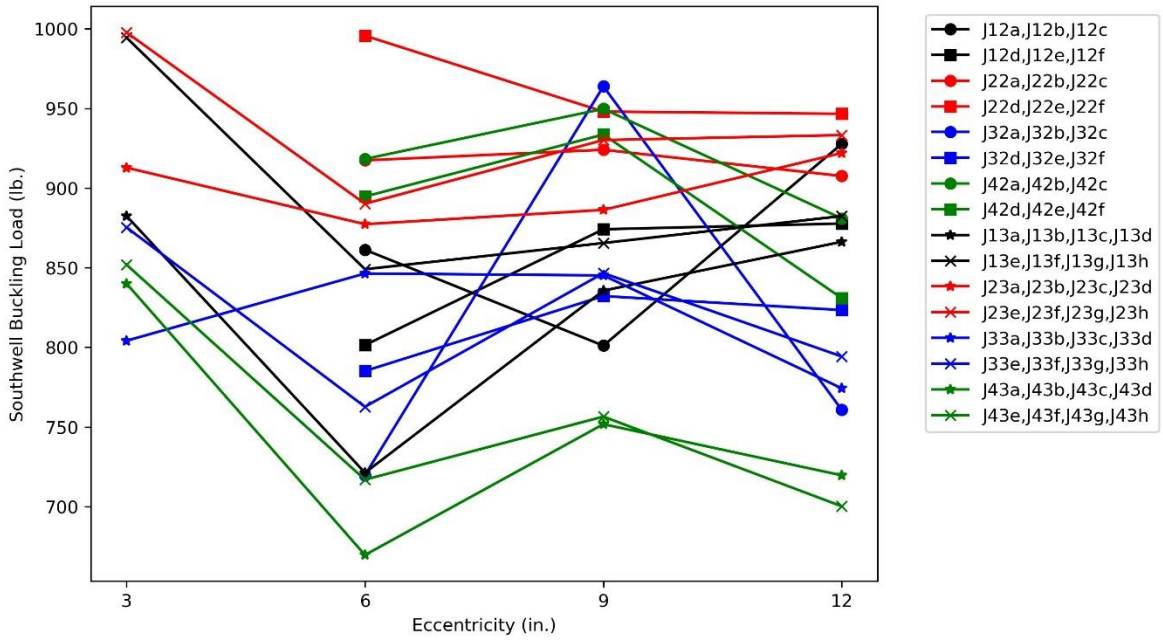


Figure 25. Influence of Eccentricity to Southwell Buckling Load

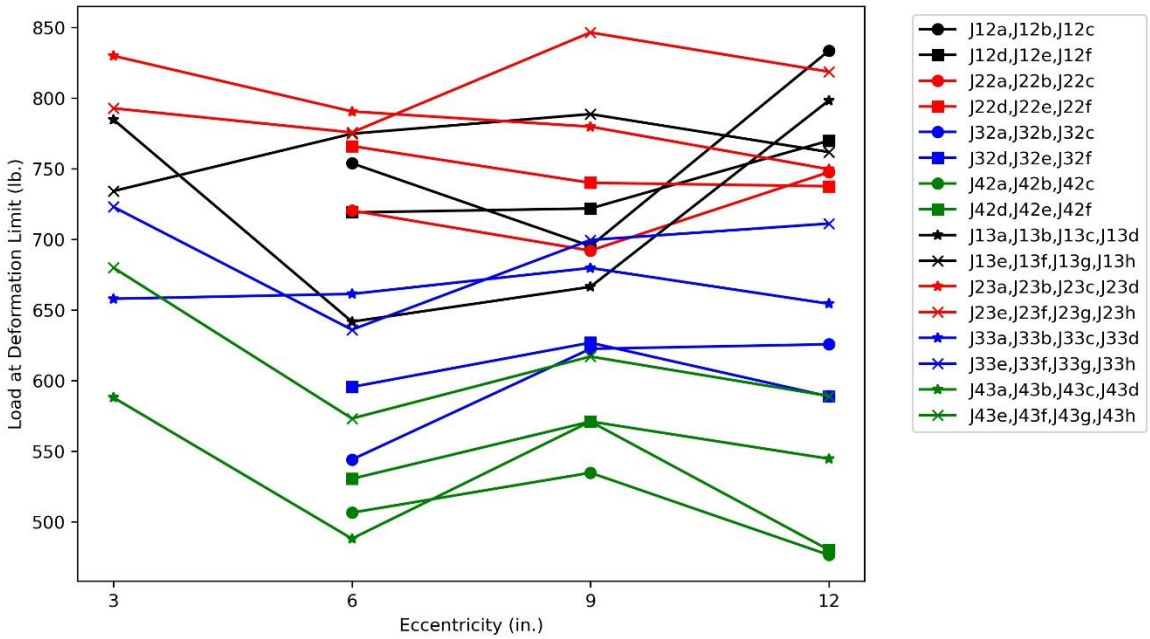


Figure 26. Influence of Eccentricity to Load at Deflection Limit

For the flush frame joists, the back-calculated effective length factor ranges from 0.641 for the Southwell buckling load for J23e to 0.784 for the deflection limit load for J42c. Average values for the effective length factor range from 0.687 to 0.771 for the deflection limit load and from 0.654 to 0.705 for the Southwell buckling load. Based on these results, a value of $k = 0.75$ appears to be appropriate for design of the erection bridging for flush frame joists. Note, however, that the critical load was shown to vary with connection eccentricity and girder connection plate thickness. These values of $k$ should not be used for thinner plates or larger eccentricities than those tested in this study where the flexibility of the connection could be greater and the critical buckling load lower.

The back-calculated effective length factor results also help shed light on the strength results. The increase in strength for a flush frame joist in comparison to a bearing seat joist was less for the J1 and J4 series joists than it was for the J2 and J3 series joists. The effective length factors for the flush frame joists are relatively consistent. The effective length factors for the bearing seat joists are less consistent. Based on the Southwell buckling load, $k = 0.723$ and 0.709 for joists J11 and J41, respectively; and $k = 0.786$ and 0.807 for joists J21 and J31, respectively. These results indicate that the reason that there was less difference in strength between the bearing seat joists and the flush frame joist for the J1 and J4 series joists is because the bearing seat joists were relatively strong and not because the flush frame joists were relatively weak. Table 7. Cross-sectional properties of the chords were computed using the dimensions listed in Table 4 and assuming the angles had the shape of two rectangles, neglecting corner radii.

Table 8 lists the calculated critical load, $P$, from the Minkoff equation (Equation 11a) for each series of joists and different values of effective length factor, $k$. The critical loads with $k = 1.00$, i.e., the value from the original derivation by Minkoff (1975), are less than the experimentally obtained strengths across all joists and connection configurations. The critical loads with $k = 0.85$, i.e., the value specified in the SJI *Specifications* (2020), are less than the experimentally obtained strengths for all joists and connection configurations except the deflection limit load for J31, a joist with a bearing seat connection.

The value of the effective length factor that results in the Minkoff equation giving the same critical load as from the experiment was back-calculated using an iterative approach and is listed for each configuration and both definitions of experimental critical load in Table 9.

The buckling loads of the bearing seat joists are generally lower than those for the flush frame joists, thus their back-calculated effective length factor is higher. Only for the deflection limit load for J31 is the effective length factor greater than 0.85, the value listed in the SJI *Specifications* (2020). The back-calculated effective length factor for J31 is 0.861 for the deflection limit load and 0.807 for the Southwell buckling load. The effective length factor for the bearing seat joists is as low as 0.709 for the Southwell buckling load for J41. These results confirm that the use of $k = 0.85$ is conservative in cases but appropriate overall for bearing seat joists.

For the flush frame joists, the back-calculated effective length factor ranges from 0.641 for the Southwell buckling load for J23e to 0.784 for the deflection limit load for J42c. Average values for the effective length factor range from 0.687 to 0.771 for the deflection limit load and from 0.654 to 0.705 for the Southwell buckling load. Based on these results, a value of $k = 0.75$ appears to be appropriate for design of the erection bridging for flush frame joists. Note, however, that the critical load was shown to vary with connection eccentricity and girder connection plate thickness. These values of $k$ should not be used for thinner plates or larger eccentricities than those tested in this study where the flexibility of the connection could be greater and the critical buckling load lower.

The back-calculated effective length factor results also help shed light on the strength results. The increase in strength for a flush frame joist in comparison to a bearing seat joist was less for the J1 and J4 series joists than it was for the J2 and J3 series joists. The effective length factors for the flush frame joists are relatively consistent. The effective length factors for the bearing seat joists are less consistent. Based on the Southwell buckling load, $k = 0.723$ and 0.709 for joists J11 and J41, respectively; and $k = 0.786$ and 0.807 for joists J21 and J31, respectively. These results indicate that the reason that there was less difference in strength between the bearing seat joists and the flush frame joist for the J1 and J4 series joists is because the bearing seat joists were relatively strong and not because the flush frame joists were relatively weak.

Table 7. Parameters for the Minkoff Equation

| | | Joist Designation | | | |
|---|---|---|---|---|---|
| **Parameter** | **Units** | **J1** | **J2** | **J3** | **J4** |
| $d$ | in. | 18 | 30 | 30 | 32 |
| $L$ | in. | 384 | 528 | 648 | 720 |
| $y$ | in. | 7.17 | 13.19 | 13.43 | 15.30 |
| $y_t$ | in. | 0.432 | 0.551 | 0.592 | 0.703 |
| $y_b$ | in. | 0.361 | 0.432 | 0.580 | 0.703 |
| $y_o$ | in. | -0.802 | -2.273 | -0.097 | 0 |
| $d_e$ | in. | 17.21 | 29.02 | 28.83 | 30.59 |
| $t_t$ | in. | 0.155 | 0.137 | 0.250 | 0.212 |
| $t_b$ | in. | 0.133 | 0.155 | 0.216 | 0.212 |
| $A_t$ | $in.^2$ | 0.882 | 1.058 | 1.875 | 2.030 |
| $A_b$ | $in.^2$ | 0.630 | 0.882 | 1.635 | 2.030 |
| $I_{yt}$ | $in.^4$ | 0.954 | 1.581 | 2.930 | 4.158 |
| $I_{yb}$ | $in.^4$ | 0.560 | 0.954 | 2.520 | 4.158 |
| $I_y$ | $in.^4$ | 1.514 | 2.535 | 5.450 | 8.316 |
| $I_x$ | $in.^4$ | 108.8 | 405.1 | 725.8 | 950.0 |
| $a_e$ | in | 7.30 | 11.97 | 14.42 | 16.50 |
| $J$ | $in.^4$ | 0.011 | 0.014 | 0.064 | 0.061 |
| $C_w$ | $in.^6$ | 104.4 | 500.9 | 1126 | 1946 |
| $\beta_x$ | in. | 4.476 | 7.186 | 2.168 | 0 |

| | | | | | |
|---|---|---|---|---|---|
| *w* | lb./in. | 0.571 | 0.712 | 1.142 | 1.345 |

Table 8. Minkoff Equation Results

| **Joist Designation** | **Calculated *P* (lbs)** | |
|---|---|---|
| | **with *k* = 0.85** | **with *k* = 1.00** |
| J1 | 434 | 257 |
| J2 | 381 | 194 |
| J3 | 376 | 149 |
| J4 | 315 | 73.5 |

Table 9. Back-Calculated Effective Length Factors

| Specimen | Southwell Buckling Load (lbs) | Effective Length Factor, *k* | Load at Deflection Limit (lbs) | Effective Length Factor, *k* |
|---|---|---|---|---|
| J11 | 709 | 0.723 | 632 | 0.752 |
| J12a | 861 | 0.678 | 754 | 0.709 |
| J12b | 801 | 0.694 | 695 | 0.728 |
| J12c | 928 | 0.661 | 833 | 0.685 |
| J12d | 801 | 0.694 | 719 | 0.720 |
| J12e | 874 | 0.674 | 722 | 0.719 |
| J12f | 878 | 0.673 | 770 | 0.704 |
| Average for J12 | 857 | 0.679 | 749 | 0.711 |
| J13a | 882 | 0.672 | 785 | 0.699 |
| J13b | 721 | 0.719 | 642 | 0.748 |
| J13c | 836 | 0.684 | 666 | 0.739 |
| J13d | 866 | 0.676 | 798 | 0.695 |
| J13e | 994 | 0.646 | 734 | 0.715 |
| J13f | 849 | 0.681 | 775 | 0.702 |
| J13g | 865 | 0.677 | 789 | 0.698 |
| J13h | 882 | 0.672 | 762 | 0.706 |
| Average for J13 | 862 | 0.678 | 744 | 0.713 |
| J21 | 506 | 0.786 | 455 | 0.810 |
| J22a | 917 | 0.658 | 720 | 0.709 |
| J22b | 924 | 0.657 | 692 | 0.717 |
| J22c | 908 | 0.660 | 748 | 0.701 |
| J22d | 996 | 0.642 | 766 | 0.696 |
| J22e | 948 | 0.652 | 740 | 0.703 |
| J22f | 947 | 0.652 | 738 | 0.704 |
| Average for J22 | 940 | 0.654 | 734 | 0.705 |
| J23a | 913 | 0.659 | 830 | 0.679 |
| J23b | 877 | 0.668 | 790 | 0.689 |
| J23c | 886 | 0.666 | 780 | 0.692 |
| J23d | 922 | 0.657 | 750 | 0.700 |
| J23e | 998 | 0.641 | 793 | 0.689 |
| J23f | 890 | 0.665 | 776 | 0.693 |
| J23g | 930 | 0.656 | 846 | 0.675 |
| J23h | 933 | 0.655 | 819 | 0.682 |
| Average for J23 | 919 | 0.658 | 798 | 0.687 |

Table 9. Back-Calculated Effective Length Factors (Continued)

| Specimen | Southwell Buckling Load (lbs) | Effective Length Factor, *k* | Load at Deflection Limit (lbs) | Effective Length Factor, *k* |
|---|---|---|---|---|
| J31 | 469 | 0.807 | 354 | 0.861 |
| J32a | 720 | 0.722 | 544 | 0.778 |
| J32b | 964 | 0.663 | 623 | 0.751 |
| J32c | 761 | 0.710 | 626 | 0.750 |
| J32d | 785 | 0.704 | 596 | 0.760 |
| J32e | 832 | 0.693 | 627 | 0.749 |
| J32f | 823 | 0.695 | 589 | 0.762 |
| Average for J32 | 814 | 0.698 | 601 | 0.758 |
| J33a | 804 | 0.699 | 658 | 0.740 |
| J33b | 846 | 0.689 | 661 | 0.739 |
| J33c | 845 | 0.689 | 680 | 0.733 |
| J33d | 774 | 0.707 | 654 | 0.741 |
| J33e | 875 | 0.682 | 723 | 0.721 |
| J33f | 763 | 0.710 | 636 | 0.747 |
| J33g | 847 | 0.689 | 700 | 0.727 |
| J33h | 794 | 0.702 | 711 | 0.724 |
| Average for J33 | 819 | 0.696 | 678 | 0.734 |
| J41 | 735 | 0.709 | 493 | 0.779 |
| J42a | 918 | 0.669 | 507 | 0.774 |
| J42b | 950 | 0.663 | 535 | 0.765 |
| J42c | 881 | 0.676 | 477 | 0.784 |
| J42d | 895 | 0.673 | 531 | 0.766 |
| J42e | 934 | 0.666 | 571 | 0.753 |
| J42f | 831 | 0.687 | 480 | 0.783 |
| Average for J42 | 901 | 0.672 | 517 | 0.771 |
| J43a | 840 | 0.685 | 588 | 0.748 |
| J43b | 670 | 0.725 | 488 | 0.780 |
| J43c | 752 | 0.705 | 571 | 0.753 |
| J43d | 720 | 0.712 | 545 | 0.761 |
| J43e | 852 | 0.682 | 680 | 0.723 |
| J43f | 717 | 0.713 | 573 | 0.753 |
| J43g | 757 | 0.703 | 617 | 0.740 |
| J43h | 700 | 0.717 | 589 | 0.748 |
| Average for J43 | 751 | 0.705 | 581 | 0.751 |

Joists J11, J21, and J31 all had similar bearing seat details, but joist J11 was smaller and thus the relative restraint provided by the bearing seat could have been higher. Joist J41 was an LH series joist with a larger bearing seat than the other joists (which were K series joists) and thus also could have had greater end restraint.

To illustrate the impact of different effective length factors, the length at which erection bridging is required was computed for the different joists and different values of $k$. The length was computed as the length, $L$, at which $P$ from Equation 11a equals 300 lbs. The resulting values are listed in Table 10. Changing from $k = 0.85$ to $k = 0.75$ results in an approximately 11% increase in the length at which erection bridging is required for the joists investigated.

## Out-of-Plane Stiffness

The out-of-plane stiffness measurements are shown vs connection eccentricity in Figure 27 through Figure 30. The chord and web members of the joists in a series are the same, therefore differences in out-of-plane stiffness measurements should be representative of the end conditions. It is generally expected that increasing connection eccentricity would decrease connection stiffness and that increasing connection plate thickness (as occurs in this work between connection eccentricity of 6 and 9 in.) would increase connection stiffness. These trends were observed in the critical load results (Figure 25 and Figure 26), but are not clearly visible in the out-of-plane stiffness results.

Given the lack of clearly identifiable trends in the results, it is possible that the out-of-plane experiments are flawed. The loads applied in the out-of-plane bending tests were generally small (typically less than 300 lbs) and friction in the pulley in the loading rig could have skewed the results. The girder and column assemblies could have also introduced flexibility that skewed the results.

## Effect of Number of Bolts Installed

During erection of steel buildings, it can be more efficient for the crew that is setting the members to only install the minimum number of bolts and have another crew install the remaining bolts later. OSHA 1926.756 requires two bolts per connection for solid web beams during erection before hoisting cables are released. To provide guidance on the impact of not installing all bolts on stability during erection, several joist configurations were tested with some bolts not installed.

Table 11 lists results for each of the in-plane bolt comparison tests. Data for each includes the Southwell buckling load, load at deflection limit, and percent change from the result with all three bolts installed. Table 12 lists results for each of the out-of-plane bolt comparison tests. Data for each includes the top chord stiffnesses, bottom chord stiffnesses, and percent change from the result with all three bolts installed. Figure 31 shows the Southwell buckling loads and Figure 32 shows the load at deflection limit from these tests.

The critical load is somewhat less when two bolts are installed instead of all three bolts. The average reduction among the nine specimens tested with only two bolts installed at each

Table 10. Calculated Length at Which Erection Bridging is Required

| Joist Designation | Length (ft) when $P$ = 300 lbs | | | |
|---|---|---|---|---|
| | $k$ = 1.00 | $k$ = 0.85 | $k$ = 0.75 | $k$ = 0.70 |
| J1 | 30.7 | 35.6 | 39.9 | 42.5 |
| J2 | 40.2 | 46.5 | 52.0 | 55.3 |
| J3 | 49.0 | 56.2 | 62.3 | 66.0 |
| J4 | 52.8 | 60.4 | 67.0 | 70.9 |

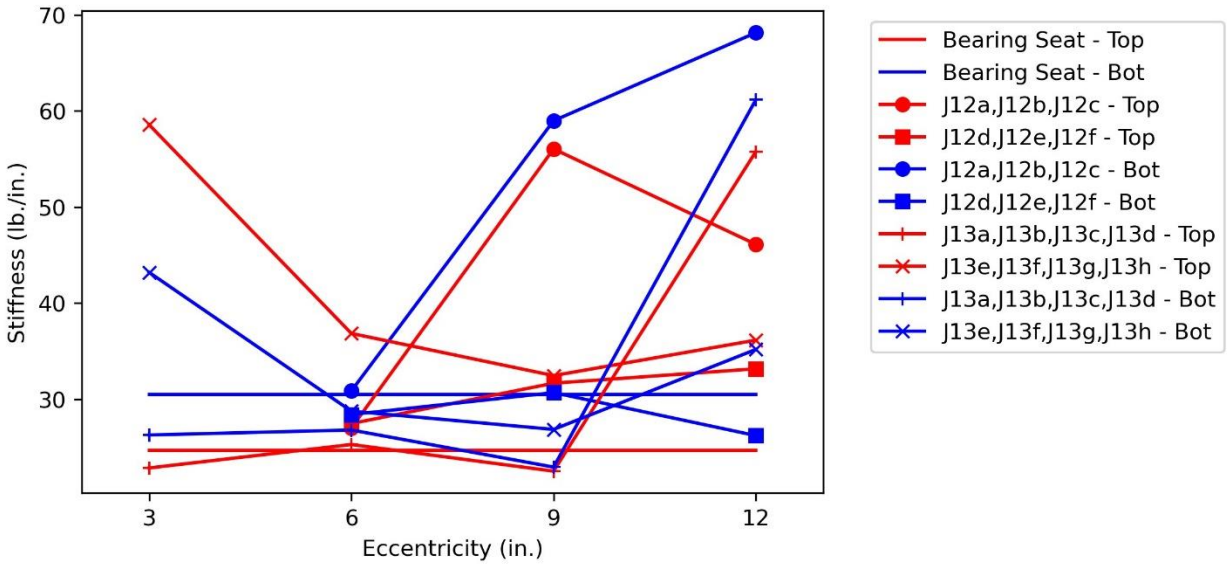


Figure 27. Out-of-Plane Stiffness Results for Joist Series J1

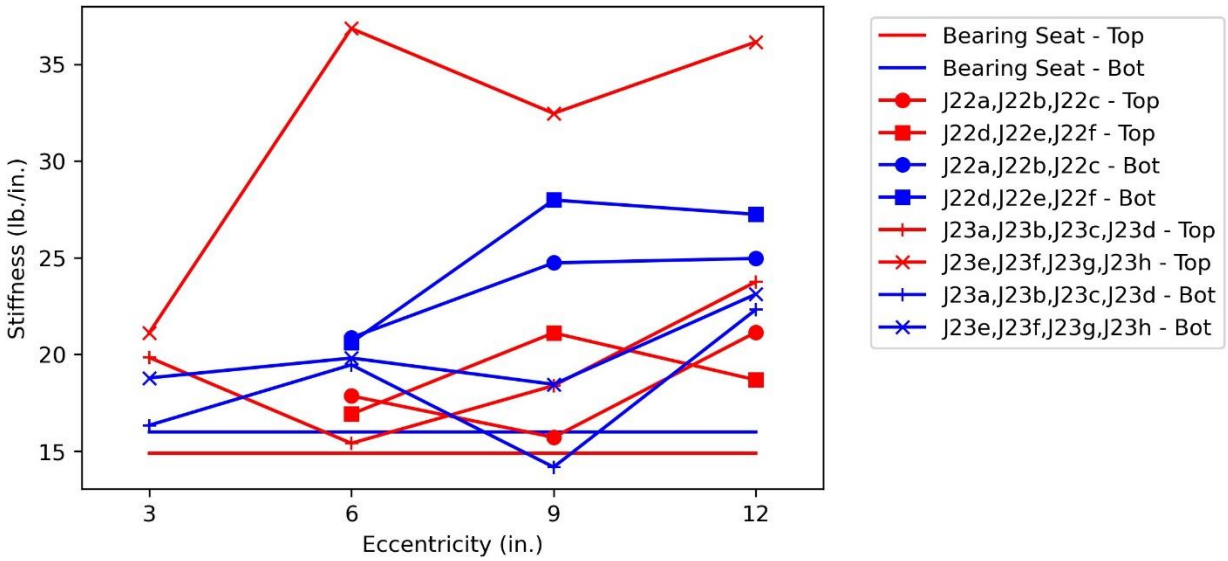


Figure 28. Out-of-Plane Stiffness Results for Joist Series J2

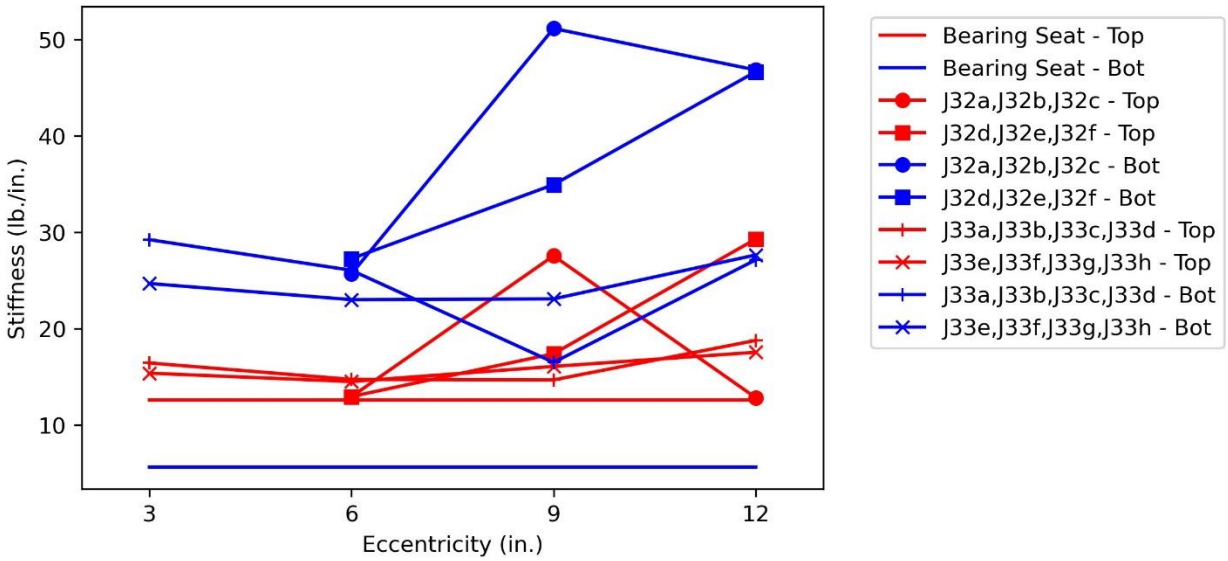


Figure 29. Out-of-Plane Stiffness Results for Joist Series J3

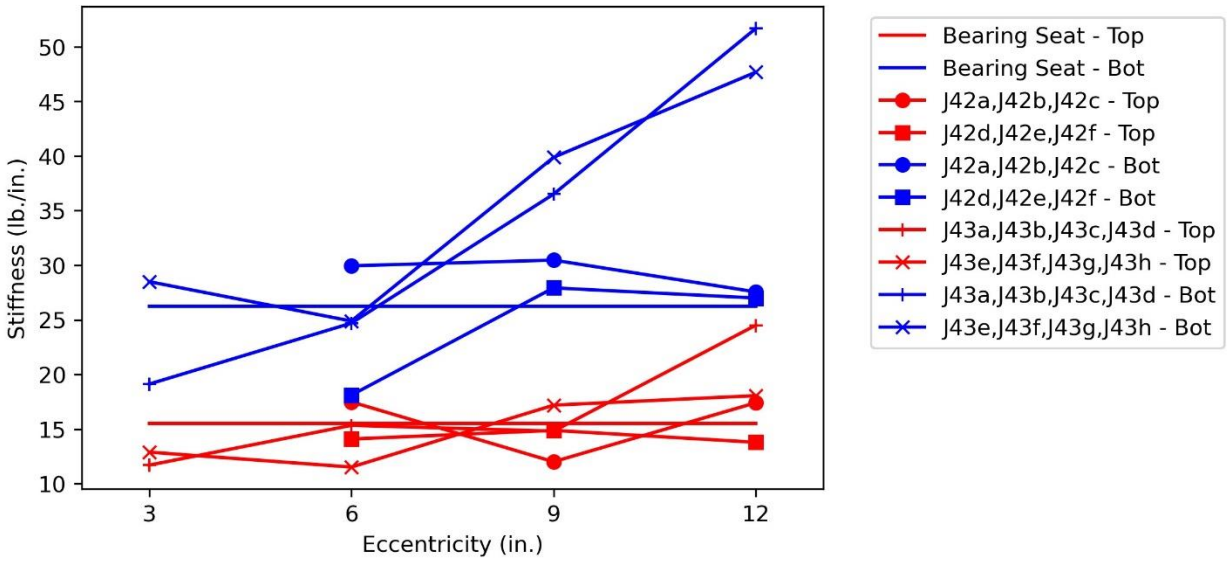


Figure 30. Out-of-Plane Stiffness Results for Joist Series J4

connection was 4.3% for the Southwell buckling load and 2.0% for the load at the deflection limit. Only one specimen was tested with one bolt in each connection. It saw a greater reduction in critical load: 12.9% for the Southwell buckling load and 9.9% for the load at the deflection limit. These results indicate that only installing two bolts can be acceptable, but only installing one bolt is not recommended.

The change in out-of-plane stiffness is more variable than the change in strength as the number of bolts installed decreases. Both increases and decreases in the out-of-plane stiffness were observed when fewer than three bolts were installed. Among the nine specimens tested with only two bolts installed at each connection, the top chord stiffness decreased by an average of 8.8% and the bottom chord stiffness increased by an average of 2.4%. As described previously for the out-of-plane stiffness data, the lack of clear trends in the stiffness data could indicate a flaw in the experiment or that the stiffness does not depend on the number of bolts installed.

Table 11. Bolt Installation Comparison from In-Plane Tests

| Specimen | Bolts | Southwell Buckling Load (lbs) | Change from 3 Bolts | Load at Deflection Limit (lbs) | Change from 3 Bolts |
|---|---|---|---|---|---|
| J13a | 3 Bolts | 882 | --- | 785 | --- |
| J13a | 2 Bolts | 856 | -3.1% | 762 | -3.0% |
| J13a | 1 Bolt | 782 | -12.9% | 714 | -9.9% |
| J32b | 3 Bolts | 964 | --- | 623 | --- |
| J32b | 2 Bolts | 804 | -19.8% | 627 | 0.8% |
| J32e | 3 Bolts | 832 | --- | 627 | --- |
| J32e | 2 Bolts | 829 | -0.4% | 613 | -2.2% |
| J33d | 3 Bolts | 774 | --- | 654 | --- |
| J33d | 2 Bolts | 797 | 2.8% | 656 | 0.3% |
| J33h | 3 Bolts | 794 | --- | 711 | --- |
| J33h | 2 Bolts | 793 | -0.2% | 704 | -1.1% |
| J42a | 3 Bolts | 918 | --- | 507 | --- |
| J42a | 2 Bolts | 905 | -1.4% | 503 | -0.7% |
| J42d | 3 Bolts | 895 | --- | 531 | --- |
| J42d | 2 Bolts | 906 | 1.2% | 504 | -5.3% |
| J43a | 3 Bolts | 840 | --- | 588 | --- |
| J43a | 2 Bolts | 805 | -4.3% | 569 | -3.4% |
| J43e | 3 Bolts | 852 | --- | 680 | --- |
| J43e | 2 Bolts | 749 | -13.7% | 659 | -3.2% |
| | **Average for 2 Bolts:** | | -4.3% | | -2.0% |

Table 12. Bolt Installation Comparison from Out-of-Plane Tests

| Specimen | Bolts | Top Chord Stiffness (lbs/in.) | Change from 3 Bolts | Bottom Chord Stiffness (lbs/in.) | Change from 3 Bolts |
|---|---|---|---|---|---|
| J13a | 3 Bolts | 22.9 | --- | 26.3 | --- |
| J13a | 2 Bolts | 19.7 | -15.9% | 32.3 | 18.7% |
| J13a | 1 Bolt | 28.1 | 18.7% | 31.8 | 17.4% |
| J32b | 3 Bolts | 27.6 | --- | 51.2 | --- |
| J32b | 2 Bolts | 17.7 | -55.4% | 34.4 | -48.6% |
| J32e | 3 Bolts | 17.4 | --- | 34.9 | --- |
| J32e | 2 Bolts | 16.9 | -2.9% | 30.0 | -16.4% |
| J33d | 3 Bolts | 18.8 | --- | 27.1 | --- |
| J33d | 2 Bolts | 16.5 | -14.0% | 35.0 | 22.5% |
| J33h | 3 Bolts | 17.5 | --- | 27.6 | --- |
| J33h | 2 Bolts | 26.5 | 33.8% | 33.1 | 16.4% |
| J42a | 3 Bolts | 17.5 | --- | 30.0 | --- |
| J42a | 2 Bolts | 16.3 | -7.2% | 24.7 | -21.4% |
| J42d | 3 Bolts | 14.1 | --- | 18.1 | --- |
| J42d | 2 Bolts | 9.7 | -45.7% | 23.7 | 23.5% |
| J43a | 3 Bolts | 11.7 | --- | 19.1 | --- |
| J43a | 2 Bolts | 13.3 | 12.0% | 25.7 | 25.6% |
| J43e | 3 Bolts | 12.9 | --- | 28.5 | --- |
| J43e | 2 Bolts | 15.4 | 16.4% | 28.9 | 1.3% |
| | | **Average for 2 Bolts:** | -8.8% | | 2.4% |

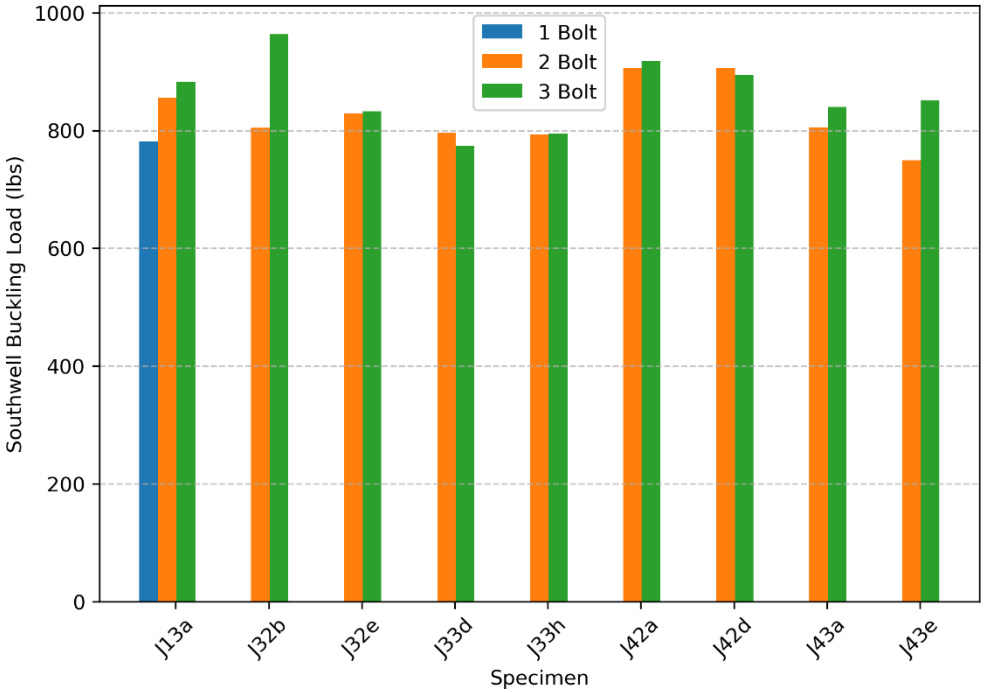


Figure 31. Bolt Installation Comparison – Southwell Buckling

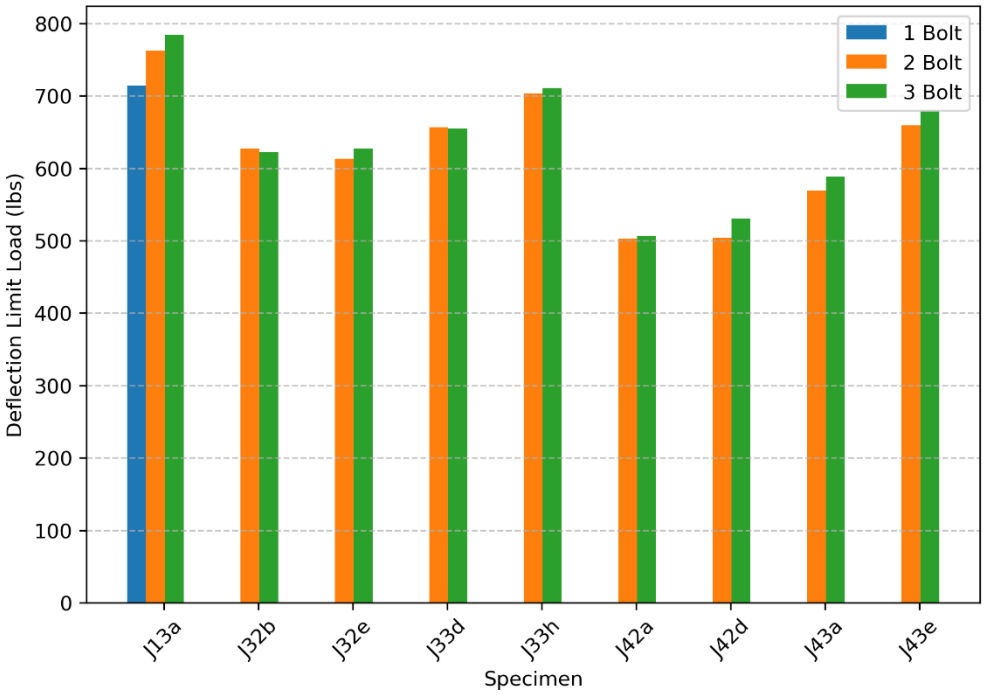


Figure 32. Bolt Installation Comparison – Deflection Limit

# CHAPTER FOUR

# NUMERICAL ANALYSIS

Previous studies on the stability of open web steel joists have included numerical analyses. Eberle et al. (2012) investigated systems of one to ten parallel joists. They considered cases without decking to evaluate construction bridging requirements and with decking to evaluate permanent bridging requirements. They used the finite element analysis software MASTAN2 with line elements that did not consider warping to model the joist members and spring elements to model the stiffness of the bearing seat connections at the joist ends. Rojahn and Ziemian (2021) evaluated the buckling strength of open web steel joists using line elements in MASTAN2 and shell elements in the finite element analysis software Strand7. They found that using two parallel line elements for the joist top and bottom chords (i.e., each line of elements representing a single angle of the double angle chord) provided improved results. The short elements that linked the two chord members were modeled with the properties of a 1 in. diameter steel rod.

Numerical analyses were performed in this work to bring greater context to the experimental results and to expand the range of investigation. Twelve joist models were created in MASTAN2 using best practices identified in previous studies. Each model represented one of the twelve physical joists used in the experimental investigation. Two lines of frame elements, with each line representing a single angle, were defined for the chords. Web members were represented by a single line of frame elements. Cross-sectional properties of each element were defined to match those in the physical joists as described in the Appendix. The local axes of the elements were oriented to match the physical orientation of the members. Four elements were used for each line between work points. The modulus of elasticity was set to 29,000,000 psi and the density was calibrated to match the measured self-weight of the bearing seat joist of each designation. At each work point, elements oriented perpendicular to the members were added to connect the chord members to each other and to the web member. These elements were assigned the properties of a 1 in. diameter steel rod. Elements with the same properties were added at locations of fillers in the top chord. An example of the joist model is shown in Figure 33.

Special end conditions were defined for bearing seat connections, top chord flush frame connections, and full depth flush frame connections as shown in Figure 34 and Figure 35. The point at which the end conditions were applied was the work point for the bearing seat connections and the centroid of the bolt group for the flush frame connections. Additional frame elements were added to the models of the joists with flush frame connections to represent the connection plates. Translational degrees of freedom at the ends were defined as a pin and roller. In-plane rotation (i.e., rotation about the $z$ axis) was unrestrained. Out-of-plane rotation and twist of the cross section were either fully or partially restrained. Partial restraint was achieved by defining a 12 in. long stiff frame element perpendicular to the joist at each end. Connection stiffnesses $k_z$ and $k_y$ were defined for these elements which correspond to the torsional stiffness and out-of-plane rotational stiffness, respectively. Analyses were performed with various values of $k_z$ and $k_y$. The same pair of values was used at both ends of the joist.

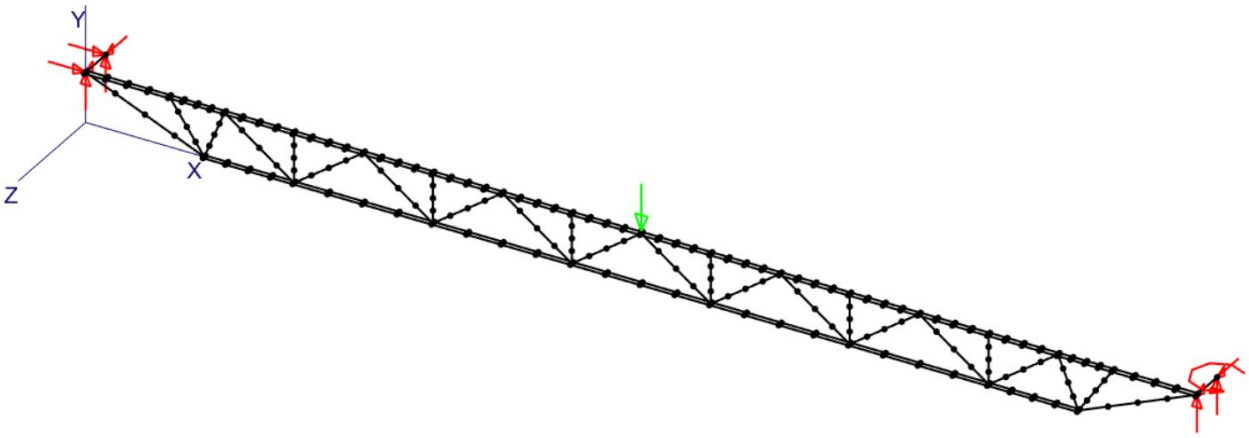


Figure 33. Three-dimensional View of the MASTAN2 Model of Joist J11

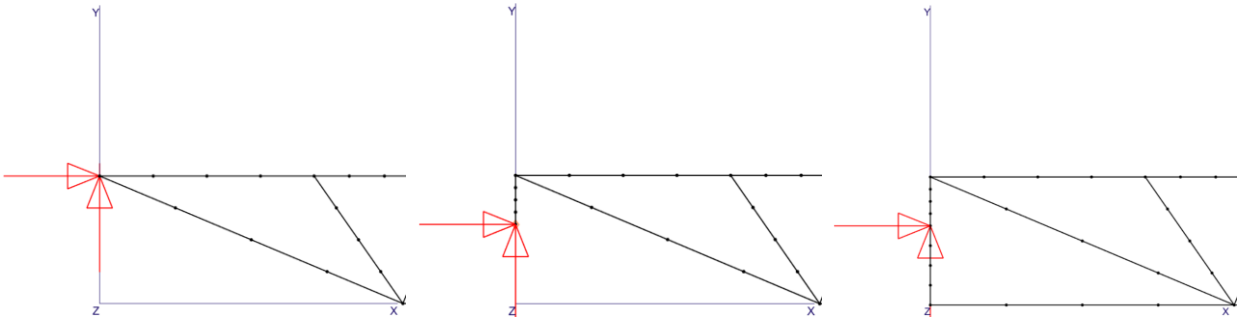

(a) Bearing Seat Configuration (b) Top Chord Flush Frame Configuration (c) Full Depth Flush Frame Configuration

Figure 34. Side View of End Configurations for Joist Models (18K3 Shown)

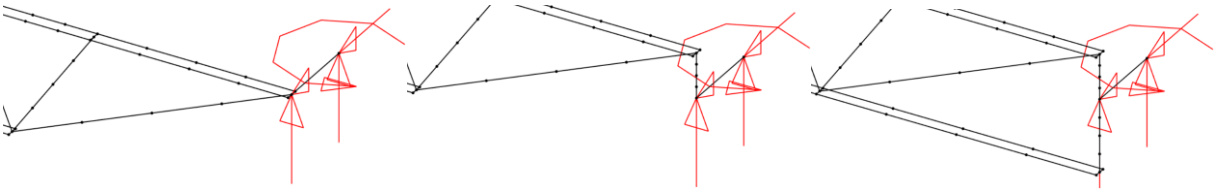

(a) Bearing Seat Configuration (b) Top Chord Flush Frame Configuration (c) Full Depth Flush Frame Configuration

Figure 35. Isometric View of End Configurations for Joist Models (18K3 Shown)

The point load was applied 0.5 in. above the top of the top chord at the center of the midspan as shown in Figure 36. A frame element with properties of a 1 in. diameter bar linked the work point to the point of load application.

Elastic eigenvalue buckling analyses were performed to determine the critical load. MASTAN2 calculates the critical load as a ratio of the applied loads, including both the applied point load and the self-weight. To determine the critical point load for a given self-weight, the magnitude of the point load was adjusted by hand until the applied load ratio was 1.0. An example buckled shape is shown in Figure 37.

## End Restraint

The values of end restraint stiffnesses $k_y$ and $k_z$ were calibrated to the results of the physical experiments. Ideally, the stiffnesses would be calibrated to the results of the out-of-plane bending tests and subsequently validated through comparison to the buckling loads from the in-plane bending tests. However, calibration to the results of the out-of-plane bending tests was unsuccessful because the stiffness from the model was greater than that from the experiments even when the ends were free to rotate out-of-plane. Therefore, the values $k_y$ and $k_z$ were calibrated to the results of the in-plane tests directly.

The variation of the torsional stiffness, $k_z$, from very soft to fully rigid and the out-of-plane rotational stiffness, $k_y$, from zero to fully rigid provide a wide range of buckling loads. As a result, the differences in strength between the joists observed in the physical experiments can be explained by different end conditions. Critical load from MASTAN2 for different values of $k_y$ and $k_z$ are shown in Figure 38 for the J3 series joists.

Values of $k_y$ and $k_z$ were selected for each joist through a trial-and-error process such that the buckling load from MASTAN2 matched the Southwell buckling load from the experiments. For the flush frame joists, the average of the Southwell buckling load for the different configurations was used. The Southwell buckling load was used instead of the load at the deflection limit because the Southwell buckling load is more calculated with the calculated buckling load, especially considering no initial geometric imperfections were included in the MASTAN2 model. The resulting values are listed in Table 13. Both values affect the buckling load and thus the selected values are not unique and represent only one pair of values that gives the same critical load as the experiments.

End conditions that result in critical loads that match the experiments were achieved for all the joists. As expected, the stiffnesses were generally smaller for the bearing seat connections. For the bearing seat joists, the torsional stiffness ranged from 30 kip-in./rad to fully rigid and the out-of-plane rotational stiffnesses ranged from 52 to 100 kip-in./rad. For the top chord flush frame joists, the torsional stiffness ranged from 180 kip-in./rad to fully rigid and the out-of-plane rotational stiffnesses ranged from 90 to 1700 kip-in./rad. For the full depth flush frame joists, the torsional stiffness was fully rigid and the out-of-plane rotational stiffnesses ranged from 10 to 225 kip-in./rad.

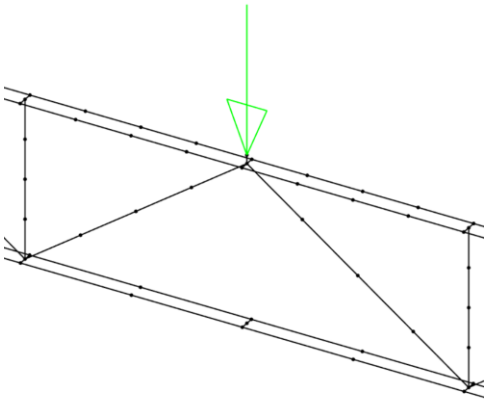

Figure 36. Load Application

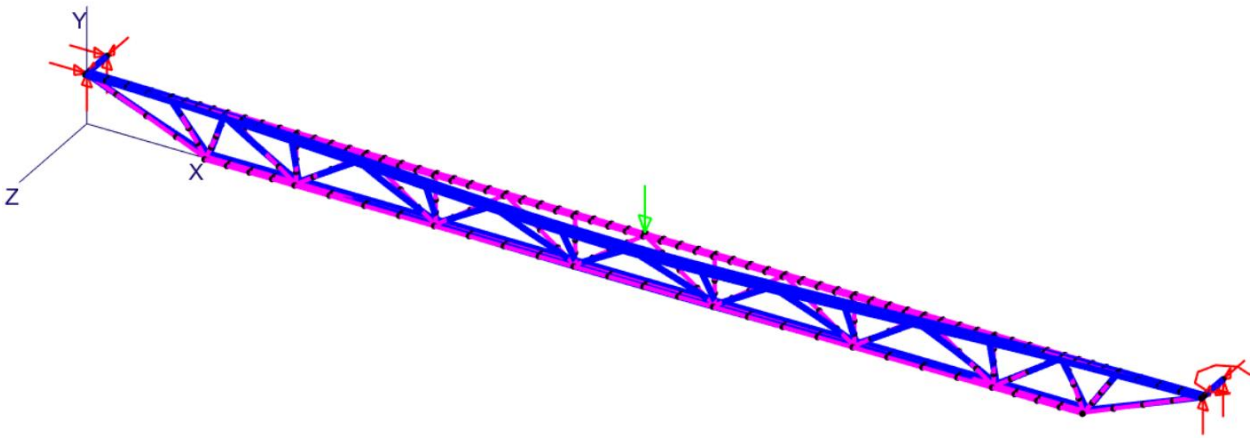


Figure 37. Three-Dimensional View of the Buckled Shape from MASTAN2 of Joist J11

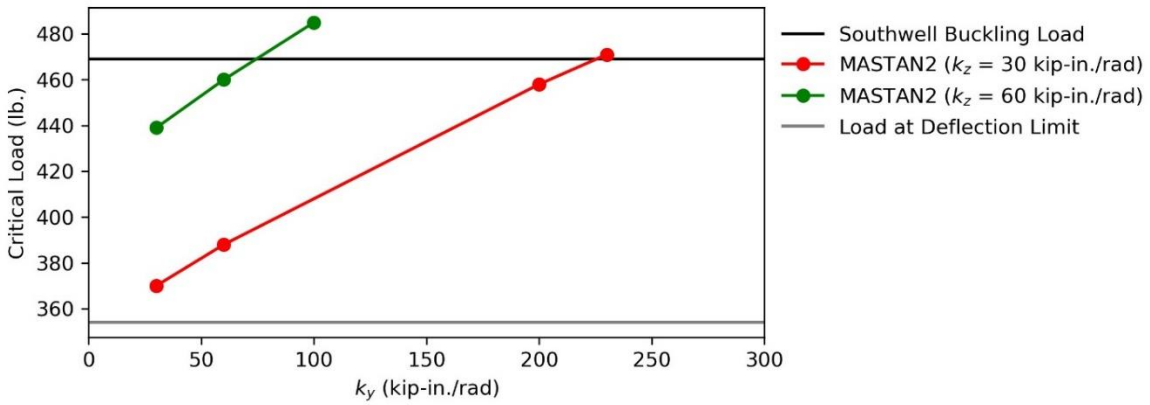


(a) Joist J31

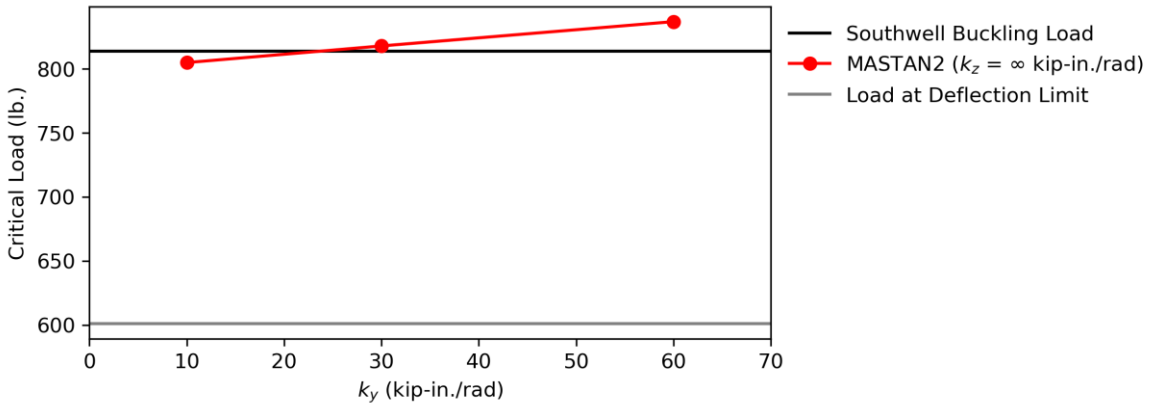


(b) Joist J32

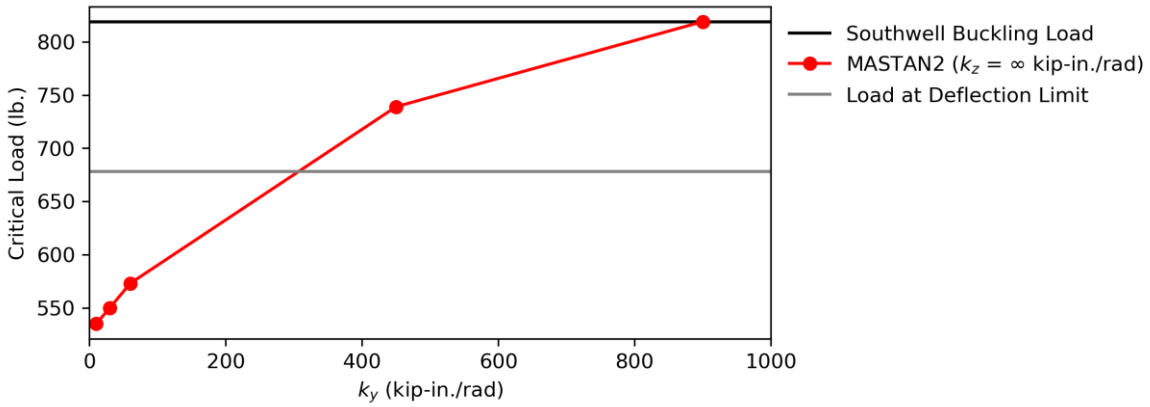


(c) Joist J33

Figure 38. Variation of Critical Load with Stiffness Values

Table 13. Calibrated End Restraint Stiffnesses

| Joist | Buckling Load (lbs) | $k_z$ (kip-in./rad) | $k_y$ (kip-in./rad) |
|---|---|---|---|
| J11 | 709 | ∞ | 52 |
| J12 | 857 | ∞ | 140 |
| J13 | 862 | ∞ | 399 |
| J21 | 506 | 30 | 98 |
| J22 | 940 | ∞ | 225 |
| J23 | 919 | ∞ | 1700 |
| J31 | 469 | 60 | 73 |
| J32 | 814 | ∞ | 25 |
| J33 | 819 | ∞ | 900 |
| J41 | 735 | 140 | 100 |
| J42 | 901 | ∞ | 10 |
| J43 | 751 | 180 | 90 |

## Critical Load When Braced

If a joist with a span of 60 ft or less in length is shown to require erection bridging by the Minkoff equation, then one row of erection bridging is provided without explicit evaluation that the braced configuration is sufficiently strong. To evaluate the strength of the joists when braced, the critical buckling load was computed using MASTAN2 for cases where the top and bottom are restrained from out-of-plane movement at midspan. The critical load was determined for the load at midspan and for load at a quarter point. The resulting critical loads are listed in Table 14. The buckled shape of one case with load at a quarter point is shown in Figure 39. When braced at midspan the critical load is, on average, nearly three times the critical load when unbraced.

## Strength With Lateral Load

To investigate the strength of joists subject to self-weight, a point load at midspan 0.5 in. above the top chord, and lateral wind loading proportional to the member's width of horizontal projection, two plots were generated showing total applied vertical load vs total applied lateral load. The plots, shown in Figure 40 and Figure 41, show elastic critical buckling load results and second-order inelastic analysis results.

The joist models as described before were used for these analyses, but with two cases of boundary conditions each. One with end connection stiffnesses applied to match the Southwell buckling load. The other with pinned end connections.

The elastic critical buckling load, shown as a horizontal dashed line, is the magnitude of the point load that causes elastic buckling concurrent with self-weight. In MASTAN2, the output of elastic critical buckling load analysis is the applied load ratio (ALR) which is the ratio that when applied to all loads produces a loading pattern that results in buckling. For this analysis, the self-weight was to be constant, therefore a series of buckling analyses was performed with varying material density such that when the defined material density is multiplied by ALR, it is equal to the actual applied load ratio. The applied point load times ALR is the critical point load for this case.

The points along the curve represent the applied vertical load concurrent with self-weight and applied lateral wind load that causes inelastic buckling. The ALR is also the output for MASTAN2's second-order inelastic analysis. For this analysis, the self-weight still remained constant by varying the material density as described before. The applied point load times ALR and the lateral wind load times ALR was the critical buckling loads for these cases. To create a series of points, the point load would be increased by some amount and the material density would be adjusted accordingly. These adjustments would generally increase applied vertical load and decrease applied lateral load all while keeping self-weight constant.

The first yield strength and plastic moment capacity, shown as vertical lines, was calculated using the two double angle sections with bending in the out-of-plane direction.

The relationship between vertical and lateral loads is non-linear, with an increase in vertical load generally leading to a decrease in lateral load capacity. However, for the 18K3 joist, an applied

Table 14. Calculated Buckling Loads with Bracing at Midspan

| | Critical Load from MASTAN2 with Bracing (lbs) | |
|---|---|---|
| **Joist** | **Load at Midspan** | **Load at Quarter Point** |
| J11 | 2,772 | 2,325 |
| J12 | 3,042 | 2,680 |
| J13 | 2,990 | 2,520 |
| J21 | 2,704 | 2,124 |
| J22 | 3,505 | 3,130 |
| J23 | 3,470 | 2,880 |
| J31 | 2,750 | 2,238 |
| J32 | 3,465 | 3,157 |
| J33 | 3,300 | 2,777 |
| J41 | 3,462 | 3,020 |
| J42 | 3,975 | 3,784 |
| J43 | 3,482 | 3,060 |

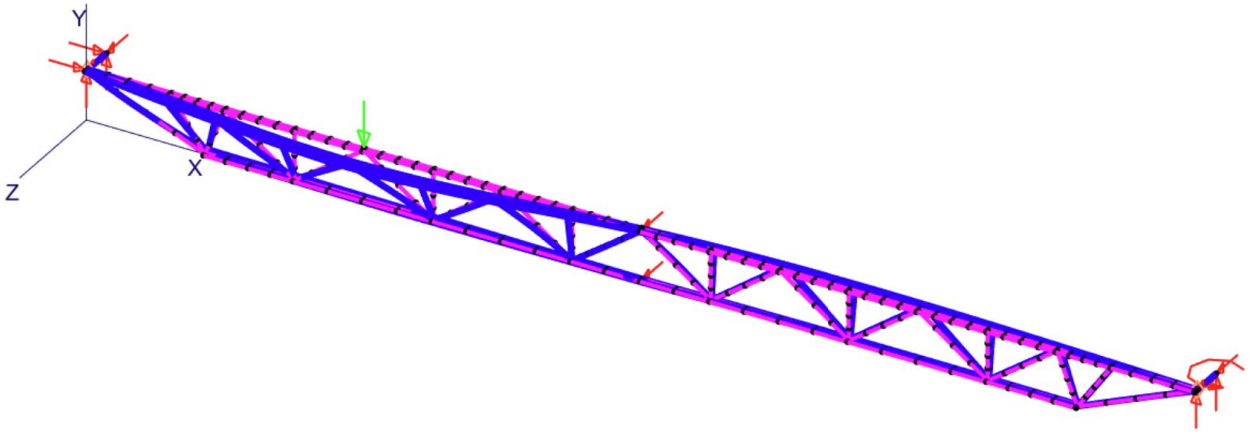


Figure 39. Three-Dimensional View of the Buckled Shape from MASTAN2 of Joist J11 with Bracing

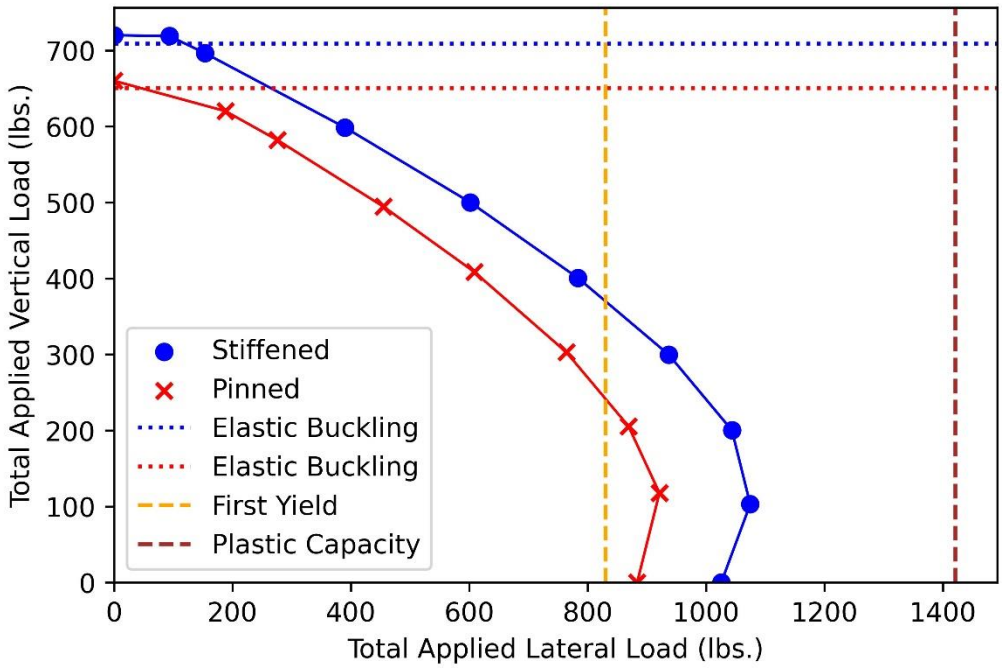


Figure 40. 2nd Order Inelastic Buckling Analysis Plot of the 18K3 Joist

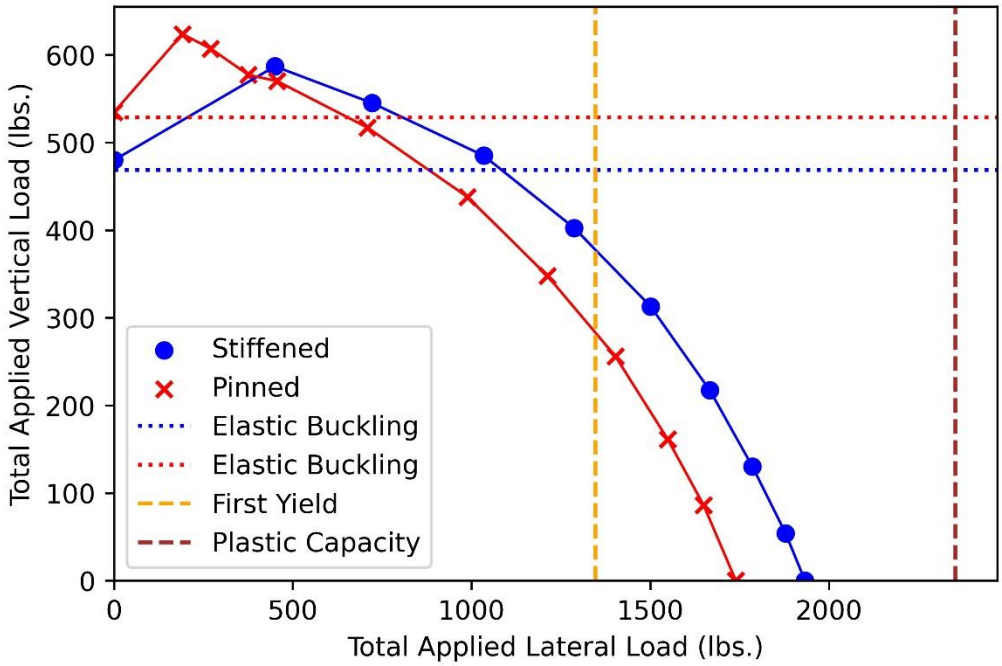


Figure 41. 2nd Order Inelastic Buckling Analysis Plot of the 30K12 Joist

vertical load in the range of 100-200 lbs. led to an increase in the lateral load capacity. The plots of the second-order inelastic analysis converge to their respective elastic buckling load when no lateral load is applied.

# CHAPTER FIVE

# CONCLUSIONS AND RECOMENDATIONS

Accurately evaluating the potential for lateral-torsional buckling is critical for safe and efficient erection of open web steel joists. If a joist cannot support its own weight and the weight of an erector, bridging must be installed before the hoisting cables are released. The potential for lateral-torsional buckling of joists is evaluated in practice using the Minkoff equation which was derived and validated for joists with typical bearing seat connections. Flush frame connections for joists have been recently developed and are particularly attractive in composite floor systems controlled by vibrations. Flush frame connections also provide greater connection stiffness than bearing seat connections. However, the greater stiffness provided by flush frame connections is not yet recognized in the design of erection bridging.

This study investigated the erection stability of joists with flush frame connections with physical experiments and numerical analyses to better understand the impact of the increased connection stiffness and develop recommendations for design. Bending tests of 60 different joist and connection configurations without bridging were performed to determine the critical load and out-of-plane stiffness. The critical load of joists with flush frame connections was almost always greater than that for joists with bearing seat connections. The Minkoff equation with an effective length factor of $k = 0.75$ was found to provide a generally conservative approximation of the strength of joists with flush frame connections. Numerical analyses demonstrated that differences in strength can be explained by differences in connection stiffness.

Based on these results, a modification to the SJI *Specifications* to allow the use of $k = 0.75$ in the Minkoff equation for joists with flush frame connections is recommended. Noting that the stiffness of flush frame connections depends on connection eccentricity and plate thickness, without further research, the recommended effective length factor should not be used for connections less stiff than those tested in this study. Specifically, the recommended effective length factor should be used only when the girder connection plate thickness is greater than or equal to 1/4 in. when the eccentricity is less than or equal to 6 in. and 1/2 in. when the eccentricity is between 6 and 12 in.

Use of the recommended effective length factor will allow more joists to be erected without erection bridging and without compromising safety. For ease of use, limiting lengths for all standard SJI joists should be calculated and provided to engineers. Additional research on the erection stability of other types of joists for which the Minkoff equation does not directly apply, such as pitched joists, is also recommended.

## LIST OF REFERENCES


Davis, B., and Murray, T. M. (2022). "Vulcraft Vibration Research Composite Joists with Flush Framed Connections 1785 Columbus Avenue, Boston, MA."

Eberle, J. R., Ziemian, R. D., and Potts, D. R. (2012). "Computational studies aimed at defining bridging requirements for steel joists." *Proceedings of the Annual Stability Conference Structural Stability Research Council*, SSRC, Grapevine, Texas.

Galambos, T. V. (1993). "Bracing of Trussed Beams." *Is Your Structure Suitably Braced?*, Structural Stability Research Council, Milwaukee, Wisconsin.

Green, P. S., and Holtermann, T. (2008). "Bridging of Open-Web Steel Joists and Joist Girders." *Structures Congress 2008*, ASCE, Vancouver, British Columbia, Canada.

Green, P. S., Winarta, M., and Davis, G. (2008). *Handling and Erection of Steel Joists and Joist Girders*. Technical Digest 9, Steel Joist Institute, Myrtle Beach, South Carolina.

Mandal, P., and Calladine, C. R. (2002). "Lateral-torsional buckling of beams and the Southwell plot." *International Journal of Mechanical Sciences*, 44(12), 2557–2571.

Minkoff, R. M. (1975). "Stability of Joists During Erection." M.S. Thesis, Washington University, St. Louis, Missouri.

Murray, T. M., and Davis, B. (2020). "Vibration of Vulcraft Steel Joists with Flush Framed and Flush Bearing Seat Connections."

OSHA. (2001). *Open web steel joists*. Subpart R of Part 1926, Standard Number 1926.757, Occupational Safety and Health Administration, United States Department of Labor, Washington, DC.

Rojahn, G. M. K., and Ziemian, R. D. (2021). "Finite Element Modeling Considerations for the Stability Analysis of Open Web Steel Joists." *Proceedings of the Annual Stability Conference*, Structural Stability Research Council.

SJI. (2020). *Standard Specifications for K-Series, LH-Series, and DLH-Series Open Web Steel Joists, and for Joist Girders*. ANSI/SJI 100-2020, Steel Joist Institute, Florence, South Carolina.

Slein, R., Buth, J. S., Latif, W., Kamath, A. M., Alshannaq, A. A., Sherman, R. J., Scott, D. W., and White, D. W. (2020). "Large-scale experimental lateral-torsional buckling tests of welded I-section members." *Proceedings of the Annual Stability Conference*, Structural Stability Research Council, Atlanta, Georgia.

Vulcraft. (2023). "Joist Flush Frame Connections." <https://vulcraft.com/Products/FlushFrameConnections>.

Ziemian, R. D., Schwarz, J. E., Emerson, M. R., and Potts, D. R. (2004). "Stability of Unbraced Steel Joists Subject to Min-Span Loading." *Proceedings of the Annual Stability Conference, Structural Stability Research Council*, Long Beach, California.

# APPENDIX

J11

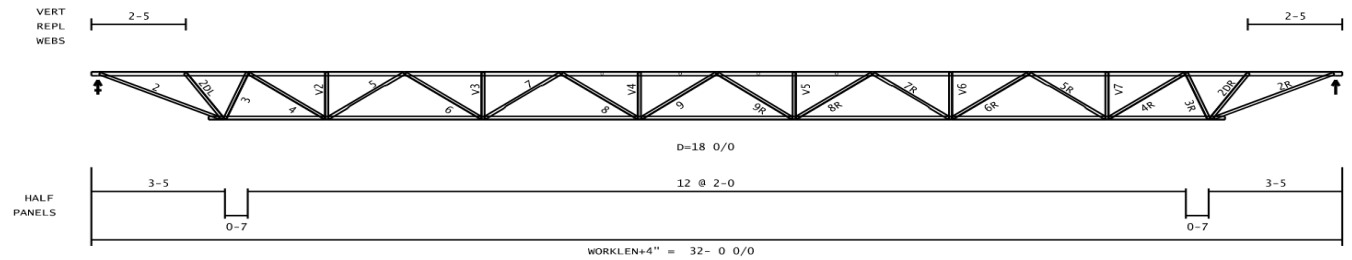


TCXL = 0- 0 0/0 | TOP CHORD 2 L 1-1/2X 1-1/2X~~.113~~ .155 | TCXR = 0- 0 0/0

BCXL = 0- 5 0/0 | BOTTOM CHORD 2 L 1-1/4X 1-1/4X~~.109~~ .133 | BCXR = 0- 5 0/0

| WEB | QTY | SIZE | WELD SIZE |
|---|---|---|---|
| 2 | 1 | ~~"15/16"" ROUND~~" | 2.0X0.222 1" ROUND |
| 2DL | 1 | L 1 X 1 X .109 | 1.5X0.109 |
| 3 | 1 | ~~L 1 X 1 X .109~~ | 1.5X0.109 L1.25x1.25x.109 |
| 4 | 1 | ~~L 1 X 1 X .109~~ | 2.3X0.109 L1.25x1.25x.109 |
| V2 | 1 | L 1 X 1 X .109 | 1.5X0.109 |
| 5 | 1 | L 1-1/4X 1-1/4X.109 | 2.0X0.109 |
| 6 | 1 | ~~L 1 X 1 X .109~~ | 1.9X0.109 L1.25x1.25x.109 |
| V3 | 1 | L 1 X 1 X .109 | 1.5X0.109 |
| 7 | 1 | L 1-1/4X 1-1/4X.109 | 1.5X0.109 |
| 8 | 1 | ~~L 1 X 1 X .109~~ | 1.5X0.109 L1.25x1.25x.109 |
| V4 | 1 | L 1 X 1 X .109 | 1.5X0.109 |
| 9 | 1 | ~~L 1 X 1 X .109~~ | 1.5X0.109 L1.25x1.25x.109 |

| WEB | QTY | SIZE | WELD SIZE |
|---|---|---|---|
| 9R | 1 | ~~L 1 X 1 X .109~~ | 1.5X0.109 L1.25x1.25x.109 |
| V5 | 1 | L 1 X 1 X .109 | 1.5X0.109 |
| 8R | 1 | ~~L 1 X 1 X .109~~ | 1.5X0.109 L1.25x1.25x.109 |
| 7R | 1 | L 1-1/4X 1-1/4X.109 | 1.5X0.109 |
| V6 | 1 | L 1 X 1 X .109 | 1.5X0.109 |
| 6R | 1 | ~~L 1 X 1 X .109~~ | 1.9X0.109 L1.25x1.25x.109 |
| 5R | 1 | L 1-1/4X 1-1/4X.109 | 2.0X0.109 |
| V7 | 1 | L 1 X 1 X .109 | 1.5X0.109 |
| 4R | 1 | ~~L 1 X 1 X .109~~ | 2.3X0.109 L1.25x1.25x.109 |
| 3R | 1 | ~~L 1 X 1 X .109~~ | 1.5X0.109 L1.25x1.25x.109 |
| 2DR | 1 | L 1 X 1 X .109 | 1.5X0.109 |
| 2R | 1 | ~~"15/16"" ROUND~~" | 2.0X0.222 1" SQUARE |

J11 18K3 2-MAY-2023 08:14:04

# J12

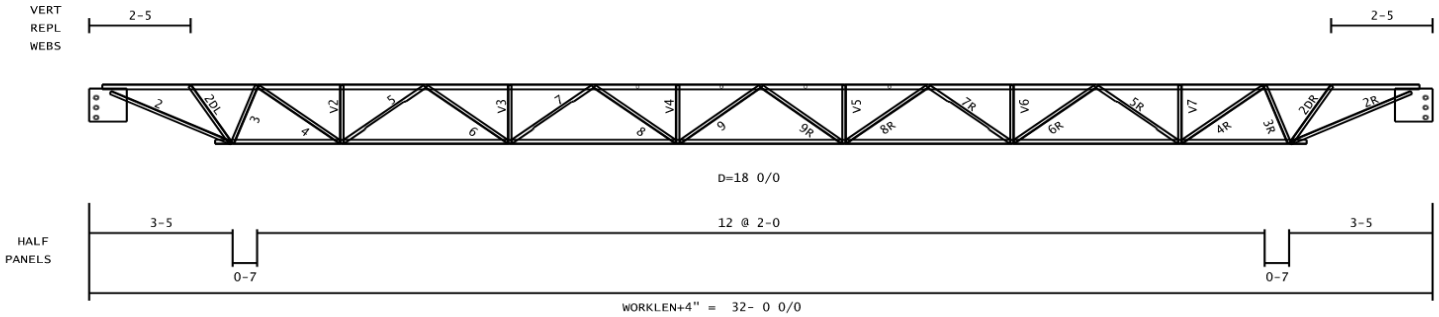


TCXL = 0- 0 0/0 | TOP CHORD 2 L 1-1/2X 1-1/2X~~.113~~ .155 | TCXR = 0- 0 0/0

BCXL = 0- 5 0/0 | BOTTOM CHORD 2 L 1-1/4X 1-1/4X~~.109~~ .133 | BCXR = 0- 5 0/0

| WEB | QTY | SIZE | WELD SIZE |
|---|---|---|---|
| 2 | 2 | ~~L 1 X 1 X .109~~ | 4.1X0.109 G 2L1.25x1.25x.109 |
| 2DL | 1 | L 1 X 1 X .109 | 1.5X0.109 |
| 3 | 1 | ~~L 1 X 1 X .109~~ | 1.5X0.109 L1.25x1.25x.109 |
| 4 | 1 | ~~L 1 X 1 X .109~~ | 2.3X0.109 L1.25x1.25x.109 |
| V2 | 1 | L 1 X 1 X .109 | 1.5X0.109 |
| 5 | 1 | L 1-1/4X 1-1/4X.109 | 2.0X0.109 |
| 6 | 1 | ~~L 1 X 1 X .109~~ | 1.9X0.109 L1.25x1.25x.109 |
| V3 | 1 | L 1 X 1 X .109 | 1.5X0.109 |
| 7 | 1 | L 1-1/4X 1-1/4X.109 | 1.5X0.109 |
| 8 | 1 | ~~L 1 X 1 X .109~~ | 1.5X0.109 L1.25x1.25x.109 |
| V4 | 1 | L 1 X 1 X .109 | 1.5X0.109 |
| 9 | 1 | ~~L 1 X 1 X .109~~ | 1.5X0.109 L1.25x1.25x.109 |

| WEB | QTY | SIZE | WELD SIZE |
|---|---|---|---|
| 9R | 1 | ~~L 1 X 1 X .109~~ | 1.5X0.109 L1.25x1.25x.109 |
| V5 | 1 | L 1 X 1 X .109 | 1.5X0.109 |
| 8R | 1 | ~~L 1 X 1 X .109~~ | 1.5X0.109 L1.25x1.25x.109 |
| 7R | 1 | L 1-1/4X 1-1/4X.109 | 1.5X0.109 |
| V6 | 1 | L 1 X 1 X .109 | 1.5X0.109 |
| 6R | 1 | ~~L 1 X 1 X .109~~ | 1.9X0.109 L1.25x1.25x.109 |
| 5R | 1 | L 1-1/4X 1-1/4X.109 | 2.0X0.109 |
| V7 | 1 | L 1 X 1 X .109 | 1.5X0.109 |
| 4R | 1 | ~~L 1 X 1 X .109~~ | 2.3X0.109 L1.25x1.25x.109 |
| 3R | 1 | ~~L 1 X 1 X .109~~ | 1.5X0.109 L1.25x1.25x.109 |
| 2DR | 1 | L 1 X 1 X .109 | 1.5X0.109 |
| 2R | 2 | ~~L 1 X 1 X .109~~ | 4.1X0.109 G 2L1.25x1.25x.109 |

J12 18K3 2-MAY-2023 08:14:04

# J13

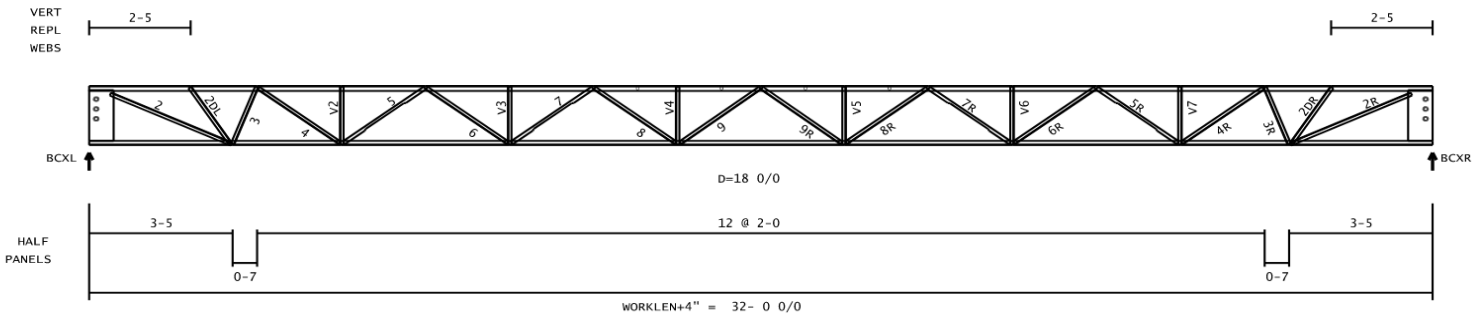


TCXL = 0- 0 0/0 | TOP CHORD 2 L 1-1/2X 1-1/2X~~.113~~ .155 | TCXR = 0- 0 0/0

BCXL = 3- 5 0/0 | BOTTOM CHORD 2 L 1-1/4X 1-1/4X~~.109~~ .133 | BCXR = 3- 5 0/0

| WEB | QTY | SIZE | WELD SIZE |
|---|---|---|---|
| 2 | 2 | ~~L 1 X 1 X .109~~ | 4.1X0.109 G 2L1.25x1.25x.109 |
| 2DL | 1 | L 1 X 1 X .109 | 1.5X0.109 |
| 3 | 1 | ~~L 1 X 1 X .109~~ | 1.5X0.109 L1.25x1.25x.109 |
| 4 | 1 | ~~L 1 X 1 X .109~~ | 2.3X0.109 L1.25x1.25x.109 |
| V2 | 1 | L 1 X 1 X .109 | 1.5X0.109 |
| 5 | 1 | L 1-1/4X 1-1/4X.109 | 2.0X0.109 |
| 6 | 1 | ~~L 1 X 1 X .109~~ | 1.9X0.109 L1.25x1.25x.109 |
| V3 | 1 | L 1 X 1 X .109 | 1.5X0.109 |
| 7 | 1 | L 1-1/4X 1-1/4X.109 | 1.5X0.109 |
| 8 | 1 | ~~L 1 X 1 X .109~~ | 1.5X0.109 L1.25x1.25x.109 |
| V4 | 1 | L 1 X 1 X .109 | 1.5X0.109 |
| 9 | 1 | ~~L 1 X 1 X .109~~ | 1.5X0.109 L1.25x1.25x.109 |

| WEB | QTY | SIZE | WELD SIZE |
|---|---|---|---|
| 9R | 1 | ~~L 1 X 1 X .109~~ | 1.5X0.109 L1.25x1.25x.109 |
| V5 | 1 | L 1 X 1 X .109 | 1.5X0.109 |
| 8R | 1 | ~~L 1 X 1 X .109~~ | 1.5X0.109 L1.25x1.25x.109 |
| 7R | 1 | L 1-1/4X 1-1/4X.109 | 1.5X0.109 |
| V6 | 1 | L 1 X 1 X .109 | 1.5X0.109 |
| 6R | 1 | ~~L 1 X 1 X .109~~ | 1.9X0.109 L1.25x1.25x.109 |
| 5R | 1 | L 1-1/4X 1-1/4X.109 | 2.0X0.109 |
| V7 | 1 | L 1 X 1 X .109 | 1.5X0.109 |
| 4R | 1 | ~~L 1 X 1 X .109~~ | 2.3X0.109 L1.25x1.25x.109 |
| 3R | 1 | ~~L 1 X 1 X .109~~ | 1.5X0.109 L1.25x1.25x.109 |
| 2DR | 1 | L 1 X 1 X .109 | 1.5X0.109 |
| 2R | 2 | ~~L 1 X 1 X .109~~ | 4.1X0.109 G 2L1.25x1.25x.109 |

J13 18K3 2-MAY-2023 08:14:04

# J21

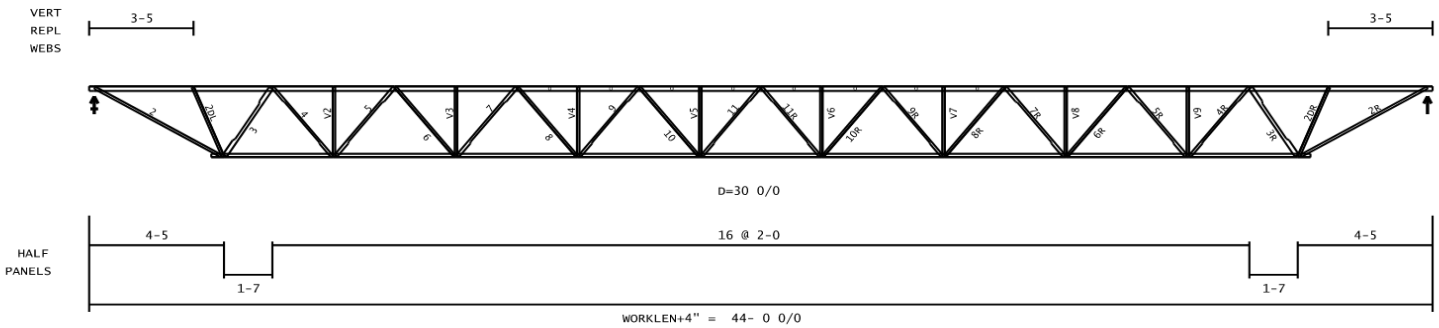


| | | | | | |
|---|---|---|---|---|---|
| TCXL = | 0- 0 0/0 | TOP CHORD | 2 | L 2 X 2 X .137 | TCXR = 0- 0 0/0 |
| BCXL = | 0- 5 0/0 | BOTTOM CHORD | 2 | L 1-1/2X 1-1/2X.155 | BCXR = 0- 5 0/0 |

| WEB | QTY | SIZE | WELD SIZE |
|---|---|---|---|
| 2 | 1 | "1"" ROUND" | 2.3X0.230 |
| 2DL | 1 | L 1 X 1 X .109 | 1.5X0.109 |
| 3 | 1 | L 2 X 2 X .137 | 2.7X0.137 |
| 4 | 1 | L 1-1/4X 1-1/4X.109 | 3.4X0.109 |
| V2 | 1 | L 1 X 1 X .109 | 1.5X0.109 |
| 5 | 1 | L 1-1/2X 1-1/2X.155 | 2.2X0.155 |
| 6 | 1 | L 1 X 1 X .109 | 2.7X0.109 |
| V3 | 1 | L 1 X 1 X .109 | 1.5X0.109 |
| 7 | 1 | L 1-1/2X 1-1/2X.123 | 2.1X0.123 |
| 8 | 1 | L 1 X 1 X .109 | 2.0X0.109 |
| V4 | 1 | L 1 X 1 X .109 | 1.5X0.109 |
| 9 | 1 | L 1-1/4X 1-1/4X.109 | 1.7X0.109 |
| 10 | 1 | L 1 X 1 X .109 | 1.5X0.109 |
| V5 | 1 | L 1 X 1 X .109 | 1.5X0.109 |
| 11 | 1 | L 1-1/4X 1-1/4X.109 | 1.5X0.109 |

| WEB | QTY | SIZE | WELD SIZE |
|---|---|---|---|
| 11R | 1 | L 1-1/4X 1-1/4X.109 | 1.5X0.109 |
| V6 | 1 | L 1 X 1 X .109 | 1.5X0.109 |
| 10R | 1 | L 1 X 1 X .109 | 1.5X0.109 |
| 9R | 1 | L 1-1/4X 1-1/4X.109 | 1.7X0.109 |
| V7 | 1 | L 1 X 1 X .109 | 1.5X0.109 |
| 8R | 1 | L 1 X 1 X .109 | 2.0X0.109 |
| 7R | 1 | L 1-1/2X 1-1/2X.123 | 2.1X0.123 |
| V8 | 1 | L 1 X 1 X .109 | 1.5X0.109 |
| 6R | 1 | L 1 X 1 X .109 | 2.7X0.109 |
| 5R | 1 | L 1-1/2X 1-1/2X.155 | 2.2X0.155 |
| V9 | 1 | L 1 X 1 X .109 | 1.5X0.109 |
| 4R | 1 | L 1-1/4X 1-1/4X.109 | 3.4X0.109 |
| 3R | 1 | L 2 X 2 X .137 | 2.7X0.137 |
| 2DR | 1 | L 1 X 1 X .109 | 1.5X0.109 |
| 2R | 1 | "1"" ROUND" | 2.3X0.230 |

J21 30K7

2-MAY-2023 08:14:04

# J22

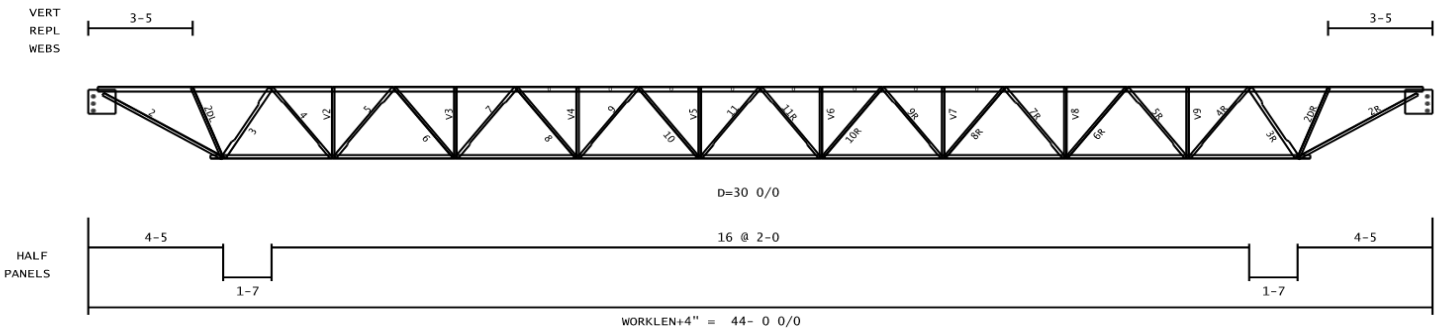


| | | | | | |
|---|---|---|---|---|---|
| TCXL = 0- 0 0/0 | TOP CHORD | 2 | L 2 X 2 X .137 | TCXR = 0- 0 0/0 |
| BCXL = 0- 5 0/0 | BOTTOM CHORD | 2 | L 1-1/2X 1-1/2X.155 | BCXR = 0- 5 0/0 |

| WEB | QTY | SIZE | WELD SIZE | |
|---|---|---|---|---|
| 2 | 2 | ~~L 1-1/4X 1-1/4X.109~~ | 6.7X0.109 G | 2L1.5x1.5x.155 |
| 2DL | 1 | L 1 X 1 X .109 | 1.5X0.109 | |
| 3 | 1 | L 2 X 2 X .137 | 2.7X0.137 | |
| 4 | 1 | L 1-1/4X 1-1/4X.109 | 3.4X0.109 | |
| V2 | 1 | L 1 X 1 X .109 | 1.5X0.109 | |
| 5 | 1 | L 1-1/2X 1-1/2X.155 | 2.2X0.155 | |
| 6 | 1 | L 1 X 1 X .109 | 2.7X0.109 | |
| V3 | 1 | L 1 X 1 X .109 | 1.5X0.109 | |
| 7 | 1 | L 1-1/2X 1-1/2X.123 | 2.1X0.123 | |
| 8 | 1 | L 1 X 1 X .109 | 2.0X0.109 | |
| V4 | 1 | L 1 X 1 X .109 | 1.5X0.109 | |
| 9 | 1 | L 1-1/4X 1-1/4X.109 | 1.7X0.109 | |
| 10 | 1 | L 1 X 1 X .109 | 1.5X0.109 | |
| V5 | 1 | L 1 X 1 X .109 | 1.5X0.109 | |
| 11 | 1 | L 1-1/4X 1-1/4X.109 | 1.5X0.109 | |

| WEB | QTY | SIZE | WELD SIZE | |
|---|---|---|---|---|
| 11R | 1 | L 1-1/4X 1-1/4X.109 | 1.5X0.109 | |
| V6 | 1 | L 1 X 1 X .109 | 1.5X0.109 | |
| 10R | 1 | L 1 X 1 X .109 | 1.5X0.109 | |
| 9R | 1 | L 1-1/4X 1-1/4X.109 | 1.7X0.109 | |
| V7 | 1 | L 1 X 1 X .109 | 1.5X0.109 | |
| 8R | 1 | L 1 X 1 X .109 | 2.0X0.109 | |
| 7R | 1 | L 1-1/2X 1-1/2X.123 | 2.1X0.123 | |
| V8 | 1 | L 1 X 1 X .109 | 1.5X0.109 | |
| 6R | 1 | L 1 X 1 X .109 | 2.7X0.109 | |
| 5R | 1 | L 1-1/2X 1-1/2X.155 | 2.2X0.155 | |
| V9 | 1 | L 1 X 1 X .109 | 1.5X0.109 | |
| 4R | 1 | L 1-1/4X 1-1/4X.109 | 3.4X0.109 | |
| 3R | 1 | L 2 X 2 X .137 | 2.7X0.137 | |
| 2DR | 1 | L 1 X 1 X .109 | 1.5X0.109 | |
| 2R | 2 | ~~L 1-1/4X 1-1/4X.109~~ | 6.7X0.109 G | 2L1.5x1.5x.155 |

# J23

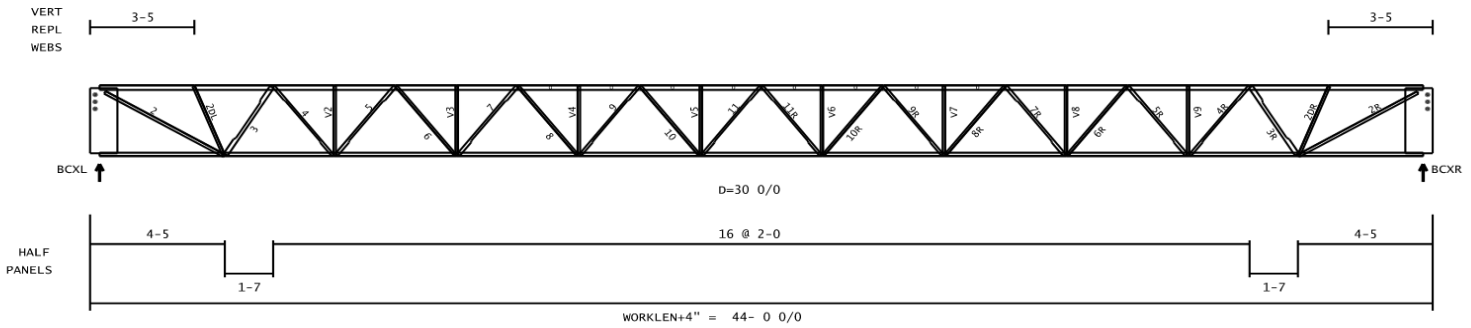


| | | | | | |
|---|---|---|---|---|---|
| TCXL = 0- 0 0/0 | TOP CHORD | 2 | L 2 X 2 X .137 | TCXR = 0- 0 0/0 |
| BCXL = 4- 1 1/4 | BOTTOM CHORD | 2 | L 1-1/2X 1-1/2X.155 | BCXR = 4- 1 1/4 |

| WEB | QTY | SIZE | WELD SIZE | |
|---|---|---|---|---|
| 2 | 2 | ~~L 1-1/4X 1-1/4X.109~~ | 6.7X0.109 G | 2L1.5x1.5x.155 |
| 2DL | 1 | L 1 X 1 X .109 | 1.5X0.109 | |
| 3 | 1 | L 2 X 2 X .137 | 2.7X0.137 | |
| 4 | 1 | L 1-1/4X 1-1/4X.109 | 3.4X0.109 | |
| V2 | 1 | L 1 X 1 X .109 | 1.5X0.109 | |
| 5 | 1 | L 1-1/2X 1-1/2X.155 | 2.2X0.155 | |
| 6 | 1 | L 1 X 1 X .109 | 2.7X0.109 | |
| V3 | 1 | L 1 X 1 X .109 | 1.5X0.109 | |
| 7 | 1 | L 1-1/2X 1-1/2X.123 | 2.1X0.123 | |
| 8 | 1 | L 1 X 1 X .109 | 2.0X0.109 | |
| V4 | 1 | L 1 X 1 X .109 | 1.5X0.109 | |
| 9 | 1 | L 1-1/4X 1-1/4X.109 | 1.7X0.109 | |
| 10 | 1 | L 1 X 1 X .109 | 1.5X0.109 | |
| V5 | 1 | L 1 X 1 X .109 | 1.5X0.109 | |
| 11 | 1 | L 1-1/4X 1-1/4X.109 | 1.5X0.109 | |

| WEB | QTY | SIZE | WELD SIZE | |
|---|---|---|---|---|
| 11R | 1 | L 1-1/4X 1-1/4X.109 | 1.5X0.109 | |
| V6 | 1 | L 1 X 1 X .109 | 1.5X0.109 | |
| 10R | 1 | L 1 X 1 X .109 | 1.5X0.109 | |
| 9R | 1 | L 1-1/4X 1-1/4X.109 | 1.7X0.109 | |
| V7 | 1 | L 1 X 1 X .109 | 1.5X0.109 | |
| 8R | 1 | L 1 X 1 X .109 | 2.0X0.109 | |
| 7R | 1 | L 1-1/2X 1-1/2X.123 | 2.1X0.123 | |
| V8 | 1 | L 1 X 1 X .109 | 1.5X0.109 | |
| 6R | 1 | L 1 X 1 X .109 | 2.7X0.109 | |
| 5R | 1 | L 1-1/2X 1-1/2X.155 | 2.2X0.155 | |
| V9 | 1 | L 1 X 1 X .109 | 1.5X0.109 | |
| 4R | 1 | L 1-1/4X 1-1/4X.109 | 3.4X0.109 | |
| 3R | 1 | L 2 X 2 X .137 | 2.7X0.137 | |
| 2DR | 1 | L 1 X 1 X .109 | 1.5X0.109 | |
| 2R | 2 | ~~L 1-1/4X 1-1/4X.109~~ | 6.7X0.109 G | 2L1.5x1.5x.155 |

J23 30K7

2-MAY-2023 08:14:04

# J31

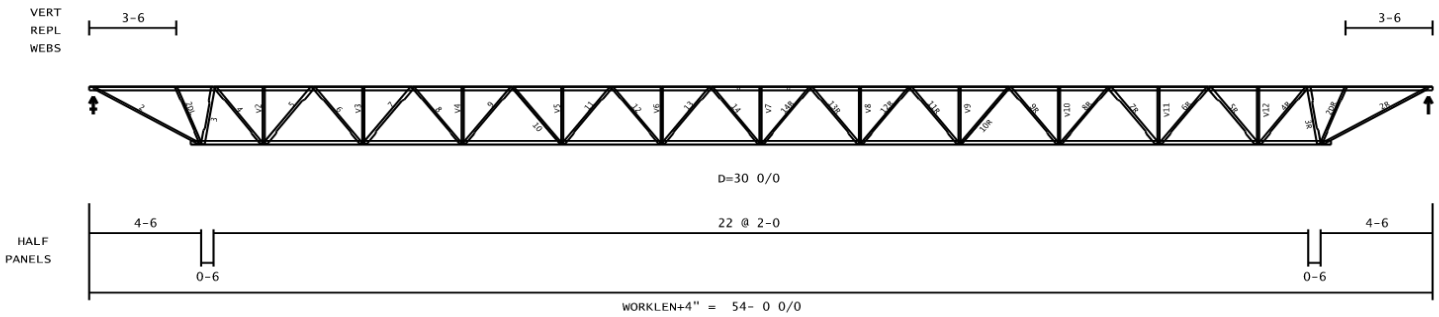


| | | | |
|---|---|---|---|
| TCXL = 0- 0 0/0 | TOP CHORD 2 | L 2 X 2 X .250 | TCXR = 0- 0 0/0 |
| BCXL = 0- 5 0/0 | BOTTOM CHORD 2 | L 2 X 2 X .216 | BCXR = 0- 5 0/0 |

| WEB | QTY | SIZE | WELD SIZE |
|---|---|---|---|
| 2 | 1 | "1"" ROUND" | 3.5X0.230 |
| 2DL | 1 | L 1-1/4X 1-1/4X.109 | 1.5X0.109 |
| 3 | 1 | L 2 X 2 X .187 | 2.7X0.188 |
| 4 | 1 | L 1-1/2X 1-1/2X.155 | 4.1X0.155 |
| V2 | 1 | L 1 X 1 X .109 | 1.5X0.109 |
| 5 | 1 | L 2 X 2 X .137 | 4.2X0.137 |
| 6 | 1 | L 1-1/2X 1-1/2X.123 | 4.3X0.123 |
| V3 | 1 | L 1 X 1 X .109 | 1.5X0.109 |
| 7 | 1 | L 2 X 2 X .137 | 3.5X0.137 |
| 8 | 1 | L 1-1/4X 1-1/4X.109 | 3.9X0.109 |
| V4 | 1 | L 1 X 1 X .109 | 1.5X0.109 |
| 9 | 1 | L 1-1/2X 1-1/2X.155 | 2.5X0.155 |
| 10 | 1 | L 1 X 1 X .109 | 3.1X0.109 |
| V5 | 1 | L 1 X 1 X .109 | 1.5X0.109 |
| 11 | 1 | L 1-1/2X 1-1/2X.123 | 2.4X0.123 |
| 12 | 1 | L 1-1/4X 1-1/4X.109 | 2.4X0.109 |
| V6 | 1 | L 1 X 1 X .109 | 1.5X0.109 |
| 13 | 1 | L 1-1/2X 1-1/2X.123 | 1.8X0.123 |
| 14 | 1 | L 1-1/4X 1-1/4X.109 | 1.7X0.109 |

| WEB | QTY | SIZE | WELD SIZE |
|---|---|---|---|
| V7 | 1 | L 1 X 1 X .109 | 1.5X0.109 |
| 14R | 1 | L 1-1/4X 1-1/4X.109 | 1.7X0.109 |
| 13R | 1 | L 1-1/2X 1-1/2X.123 | 1.8X0.123 |
| V8 | 1 | L 1 X 1 X .109 | 1.5X0.109 |
| 12R | 1 | L 1-1/4X 1-1/4X.109 | 2.4X0.109 |
| 11R | 1 | L 1-1/2X 1-1/2X.123 | 2.4X0.123 |
| V9 | 1 | L 1 X 1 X .109 | 1.5X0.109 |
| 10R | 1 | L 1 X 1 X .109 | 3.1X0.109 |
| 9R | 1 | L 1-1/2X 1-1/2X.155 | 2.5X0.155 |
| V10 | 1 | L 1 X 1 X .109 | 1.5X0.109 |
| 8R | 1 | L 1-1/4X 1-1/4X.109 | 3.9X0.109 |
| 7R | 1 | L 2 X 2 X .137 | 3.5X0.137 |
| V11 | 1 | L 1 X 1 X .109 | 1.5X0.109 |
| 6R | 1 | L 1-1/2X 1-1/2X.123 | 4.3X0.123 |
| 5R | 1 | L 2 X 2 X .137 | 4.2X0.137 |
| V12 | 1 | L 1 X 1 X .109 | 1.5X0.109 |
| 4R | 1 | L 1-1/2X 1-1/2X.155 | 4.1X0.155 |
| 3R | 1 | L 2 X 2 X .187 | 2.7X0.188 |
| 2DR | 1 | L 1-1/4X 1-1/4X.109 | 1.5X0.109 |
| 2R | 1 | "1"" ROUND" | 3.5X0.230 |

J31 30K12 2-MAY-2023 08:14:04

# J32

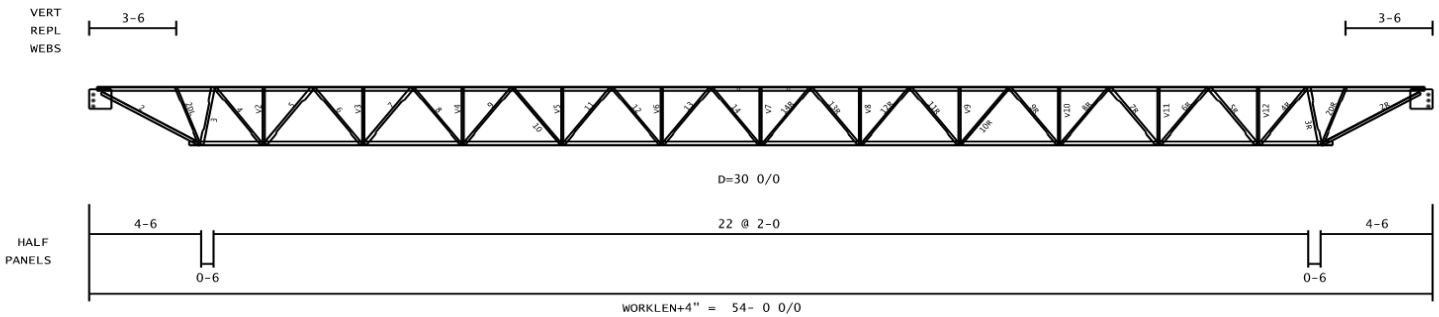


| | | | |
|---|---|---|---|
| TCXL = 0- 0 0/0 | TOP CHORD 2 | L 2 X 2 X .250 | TCXR = 0- 0 0/0 |
| BCXL = 0- 5 3/4 | BOTTOM CHORD 2 | L 2 X 2 X .216 | BCXR = 0- 5 3/4 |

| WEB | QTY | SIZE | WELD SIZE |
|---|---|---|---|
| 2 | 2 | L 1-1/2X 1-1/2X.123 | 9.3X0.123 G |
| 2DL | 1 | L 1-1/4X 1-1/4X.109 | 1.5X0.109 |
| 3 | 1 | L 2 X 2 X .187 | 2.7X0.188 |
| 4 | 1 | L 1-1/2X 1-1/2X.155 | 4.1X0.155 |
| V2 | 1 | L 1 X 1 X .109 | 1.5X0.109 |
| 5 | 1 | L 2 X 2 X .137 | 4.2X0.137 |
| 6 | 1 | L 1-1/2X 1-1/2X.123 | 4.3X0.123 |
| V3 | 1 | L 1 X 1 X .109 | 1.5X0.109 |
| 7 | 1 | L 2 X 2 X .137 | 3.5X0.137 |
| 8 | 1 | L 1-1/4X 1-1/4X.109 | 3.9X0.109 |
| V4 | 1 | L 1 X 1 X .109 | 1.5X0.109 |
| 9 | 1 | L 1-1/2X 1-1/2X.155 | 2.5X0.155 |
| 10 | 1 | L 1 X 1 X .109 | 3.1X0.109 |
| V5 | 1 | L 1 X 1 X .109 | 1.5X0.109 |
| 11 | 1 | L 1-1/2X 1-1/2X.123 | 2.4X0.123 |
| 12 | 1 | L 1-1/4X 1-1/4X.109 | 2.4X0.109 |
| V6 | 1 | L 1 X 1 X .109 | 1.5X0.109 |
| 13 | 1 | L 1-1/2X 1-1/2X.123 | 1.8X0.123 |
| 14 | 1 | L 1-1/4X 1-1/4X.109 | 1.7X0.109 |

| WEB | QTY | SIZE | WELD SIZE |
|---|---|---|---|
| V7 | 1 | L 1 X 1 X .109 | 1.5X0.109 |
| 14R | 1 | L 1-1/4X 1-1/4X.109 | 1.7X0.109 |
| 13R | 1 | L 1-1/2X 1-1/2X.123 | 1.8X0.123 |
| V8 | 1 | L 1 X 1 X .109 | 1.5X0.109 |
| 12R | 1 | L 1-1/4X 1-1/4X.109 | 2.4X0.109 |
| 11R | 1 | L 1-1/2X 1-1/2X.123 | 2.4X0.123 |
| V9 | 1 | L 1 X 1 X .109 | 1.5X0.109 |
| 10R | 1 | L 1 X 1 X .109 | 3.1X0.109 |
| 9R | 1 | L 1-1/2X 1-1/2X.155 | 2.5X0.155 |
| V10 | 1 | L 1 X 1 X .109 | 1.5X0.109 |
| 8R | 1 | L 1-1/4X 1-1/4X.109 | 3.9X0.109 |
| 7R | 1 | L 2 X 2 X .137 | 3.5X0.137 |
| V11 | 1 | L 1 X 1 X .109 | 1.5X0.109 |
| 6R | 1 | L 1-1/2X 1-1/2X.123 | 4.3X0.123 |
| 5R | 1 | L 2 X 2 X .137 | 4.2X0.137 |
| V12 | 1 | L 1 X 1 X .109 | 1.5X0.109 |
| 4R | 1 | L 1-1/2X 1-1/2X.155 | 4.1X0.155 |
| 3R | 1 | L 2 X 2 X .187 | 2.7X0.188 |
| 2DR | 1 | L 1-1/4X 1-1/4X.109 | 1.5X0.109 |
| 2R | 2 | L 1-1/2X 1-1/2X.123 | 9.3X0.123 G |

J32 30K12 2-MAY-2023 08:14:04

# J33

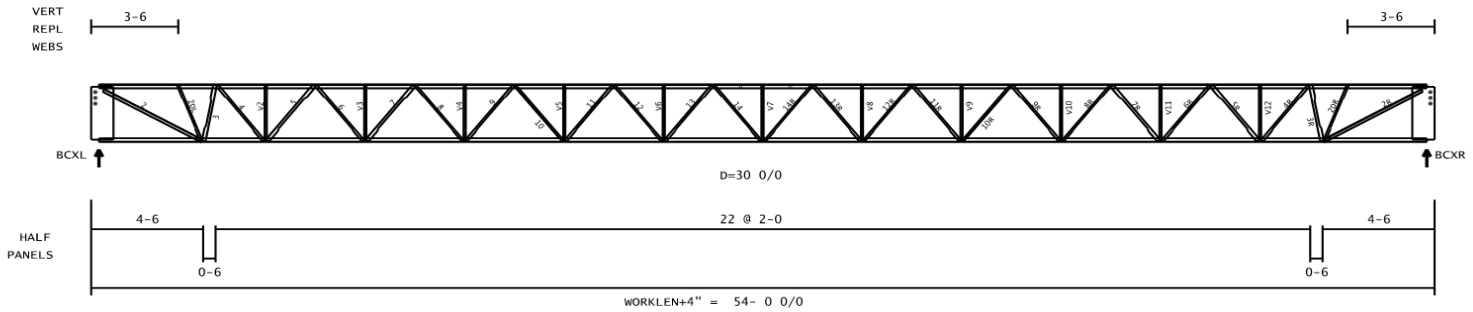


TCXL = 0- 0 0/0 | TOP CHORD 2 L 2 X 2 X .250 | TCXR = 0- 0 0/0

BCXL = 4- 2 1/4 | BOTTOM CHORD 2 L 2 X 2 X .216 | BCXR = 4- 2 1/4

| WEB | QTY | SIZE | WELD SIZE |
|---|---|---|---|
| 2 | 2 | L 1-1/2X 1-1/2X.123 | 9.3X0.123 G |
| 2DL | 1 | L 1-1/4X 1-1/4X.109 | 1.5X0.109 |
| 3 | 1 | L 2 X 2 X .187 | 2.7X0.188 |
| 4 | 1 | L 1-1/2X 1-1/2X.155 | 4.1X0.155 |
| V2 | 1 | L 1 X 1 X .109 | 1.5X0.109 |
| 5 | 1 | L 2 X 2 X .137 | 4.2X0.137 |
| 6 | 1 | L 1-1/2X 1-1/2X.123 | 4.3X0.123 |
| V3 | 1 | L 1 X 1 X .109 | 1.5X0.109 |
| 7 | 1 | L 2 X 2 X .137 | 3.5X0.137 |
| 8 | 1 | L 1-1/4X 1-1/4X.109 | 3.9X0.109 |
| V4 | 1 | L 1 X 1 X .109 | 1.5X0.109 |
| 9 | 1 | L 1-1/2X 1-1/2X.155 | 2.5X0.155 |
| 10 | 1 | L 1 X 1 X .109 | 3.1X0.109 |
| V5 | 1 | L 1 X 1 X .109 | 1.5X0.109 |
| 11 | 1 | L 1-1/2X 1-1/2X.123 | 2.4X0.123 |
| 12 | 1 | L 1-1/4X 1-1/4X.109 | 2.4X0.109 |
| V6 | 1 | L 1 X 1 X .109 | 1.5X0.109 |
| 13 | 1 | L 1-1/2X 1-1/2X.123 | 1.8X0.123 |
| 14 | 1 | L 1-1/4X 1-1/4X.109 | 1.7X0.109 |

| WEB | QTY | SIZE | WELD SIZE |
|---|---|---|---|
| V7 | 1 | L 1 X 1 X .109 | 1.5X0.109 |
| 14R | 1 | L 1-1/4X 1-1/4X.109 | 1.7X0.109 |
| 13R | 1 | L 1-1/2X 1-1/2X.123 | 1.8X0.123 |
| V8 | 1 | L 1 X 1 X .109 | 1.5X0.109 |
| 12R | 1 | L 1-1/4X 1-1/4X.109 | 2.4X0.109 |
| 11R | 1 | L 1-1/2X 1-1/2X.123 | 2.4X0.123 |
| V9 | 1 | L 1 X 1 X .109 | 1.5X0.109 |
| 10R | 1 | L 1 X 1 X .109 | 3.1X0.109 |
| 9R | 1 | L 1-1/2X 1-1/2X.155 | 2.5X0.155 |
| V10 | 1 | L 1 X 1 X .109 | 1.5X0.109 |
| 8R | 1 | L 1-1/4X 1-1/4X.109 | 3.9X0.109 |
| 7R | 1 | L 2 X 2 X .137 | 3.5X0.137 |
| V11 | 1 | L 1 X 1 X .109 | 1.5X0.109 |
| 6R | 1 | L 1-1/2X 1-1/2X.123 | 4.3X0.123 |
| 5R | 1 | L 2 X 2 X .137 | 4.2X0.137 |
| V12 | 1 | L 1 X 1 X .109 | 1.5X0.109 |
| 4R | 1 | L 1-1/2X 1-1/2X.155 | 4.1X0.155 |
| 3R | 1 | L 2 X 2 X .187 | 2.7X0.188 |
| 2DR | 1 | L 1-1/4X 1-1/4X.109 | 1.5X0.109 |
| 2R | 2 | L 1-1/2X 1-1/2X.123 | 9.3X0.123 G |

J33 30K12 2-MAY-2023 08:14:04

# J41

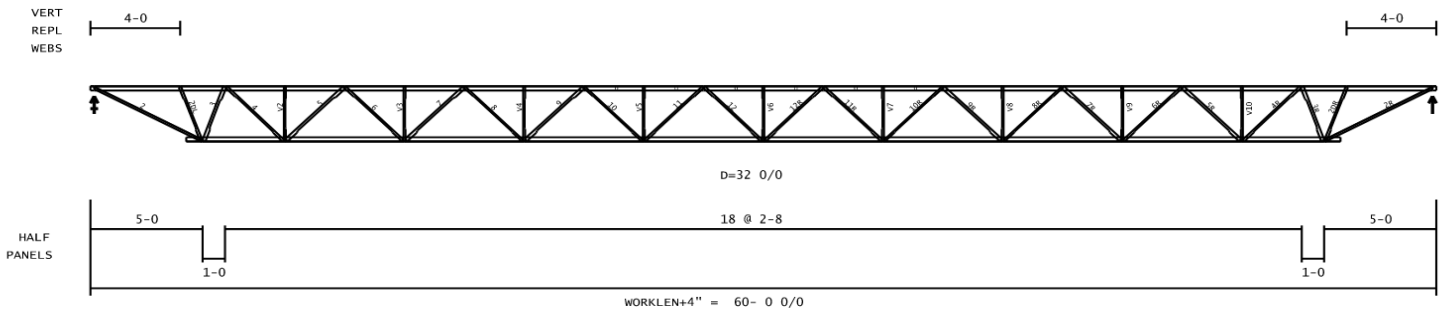


TCXL = 0- 0 0/0 | TOP CHORD 2 L 2-1/2X 2-1/2X.212 | TCXR = 0- 0 0/0

BCXL = 0- 8 3/4 | BOTTOM CHORD 2 L 2-1/2X 2-1/2X~~.188~~ .212 | BCXR = 0- 8 3/4

| WEB | QTY | SIZE | WELD SIZE | |
|---|---|---|---|---|
| 2 | 2* | ~~L 1-1/4X 1-1/4X.133~~ | 9.0X0.133 | 2L1.5x1.5x.155 |
| 2DL | 1 | L 1-1/2X 1-1/2X.155 | 1.5X0.155 | |
| 3 | 1 | L 2 X 2 X .187 | 2.8X0.188 | |
| 4 | 1 | L 1-1/2X 1-1/2X.155 | 4.5X0.155 | |
| V2 | 1 | L 1-1/4X 1-1/4X.109 | 1.5X0.109 | |
| 5 | 1 | L 2 X 2 X .187 | 3.3X0.188 | |
| 6 | 1 | L 1-1/2X 1-1/2X.155 | 3.6X0.155 | |
| V3 | 1 | L 1-1/4X 1-1/4X.109 | 1.5X0.109 | |
| 7 | 1 | L 2 X 2 X .137 | 3.6X0.137 | |
| 8 | 1 | L 1-1/4X 1-1/4X.109 | 3.9X0.109 | |
| V4 | 1 | L 1-1/4X 1-1/4X.109 | 1.5X0.109 | |
| 9 | 1 | L 2 X 2 X .137 | 2.7X0.137 | |
| 10 | 1 | L 1-1/4X 1-1/4X.109 | 2.9X0.109 | |
| V5 | 1 | L 1-1/4X 1-1/4X.109 | 1.5X0.109 | |
| 11 | 1 | L 1-1/2X 1-1/2X.155 | 1.7X0.155 | |
| 12 | 1 | L 1-1/2X 1-1/2X.155 | 1.5X0.155 | |

| WEB | QTY | SIZE | WELD SIZE | |
|---|---|---|---|---|
| V6 | 1 | L 1-1/4X 1-1/4X.109 | 1.5X0.109 | |
| 12R | 1 | L 1-1/2X 1-1/2X.155 | 1.5X0.155 | |
| 11R | 1 | L 1-1/2X 1-1/2X.155 | 1.7X0.155 | |
| V7 | 1 | L 1-1/4X 1-1/4X.109 | 1.5X0.109 | |
| 10R | 1 | L 1-1/4X 1-1/4X.109 | 2.9X0.109 | |
| 9R | 1 | L 2 X 2 X .137 | 2.7X0.137 | |
| V8 | 1 | L 1-1/4X 1-1/4X.109 | 1.5X0.109 | |
| 8R | 1 | L 1-1/4X 1-1/4X.109 | 3.9X0.109 | |
| 7R | 1 | L 2 X 2 X .137 | 3.6X0.137 | |
| V9 | 1 | L 1-1/4X 1-1/4X.109 | 1.5X0.109 | |
| 6R | 1 | L 1-1/2X 1-1/2X.155 | 3.6X0.155 | |
| 5R | 1 | L 2 X 2 X .187 | 3.3X0.188 | |
| V10 | 1 | L 1-1/4X 1-1/4X.109 | 1.5X0.109 | |
| 4R | 1 | L 1-1/2X 1-1/2X.155 | 4.5X0.155 | |
| 3R | 1 | L 2 X 2 X .187 | 2.8X0.188 | |
| 2DR | 1 | L 1-1/2X 1-1/2X.155 | 1.5X0.155 | |
| 2R | 2* | ~~L 1-1/4X 1-1/4X.133~~ | 9.0X0.133 | 2L1.5x1.5x.155 |

J41 32LH08 2-MAY-2023 08:14:30

# J42

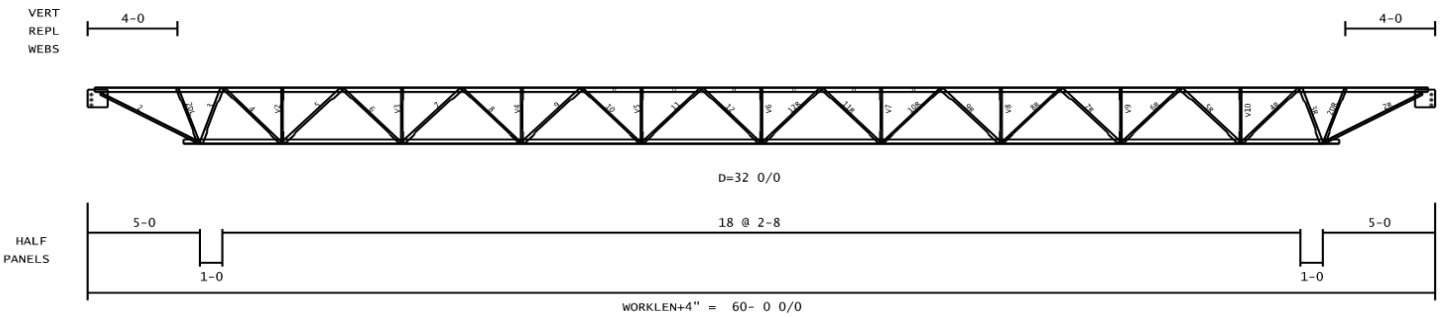


| | | | |
|---|---|---|---|
| TCXL = 0- 0 0/0 | TOP CHORD 2 | L 2-1/2X 2-1/2X.212 | TCXR = 0- 0 0/0 |
| BCXL = 0- 8 3/4 | BOTTOM CHORD 2 | L 2-1/2X 2-1/2X~~.188~~ .212 | BCXR = 0- 8 3/4 |

| WEB | QTY | SIZE | WELD SIZE | |
|---|---|---|---|---|
| 2 | 2* | ~~L 1-1/4X 1-1/4X.133~~ | 9.0X0.133 G | 2L1.5x1.5x.155 |
| 2DL | 1 | L 1-1/2X 1-1/2X.155 | 1.5X0.155 | |
| 3 | 1 | L 2 X 2 X .187 | 2.8X0.188 | |
| 4 | 1 | L 1-1/2X 1-1/2X.155 | 4.5X0.155 | |
| V2 | 1 | L 1-1/4X 1-1/4X.109 | 1.5X0.109 | |
| 5 | 1 | L 2 X 2 X .187 | 3.3X0.188 | |
| 6 | 1 | L 1-1/2X 1-1/2X.155 | 3.6X0.155 | |
| V3 | 1 | L 1-1/4X 1-1/4X.109 | 1.5X0.109 | |
| 7 | 1 | L 2 X 2 X .137 | 3.6X0.137 | |
| 8 | 1 | L 1-1/4X 1-1/4X.109 | 3.9X0.109 | |
| V4 | 1 | L 1-1/4X 1-1/4X.109 | 1.5X0.109 | |
| 9 | 1 | L 2 X 2 X .137 | 2.7X0.137 | |
| 10 | 1 | L 1-1/4X 1-1/4X.109 | 2.9X0.109 | |
| V5 | 1 | L 1-1/4X 1-1/4X.109 | 1.5X0.109 | |
| 11 | 1 | L 1-1/2X 1-1/2X.155 | 1.7X0.155 | |
| 12 | 1 | L 1-1/2X 1-1/2X.155 | 1.5X0.155 | |

| WEB | QTY | SIZE | WELD SIZE | |
|---|---|---|---|---|
| V6 | 1 | L 1-1/4X 1-1/4X.109 | 1.5X0.109 | |
| 12R | 1 | L 1-1/2X 1-1/2X.155 | 1.5X0.155 | |
| 11R | 1 | L 1-1/2X 1-1/2X.155 | 1.7X0.155 | |
| V7 | 1 | L 1-1/4X 1-1/4X.109 | 1.5X0.109 | |
| 10R | 1 | L 1-1/4X 1-1/4X.109 | 2.9X0.109 | |
| 9R | 1 | L 2 X 2 X .137 | 2.7X0.137 | |
| V8 | 1 | L 1-1/4X 1-1/4X.109 | 1.5X0.109 | |
| 8R | 1 | L 1-1/4X 1-1/4X.109 | 3.9X0.109 | |
| 7R | 1 | L 2 X 2 X .137 | 3.6X0.137 | |
| V9 | 1 | L 1-1/4X 1-1/4X.109 | 1.5X0.109 | |
| 6R | 1 | L 1-1/2X 1-1/2X.155 | 3.6X0.155 | |
| 5R | 1 | L 2 X 2 X .187 | 3.3X0.188 | |
| V10 | 1 | L 1-1/4X 1-1/4X.109 | 1.5X0.109 | |
| 4R | 1 | L 1-1/2X 1-1/2X.155 | 4.5X0.155 | |
| 3R | 1 | L 2 X 2 X .187 | 2.8X0.188 | |
| 2DR | 1 | L 1-1/2X 1-1/2X.155 | 1.5X0.155 | |
| 2R | 2* | ~~L 1-1/4X 1-1/4X.133~~ | 9.0X0.133 G | 2L1.5x1.5x.155 |

J42 32LH08 2-MAY-2023 08:14:30

# J43

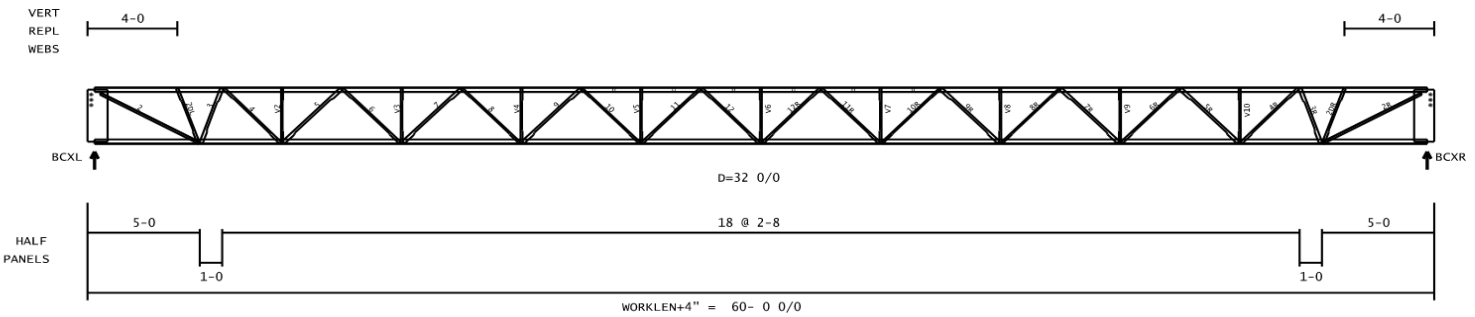


| | | | |
|---|---|---|---|
| TCXL = 0- 0 0/0 | TOP CHORD 2 | L 2-1/2x 2-1/2x.212 | TCXR = 0- 0 0/0 |
| BCXL = 4- 8 1/4 | BOTTOM CHORD 2 | L 2-1/2x 2-1/2x~~.188~~ .212 | BCXR = 4- 8 1/4 |

| WEB | QTY | SIZE | WELD SIZE | |
|---|---|---|---|---|
| 2 | 2* | ~~L 1-1/4x 1-1/4x.133~~ | 9.0X0.133 G | 2L1.5x1.5x.155 |
| 2DL | 1 | L 1-1/2X 1-1/2X.155 | 1.5X0.155 | |
| 3 | 1 | L 2 X 2 X .187 | 2.8X0.188 | |
| 4 | 1 | L 1-1/2X 1-1/2X.155 | 4.5X0.155 | |
| V2 | 1 | L 1-1/4X 1-1/4X.109 | 1.5X0.109 | |
| 5 | 1 | L 2 X 2 X .187 | 3.3X0.188 | |
| 6 | 1 | L 1-1/2X 1-1/2X.155 | 3.6X0.155 | |
| V3 | 1 | L 1-1/4X 1-1/4X.109 | 1.5X0.109 | |
| 7 | 1 | L 2 X 2 X .137 | 3.6X0.137 | |
| 8 | 1 | L 1-1/4X 1-1/4X.109 | 3.9X0.109 | |
| V4 | 1 | L 1-1/4X 1-1/4X.109 | 1.5X0.109 | |
| 9 | 1 | L 2 X 2 X .137 | 2.7X0.137 | |
| 10 | 1 | L 1-1/4X 1-1/4X.109 | 2.9X0.109 | |
| V5 | 1 | L 1-1/4X 1-1/4X.109 | 1.5X0.109 | |
| 11 | 1 | L 1-1/2X 1-1/2X.155 | 1.7X0.155 | |
| 12 | 1 | L 1-1/2X 1-1/2X.155 | 1.5X0.155 | |

| WEB | QTY | SIZE | WELD SIZE | |
|---|---|---|---|---|
| V6 | 1 | L 1-1/4X 1-1/4X.109 | 1.5X0.109 | |
| 12R | 1 | L 1-1/2X 1-1/2X.155 | 1.5X0.155 | |
| 11R | 1 | L 1-1/2X 1-1/2X.155 | 1.7X0.155 | |
| V7 | 1 | L 1-1/4X 1-1/4X.109 | 1.5X0.109 | |
| 10R | 1 | L 1-1/4X 1-1/4X.109 | 2.9X0.109 | |
| 9R | 1 | L 2 X 2 X .137 | 2.7X0.137 | |
| V8 | 1 | L 1-1/4X 1-1/4X.109 | 1.5X0.109 | |
| 8R | 1 | L 1-1/4X 1-1/4X.109 | 3.9X0.109 | |
| 7R | 1 | L 2 X 2 X .137 | 3.6X0.137 | |
| V9 | 1 | L 1-1/4X 1-1/4X.109 | 1.5X0.109 | |
| 6R | 1 | L 1-1/2X 1-1/2X.155 | 3.6X0.155 | |
| 5R | 1 | L 2 X 2 X .187 | 3.3X0.188 | |
| V10 | 1 | L 1-1/4X 1-1/4X.109 | 1.5X0.109 | |
| 4R | 1 | L 1-1/2X 1-1/2X.155 | 4.5X0.155 | |
| 3R | 1 | L 2 X 2 X .187 | 2.8X0.188 | |
| 2DR | 1 | L 1-1/2X 1-1/2X.155 | 1.5X0.155 | |
| 2R | 2* | ~~L 1-1/4X 1-1/4X.133~~ | 9.0X0.133 G | 2L1.5x1.5x.155 |

J43 32LH08 2-MAY-2023 08:14:30

## VITA

James Alex Moore was born and raised in Chattanooga, Tennessee. He and his family rooted for the Vols every Saturday in the Fall, so it was only fitting to attend the University of Tennessee. During his sophomore year, he accepted a co-op opportunity for a general contractor and spent the transformative year of 2020 mostly on construction sites. To his return to college, he wanted some extra income so he teamed up with Dr. Denavit to begin his research journey. His position as an undergraduate research assistant opened the opportunity of graduate school where stability and open web steel joists became his world and lead him to a Master's Thesis. After graduation, Alex will return home to Chattanooga to work for an engineering firm and pursue his Professional Engineer license. He gives great thanks to Dr. Denavit for his mentorship, his other professors for guidance, and his family and friends for their support.